

BOSTON UNIVERSITY
GRADUATE SCHOOL OF ARTS AND SCIENCES

Dissertation

**VISION IN THE PRESENCE OF FIXATIONAL EYE MOVEMENTS:
INSIGHTS FROM PSYCHOPHYSICS AND NEURAL MODELING**

by

GAËLLE DESBORDES

M.Sc., Laval University, Quebec City, Canada, 2001
Ingénieure de l'Ecole Nationale Supérieure des Mines de Saint-Etienne, France, 2001

Submitted in partial fulfillment of the
requirements for the degree of
Doctor of Philosophy

2007

UMI Number: 3232888

INFORMATION TO USERS

The quality of this reproduction is dependent upon the quality of the copy submitted. Broken or indistinct print, colored or poor quality illustrations and photographs, print bleed-through, substandard margins, and improper alignment can adversely affect reproduction.

In the unlikely event that the author did not send a complete manuscript and there are missing pages, these will be noted. Also, if unauthorized copyright material had to be removed, a note will indicate the deletion.

UMI[®]

UMI Microform 3232888

Copyright 2006 by ProQuest Information and Learning Company.

All rights reserved. This microform edition is protected against unauthorized copying under Title 17, United States Code.

ProQuest Information and Learning Company
300 North Zeeb Road
P.O. Box 1346
Ann Arbor, MI 48106-1346

© Copyright by
GAELLE DESBORDES
2006

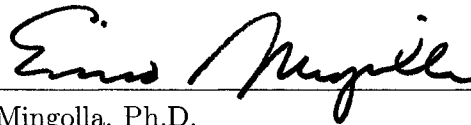
Approved by

First Reader



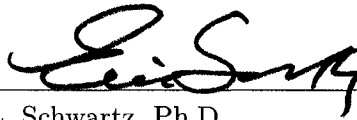
Michele Rucci, Ph.D.
Assistant Professor of Cognitive and Neural Systems

Second Reader



Ennio Mingolla, Ph.D.
Professor of Cognitive and Neural Systems, Professor of Psychology

Third Reader



Eric L. Schwartz, Ph.D.
Professor of Cognitive and Neural Systems, Professor of Electrical
and Computer Engineering, Professor of Anatomy and Neurobiology

fleeing the bees
the monkey's restless
eyes
Kobayashi Issa (1824)

Acknowledgments

This Ph.D. dissertation is the result of four years of work and could not have been possible without the invaluable help of many people. First of all, I would like to thank Professor Michele Rucci, my Ph.D. advisor, with whom I initiated this project virtually from scratch, including buying equipment for the lab and recruiting undergraduate interns. I joined the Active Perception Lab shortly after Michele had created it, and the packed room which now hosts the lab then seemed like a vast, empty, white space. I learned a lot during these first months by observing Michele establishing his scientific career.

The first year of this work owes a lot to the late Professor Jacob Beck, who sadly passed away in 2003. Jake was an outstanding mentor and provided a lot of invaluable advice. His insights in cleverly designing psychophysical experiments, his kindness, and his care will be sorely missed.

Regarding the early period of this work, I would also like to thank Thomas Cordier for his everyday support, complicity, and humour during my first two years of Ph.D. studies. In 2001–2002, while I was taking graduate courses, I had to decide which lab I wanted to join. The process of choosing the APLab certainly was not an easy one, and Thomas helped me go through these stressful times and come out stronger and more dedicated than ever before.

After about a year the APLab had gained much scope and was becoming a lively place. I would like to thank present and past lab members for their various contributions (in order of appearance): Tonino Casile, Bilgin Ersoy, Fabrizio Santini, John Watts, Gabriel Redner, Andrew Schwartz, Austin Reiter, Ramon Iovin, and Martina Poletti. Fabrizio, in particular, was a great source of encouragement and optimism. His technical and aesthetic expertise have kept the lab functioning *in stile*. Special thanks to Austin, who was dedicated, generous, and good-spirited. Even after graduating from our department, he continued to volunteer as a subject in our psychophysical experiments after the end of his workday.

Aside from my main advisor, other professors in the Department of Cognitive and Neural Systems granted me with their invaluable opinion and advice. Professors Eric Schwartz, Barb Shinn-Cunningham, Frank Guenther, Ennio Mingolla, Mike Cohen, and Dan Bullock all contributed in various ways. I am especially grateful to Eric for hundreds of hours of lively discussions about just as many topics, not only within the scope of Vision Club, but in many other informal instances as well. I am also very grateful to Barb and Frank for their warm and active support.

Regarding Vision Club, our weekly journal club consisting of lively discussions of scientific papers related to vision neuroscience, I thank present and past members (Eric Schwartz, Jon Polimeni, Aaron Seitz, Arash Yazdanbakhsh, Heiko Neumann, etc.) for sharing their insight and knowledge during these countless meetings.

Outside of our department, I would like to thank Professors Garrett Stanley, Markus Meister, and Susana Martinez-Conde, as well as the members of their respective groups, for their invaluable feedback on my work and for the opportunity to visit their labs. In particular, many thanks to Garrett for accepting me as a postdoc in his lab. I am looking forward to working there!

Special thanks to Professor Bob Steinman for several enlightening interactions, and for his help in building bite boards to use with the eyetracker. I am honored that this expert on fixational eye movements was willing to be on my Ph.D. defense committee, although unfortunately it did not work out in the end.

On a more personal level, I would like to express my deepest gratitude to Jon Polimeni, who has been an extraordinary source of support, knowledge, and motivation for me. I am also honored to know his family, which is composed of many remarkable people.

Many, many thanks to my own family, too. Maman, Papa, Mamie, Antoine, etc. have been very supportive, loving, and inspiring. Thanks also to my friends Peggy, Henry-Georges, Gwénola, François, Anne-Lise, Bénédicte, Antje, Rushi, Mukund, and many others for illuminating discussions and for showing me the path between having a life and getting a Ph.D.

Last, but not least, this work was made possible by financial support from taxpayers in the United States, through the NSF Grants EIA-0130851 and EMT-0432104, and the NIH Grant 1R03EY015732-01. Interestingly enough, the contribution of French taxpayers from the 1980s and 1990s may be just as large. Indeed, the French public educational system which bred me from kindergarten up to graduation with a *Diplôme d'Ingénieur des Grandes Ecoles* was entirely “free”—at least from my perspective. I am not sure whom in particular I should thank for this opportunity, but let me simply express my gratitude for *l'école publique gratuite, laïque et obligatoire*, a wonderful gift that we, French students, too often take for granted.

**VISION IN THE PRESENCE OF FIXATIONAL EYE MOVEMENTS:
INSIGHTS FROM PSYCHOPHYSICS AND NEURAL MODELING**

(Order No.)

GAËLLE DESBORDES

Boston University Graduate School of Arts and Sciences, 2007

Major Professor: Michele Rucci, Department of Cognitive and Neural Systems

Abstract

The projection of the visual scene onto the retina is never stationary—even during the brief intersaccadic periods of fixation that characterize natural viewing conditions. Psychophysical studies in which fixation was maintained for seconds or minutes suggest that small fixational eye movements are necessary to prevent visual percepts from fading. Neurophysiological studies indicate that neurons in the early visual system are sensitive to the input changes produced by fixational eye movements. However, the possible functions of fixational eye movements in natural viewing conditions have remained controversial.

The role of fixational eye movements was investigated by using combined psychophysical and neural modeling approaches. In psychophysical experiments a high-precision Dual-Purkinje-Image eyetracker was used to stabilize the retinal image by compensating for fixational eye movements, in order to quantify the loss of performance experienced by human observers during a short-duration visual discrimination task. Performance was significantly lower in the absence of fixational eye movements than in their presence.

Previous modeling simulations of the early visual system suggested an important role of small eye movements in the correlational structure of neural activity. The present study focuses on the temporal evolution of spatial patterns of synchronously active neurons in the primate. Macaque retinal ganglion cells with receptive fields separated by various

distances were computationally modeled. Neural responses were simulated while the cell receptive fields scanned natural images following eye movements patterns recorded in human subjects. At the onset of fixation, the responses of neighboring cells were broadly correlated over several degrees of visual angle, a distance significantly larger than the size of the receptive fields. Following this initial period, non-overlapping ganglion cells in the magnocellular pathway became, on average, uncorrelated during a typical 300-ms fixation. This dynamic spatial decorrelation was highly robust, as it originated from the temporal transience of magnocellular responses, the second-order statistics of natural images, and the retinal image motion introduced by eye movements. Spatial decorrelation facilitates a more compact neural code in the information transfer to the visual cortex. These psychophysical and computational results support the view that fixational eye movements play an important role in natural viewing conditions.

Contents

1	Introduction	1
2	Review of psychophysical, neurophysiological, and neural-modeling studies of fixational eye movements	4
2.1	Fixational eye movements in human psychophysics	6
2.1.1	Early account	7
2.1.2	Definition of fixational eye movements	8
2.1.3	Motion illusions due to fixational eye movements	10
2.1.4	Existing experimental methods to track eye movements and stabilize an image on the retina	12
2.1.5	Stabilized vision: major results	27
2.1.6	Stabilized vision: Discussion	36
2.2	Brief description of the early visual system	38
2.2.1	The retina	38
2.2.2	The lateral geniculate nucleus (LGN)	44
2.2.3	The primary visual cortex (V1)	47
2.2.4	Visual area MT	52
2.3	Influence of eye movements on the early visual system	55
2.3.1	Modulation by saccades (“Saccadic suppression” and other effects)	56
2.3.2	Modulation by fixational eye movements	58
2.4	Fixational eye movements in neural coding: results from previous modeling studies	61
2.4.1	FEM and cortical development	62
2.4.2	A functional role of fixational eye movements	65

2.4.3	Fixational eye movements as part of the neural code	72
3	Psychophysical experiments: Contributions of fixational eye movements to the discrimination of briefly presented stimuli	74
3.1	Introduction	74
3.2	Methods	76
3.2.1	Subjects	76
3.2.2	Apparatus	77
3.2.3	Stimuli	77
3.2.4	Procedure	78
3.3	Results	82
3.3.1	Experiment 1	82
3.3.2	Experiment 2	84
3.3.3	Experiment 3	87
3.3.4	Oculomotor activity	90
3.4	Discussion	92
3.4.1	Stabilization of briefly presented stimuli	95
3.4.2	Predictions from neural modeling	97
3.5	Conclusion	99
4	Fast decorrelation across primate retinal ganglion cells due to fixational eye movements	101
4.1	Introduction	101
4.2	Methods	103
4.3	Results	109
4.4	Discussion	122
4.4.1	Summary of simulation results	122
4.4.2	Validity of the result	124
4.4.3	Decorrelation and the redundancy reduction hypothesis	125
4.4.4	A dynamic, multiplexing neural code	127

4.4.5	An alternative explanation for the role of FEM in natural vision . . .	129
4.4.6	Concluding remarks about natural vision and decorrelation	129
5	Conclusion	131
5.1	Summary of results	131
5.2	Future directions	132
	References	137
	Curriculum Vitae	161

List of Figures

2.1	Pattern used for visualizing your own eye movements.	6
2.2	The Ouchi illusion.	11
2.3	Kitaoka's "rotating snakes" illusion.	12
2.4	Example of an optical lever system.	14
2.5	Examples of suction caps.	16
2.6	Modified version of a suction cap on which an optic fiber is mounted.	18
2.7	Diagram of optical components of Tulunay-Keesey's optical-electronic stabilization system.	20
2.8	Simplified schematic of the DPI eyetracker.	22
2.9	Schematic of the stimulus deflector.	24
2.10	Average contrast sensitivity functions obtained in the steady state.	31
2.11	Hubel and Wiesel's scheme for explaining the organization of simple receptive fields.	50
2.12	Dynamics of correlated activity during visual fixation in a model of the LGN.	63
3.1	An example of macroscopic and microscopic eye movements.	75
3.2	Examples of stimuli used in the experiments.	78
3.3	Main experimental procedure.	81
3.4	Contrast sensitivity functions for subjects GD and AS, measured in different experimental conditions.	83
3.5	Percentages of correct discrimination obtained in Experiment 1.	85
3.6	Percentages of correct discrimination obtained in Experiment 2.	88
3.7	Percentages of correct discrimination in early and late trials of Experiment 2.	89
3.8	Percentages of correct discrimination obtained in Experiment 3.	91

3·9 Percentages of correct discrimination in unstabilized trials that included one fixational saccade (left) and no fixational saccade (center), and in stabilized trials (right).	93
3·10 Mean area covered by fixational eye movements in unstabilized trials as a function of the subject response.	94
3·11 The rationale leading to the design of the experiments.	100
4·1 Procedure for measuring the dynamics of patterns of correlated activity in populations of model RGCs.	110
4·2 Dynamics of correlated retinal activity during visual fixation on natural images.	112
4·3 Influence of the duration of the correlation window on the dynamics of correlated activity in pairs of parafoveal M cells.	113
4·4 Spatial structure of correlated retinal activity during visual fixation on natural images.	115
4·5 Main factors contributing to the dynamic decorrelation in pairs of M cells. .	117
4·6 Influence of rectification on the dynamics of correlated activity in M cells. .	118
4·7 Influence of contrast on the dynamics of correlated activity in M cells. . . .	119
4·8 Influence of center-surround delay on the dynamics of correlated activity in M cells.	119
4·9 Example of the dynamics of correlated activity during a single fixation. . .	123

List of Abbreviations

AOSLO	Adaptive Optics Scanning Laser Ophthalmoscope
BOLD	Blood Oxygenation Level Dependent (signal)
CRT	Cathod Ray Tube
DOG	Difference Of Gaussian (functions)
DPI	Dual-Purkinje-Image (eyetracker)
EF	Early Fixation (period)
EMCD	Eye-Movement Contingent Display
fMRI	Functional Magnetic Resonance Imaging
IT	Inferotemporal (cortex)
LF	Late Fixation (period)
LGN	Lateral Geniculate Nucleus
LIP	Lateral Intraparietal (cortex)
MT	Medial Temporal (cortex)
MST	Medial Superior Temporal (cortex)
RF	Receptive Field
RGC	Retinal Ganglion Cell
SLO	Scanning Laser Ophthalmoscope
STRF	Spatiotemporal Receptive Field
V1	Primary Visual Cortex
V2	Secondary Visual Cortex
VOR	Vestibulo-Ocular Reflex

Chapter 1

Introduction

The visual input entering our eyes is continually moving. Not only do we shift our gaze several times per second to different directions; even between jump-like saccades, our eyes are constantly jittering during visual fixation, and other body movements also contribute to a considerable amount of instability. This phenomenon has been referred to by various names: fixational instability, retinal jitter, or fixational eye movements (FEM). We will use the latter.

There exist three types of fixational eye movements: *microsaccades*, which are saccades of the smallest amplitude; *ocular drifts*, during which the eye slowly drifts in a random walk; and *ocular microtremor*—a high-frequency, microscopic jitter.

Fixational eye movements have been extensively studied since the 1950's in a number of psychophysical studies. While microtremor is too small for most eyetracking methods, microsaccades and drifts have been measured extensively in many different conditions. However, their role in vision has remained elusive. According to current textbooks, the main function of microsaccades is to prevent visual percepts from fading. While it is known that visual percepts fade away after several seconds or minutes of fixation in the absence of any eye movement—a laboratory condition called “retinal stabilization” which can never happen naturally—the relevance of fading is not clear in natural vision when visual fixations typically last only a few hundreds of milliseconds.

Interest in FEM was revived with the emergence of neurophysiological experiments in awake, behaving monkeys in the late 1980's. The amplitude of FEM may be small, but receptive fields of neurons in the early visual system can be small enough to be sensitive to the microscopic motion of the retinal image induced by FEM, which covers dozens

of retinal photoreceptors. While recording the spiking activity of these neurons in awake monkeys, it became clear that their firing rate was modulated by fixational eye movements. First considered a nuisance preventing a good control of the retinal input, FEM became a topic of investigation *per se*. Chapter 2 reviews the current knowledge about fixational eye movements synthesized from several disciplines: experimental psychology, neurophysiology, and neural modeling.

The present doctoral research combines two different approaches to study the role of FEM in early vision: psychophysics and neural modeling. In a psychophysical project, we use a highly sophisticated device (the Dual-Purkinje-Image eyetracker) to record eye movements of human observers with high resolution and achieve a condition of “retinal stabilization”, or “stabilized vision”. Unlike most previous studies, our experiments investigate very short stimulus presentations, with a duration comparable to that of natural fixations (500 ms). This work is described in Chapter 3.

Our neural modeling project builds on previous work by Rucci et al. to model the influence of FEM on the neural responses in the early visual system. While these previous studies focused on long-term spatial correlations in the simulated activities of geniculate and cortical cells in the cat, our project investigates the dynamics of correlation during a 300-ms period of visual fixation in a model of macaque retinal ganglion cells (RGCs). Cell responses are simulated in the presence of a realistic visual input consisting of natural scenes scanned by real, human eye movements. This modeling project is presented in Chapter 4.

The combination of psychophysics and neural modeling offers a fresh perspective on FEM and early vision. By analyzing the impact of FEM on the properties of the visual input entering the eyes, we show that they contribute to the efficiency of neural coding in the retina. By comparing discrimination performance of human subjects in the presence and absence of FEM, we show that elimination of FEM impairs vision even for short durations in which the observers do not experience visual fading. Both results help us conclude in Chapter 5 that FEM are a significant component of the visual system. In

Chapter 5 we also propose possible extensions of the present work for future research.

Chapter 2

Review of psychophysical, neurophysiological, and neural-modeling studies of fixational eye movements

The existence of small, involuntary movements of the eye during visual fixation has been known for some time (Helmholtz, 1866). However, quantitative studies of fixational eye movements (FEM) did not start until the 1950's, when the development of electrical equipment allowed to measure them for the first time (Ratliff and Riggs, 1950; Riggs et al., 1953; Ditchburn and Ginsborg, 1953; Ditchburn, 1955; Yarbus, 1956; Nachmias, 1959; Yarbus, 1967). Ingenious methods were developed to eliminate these eye movements and study vision in their absence—a laboratory condition called *retinal stabilization* or *stabilized vision* (Yarbus, 1967; Ditchburn, 1973). Several decades of intensive psychophysical studies followed, but many questions remained unanswered (Steinman and Levinson, 1990). Findings from these experiments are reviewed in the first section of this chapter.

At the same time, progress in neurophysiology made it possible to record the activity of single neurons *in vivo*, first under anesthesia, and later in awake, behaving animals. Neural recording in awake macaques was a crucial step forward in the understanding of the primate visual system. In neuroscience, the macaque is the animal model closest to human. Not only do macaques perform eye movements very similar to humans (Skavenski et al., 1975a; Motter and Poggio, 1984; Snodderly and Kurtz, 1985; Snodderly, 1987); the early visual areas of their brains are also considered largely homologous to ours (Van Essen et al., 2001; Ejima et al., 2003; Orban et al., 2004; Van Essen, 2004; Hinds et al., 2005; Polimeni et al., 2005b). The possibility to record from neurons in the awake macaque while

the animal is performing eye movements offers a unique opportunity to study the influence of eye movements on neural coding. These studies are summarized in section 2.3, after a brief review of the physiology of the early visual system in section 2.2.

Finally, the vast amount of neurophysiological data collected in the early visual system enables to design computational models which replicate the response of neurons to various visual stimuli. This powerful and versatile approach is reviewed in section 2.4, along with previous results from our group about the influence of fixational eye movements on the development and function of the early visual system.

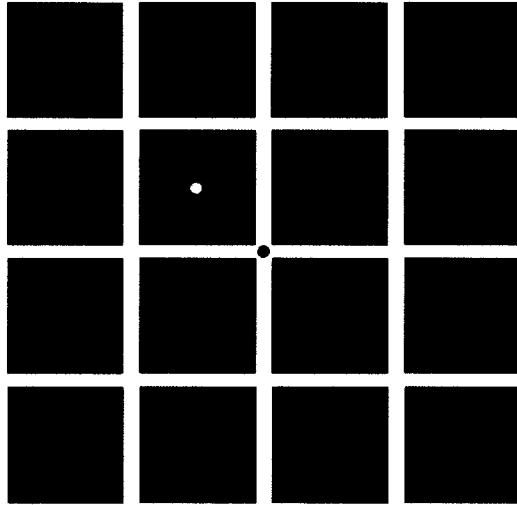


Figure 2·1: Pattern used for visualizing your own eye movements (from Verheijen, 1961). “Look at the central black dot for about a minute, then look at the white dot in the adjacent dark square. The dark after-image of the white line pattern should be seen in constant motion owing to fixational eye movements.” (Martinez-Conde et al., 2004)

2.1 Fixational eye movements in human psychophysics

In humans and other foveated animals, natural oculomotor behavior is characterized by the alternation of jump-like saccades which move the gaze to different points of the visual scene (typically 2 to 4 times per second in natural conditions), and short periods of *fixation*. The latter term is however misleading, since the projection of the visual scene on the retina is actually in constant motion. Indeed, even during the periods of visual fixation, different types of small eye movements—also known as fixational eye movements or FEM (see Martinez-Conde et al., 2004, for a review) combine with movements of the head and the body that are not perfectly compensated by the vestibulo-ocular reflex (VOR), causing *fixational instability*, or *retinal jitter*.

The existence of fixational eye movements can be experienced in some artificial conditions, such as by looking at the display shown in Figure 2·1 and following the instructions. The after-image of the stimulus, which is stabilized on the retina, appears to move on top of the real stimulus.

In this section, we review a brief history of the study of fixational eye movements, the original methods developed to eliminate them in order to achieve “stabilized vision”, and what happens to visual perception in the latter laboratory condition.

2.1.1 Early account

The existence of small eye movements of fixation in awake humans has been known for some time. Helmholtz, in his *Treatise on Physiological Optics* (1866), repeatedly mentioned the difficulty of maintaining accurate fixation, and acknowledged the importance of the “wandering of the gaze” to visual experience, as in the following excerpt (Helmholtz, 1866, Volume II, page 266):

Under ordinary circumstances, we are accustomed to let our eyes roam slowly about over the visual field continuously, so that the point of fixation glides from one part of the observed object to another. This wandering of the eye occurs involuntarily, and we are so used to it that it requires extraordinary effort and attention to focus the gaze perfectly sharply on a definite point of the visual field even for 10 or 20 seconds. The moment we do it, unusual phenomena immediately take place. Sharply defined negative after-images of the objects develop, which coincide with the objects as long as the gaze is held steady, and hence cause the objects soon to get indistinct. The result is a feeling of not seeing and of having to strain the eyes, if we persist in trying to look at the fixed place; and the impulse to move the eye becomes more and more irresistible. The little deviations of its position are scarcely noticeable in the strain, but they are revealed by parts of the negative after-images flashing up on the edges of the objects, first on one side and then on the other. This wandering of the gaze serves to keep up on all parts of the retina a continual alternation between stronger and weaker stimulation, and between different colours, and is evidently of great significance for the normality and efficiency of the visual mechanism.

2.1.2 Definition of fixational eye movements

According to the current consensus (reviewed in Martinez-Conde et al., 2004) based on observations in conditions of sustained fixation, humans exhibit several types of fixational eye movements: ocular microtremor, ocular drifts, and microsaccades.

Ocular microtremor

The smallest component, called *physiological nystagmus* or *ocular microtremor*, is an aperiodic motion of the eye (Riggs et al., 1953) with a frequency of 30–100 Hz and an amplitude smaller than 1' (one arcminute) (Ratliff and Riggs, 1950; Yarbus, 1967; Carpenter, 1988; Eizenman et al., 1985; Bolger et al., 1999). Because of its small amplitude, ocular microtremor is difficult to study and its role in vision is unknown (Martinez-Conde et al., 2004).

Ocular drifts

Slow *ocular drifts*, a second type of fixational eye movements, have an average velocity in the range of 6 to 25 arcminutes per second (Martinez-Conde et al., 2004), with great intersubject variability (St Cyr and Fender, 1969; Steinman et al., 1973). Spauschus et al. (1999) and Ditchburn and Ginsborg (1953) found drifts to be *conjugate*, that is, coordinated in both eyes. However, Yarbus (1967) and Krauskopf et al. (1960) reported non-conjugate drifts.

Microsaccades

Microsaccades are miniature versions of saccades, with amplitudes varying from 2' to 1° or 2° during sustained fixation (Martinez-Conde et al., 2004). Like larger saccades, microsaccades are conjugate (Riggs and Niehl, 1960). Under more natural viewing conditions, when brief periods of fixation alternate with larger-scale saccades, the distribution of saccade amplitudes is not bimodal. In fact, there exists a relationship between the amplitude and velocity of saccades, called the *main sequence*, which remains valid for saccades of all

sizes, including microsaccades (Zuber and Stark, 1965; Schulz, 1984; Møller et al., 2002; Martinez-Conde et al., 2000). This means that there is no clear-cut distinction between microsaccades and saccades. In general, the consensus is to reserve the term *microsaccade* for saccades shorter than 30' (e.g., Zuber and Stark, 1965), although the thresholds vary from 12' (e.g., Steinman et al., 1973) to 2° (e.g., Martinez-Conde et al., 2000).

Fixational eye movements in natural conditions

In most cases, the above statistics of drifts and microsaccades were measured in subjects who were instructed to maintain prolonged fixation. Under more natural viewing conditions, when periods of fixation only last a few hundred of milliseconds and are interspersed with saccades, other kinds of FEM exist, such as corrective saccades and *post-saccadic drifts* (e.g., Kapoula et al., 1986a). Therefore, the classic definitions must be considered with caution. Steinman has been a long-term proponent of studying “natural” conditions, in which the subjects are free to move their eyes as well as their head, and found significantly different statistics of eye movements in these conditions compared to bitebar-restricted, steady-fixation conditions (reviewed in Steinman, 2004).

Importance of microsaccades in vision

In particular, the importance of microsaccades was highly debated in the 1970s and 1980s (Ditchburn, 1980; Kowler and Steinman, 1980) and the issue still is largely unresolved (Steinman, 2004; Martinez-Conde et al., 2004), partly due to the absence of a common terminology. For instance, the characteristic range of amplitude, velocity—and even acceleration, frequency, etc.—of a microsaccade varies widely across different studies (reviewed in Martinez-Conde et al., 2004, Table 3). Interestingly enough, microsaccades may well exist only in artificial conditions in which the head is restrained and the subject has to maintain prolonged fixation, and are not to be found during shorter periods of fixation that occur naturally in normal vision (Steinman and Levinson, 1990; Steinman, 2004). Our own data seem to confirm that microsaccades are rare in free-viewing of natural images.

Torsional eye movements

It should be noted that the eye can rotate in three dimensions inside the orbit. In other words, eye movements should be described in terms of three component rotations around cardinal axes such as horizontal, vertical, and torsional. Remarkably, torsional eye rotations can have equal or larger amplitude than the horizontal and vertical components. Ferman et al. (1987a) reported that torsional instability during monocular fixation had a standard deviation of about 15' on average across 5 subjects, for fixations lasting 16 to 32 s. In Ferman et al. (1987b), mean torsional non-saccadic speed was about 46'/s when the head was held still. Therefore, it is regrettable that most eyetracking methods (described in 2.1.4), including ours (the Dual-Purkinje-Image eyetracker), can only measure horizontal and/or vertical rotations but not torsional rotations.

FEM in other animals

In addition to humans, fixational instability has been observed in many species, including the macaque (Skavenski et al., 1975a; Motter and Poggio, 1984; Snodderly and Kurtz, 1985; Snodderly, 1987), the cat (Hebbard and Marg, 1960; Pritchard and Heron, 1960; Winterson and Robinson, 1975; Conway et al., 1981a), the rabbit (Collewijn and van der Mark, 1972), the turtle (Greschner et al., 2002), the salamander (Manteuffel et al., 1977; Ölveczky et al., 2003), and even the owl (Steinbach and Money, 1973), a species whose eyes are often considered immobile. Importantly, macaques and humans exhibit very similar eye movements, including FEM (Skavenski et al., 1975a; Motter and Poggio, 1984; Snodderly and Kurtz, 1985; Snodderly, 1987). The macaque is thus a valid animal model for studying FEM in human.

2.1.3 Motion illusions due to fixational eye movements

A classic illustration of the instability of fixation is the Ouchi illusion (Ouchi, 1977; Spillmann et al., 1993), reproduced in Figure 2·2, in which the inset appears to move as we look at it, following one's own fixational eye movements.

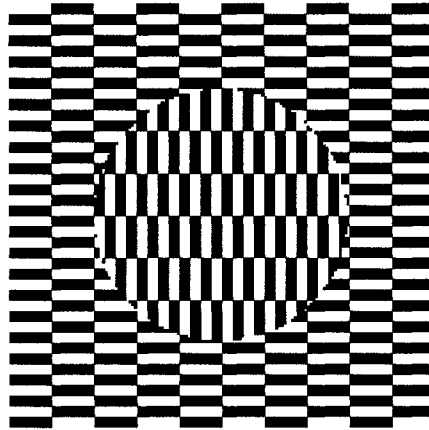


Figure 2.2: The Ouchi illusion (Ouchi, 1977).

Yet another compelling demonstration of motion illusion is the “jitter after-effect” (Murakami and Cavanagh, 1998)¹. In this illusion, observers are adapted to a patch of dynamic random noise and then view a larger pattern of static random noise. The static noise in the unadapted regions then appears to “jitter” coherently in random directions. Several control conditions indicate that this visual jitter directly reflects fixational eye movements.

In Op Art (a branch of pop art using optical illusions), there exist a growing number of similar works in which illusory motion is experienced with a static display. A popular one is the “rotating snakes” illusion by the Japanese psychologist Akiyoshi Kitaoka², reproduced in Figure 2.3.

It has been demonstrated that the motion illusion induced by this type of static display (called repeated asymmetric patterns) was due to fixational instability (Zanker et al., 2003; Zanker, 2004; Conway et al., 2005), although an alternative explanation invokes fast and slow changes over time in the neuronal representation of contrast or luminance, such as the temporal phase advance in the neural response at high contrast at the beginning of each new fixation (Backus and Oruç, 2005).

¹demonstration available online at
<http://www.brl.ntt.co.jp/people/ikuya/demo/visualjitter/VisualJitter.html>

²available on <http://www.psy.ritsumei.ac.jp/~akitaoka/index-e.html>

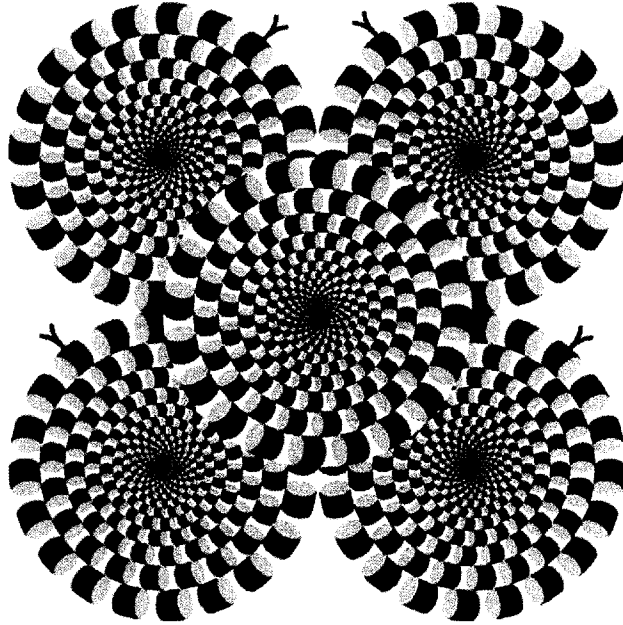


Figure 2.3: Kitaoka’s “rotating snakes” illusion (from Murakami et al., 2006).

More recently, Murakami et al. (2006) showed that the subjects with more unstable fixation experienced motion illusion more strongly. Since they did not find any correlation between the illusion strength and the frequency of microsaccades, these authors concluded that these motion illusions were mostly due to ocular drifts.

2.1.4 Existing experimental methods to track eye movements and stabilize an image on the retina

What happens if FEM are eliminated? This question has been extensively studied since the 1950’s, with the development of ingenious methods to achieve *stabilized vision*—a laboratory condition in which eye movements (including FEM) are absent or compensated for. Some of these studies focus on stationary stimuli and test different contrast levels, different chromaticity levels, and different types of artificial stimuli, from sine-wave gratings to bi-partite fields to various geometric forms. In other studies, the visual stimulus is moving according to some predefined motion pattern. In the latter case, stabilization is an important tool that allows a complete control over the retinal image motion experienced

by the subject, since retinal motion will be caused only by the well-defined stimulus motion and not by eye movements.

In this section, we will describe the major experimental methods which have been used to achieve retinal stabilization. Each method will be evaluated in terms of its degrees of spatial and temporal accuracies, its invasiveness, and its constraints on the subject—who often need substantial training in order to perform the experiment. We will then review the major results of experiments in stabilized conditions in section 2.1.5.

Paralysis of the eyes

When experimenting with animals, a common way to suppress eye movements is to induce paralysis, most often in combination with general anesthesia. These methods are usually not used on human subjects. Notable exceptions are the studies by Stevens et al. (1976) and Matin et al. (1982), who investigated visual perceptions in awake, curare-paralyzed humans. In particular, Stevens subjected himself to several experimental sessions (requiring artificial ventilation), using 15 mg to 24 mg doses of curare to induce partial paralysis, or 6 mg of curare in the addition of succinylcholine as a blocking agent to achieve complete paralysis (Stevens et al., 1976). The subject reported visual fading in both conditions, although other head and body movements (due to heart beat and artificial ventilation) were sufficient to restore visual perceptions.

Matin et al. (1982) used curare not to achieve retinal stabilization, but rather to investigate the “oculoparalytic illusion”, in which humans partially paralyzed with curare suffer from visual-field dependent spatial mislocalizations. They found that, in darkness, observers partially paralyzed with curare make large (greater than 20 degrees) gaze- and dosage-dependent errors in visually localizing eye-level-horizontal and median planes, in matching the location of a sound to a light, and in pointing at a light. The authors claimed that these impairments were due to defects in extraretinal eye position information.

Apart from these two isolated cases, paralysis has never been used to study FEM, for obvious ethical reasons. Other methods had to be developed in order to track eye move-

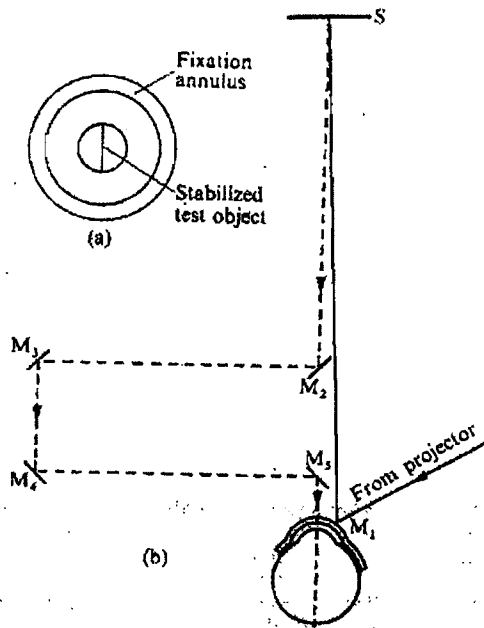


Figure 2·4: Example of an optical lever system (from Ditchburn, 1973, p. 110, after Riggs et al., 1953). The image of the target formed on the screen S is viewed by light reflected at M_2 , M_3 , M_4 , and M_5 mirrors. Inset (a): Target surrounded by fixation annulus.

ments and induce retinal stabilization in psychophysical experiments on human subjects. These methods, described below, include: optical lever systems, suction caps, an optical-electronic active feedback system, and the Dual-Purkinje-Image eyetracker combined with a stimulus deflector. Recent methods using the Adaptive Optics Scanning Laser Ophthalmoscope (AOSLO) allow to measure FEM with a significantly better resolution, but to date they have not been used to achieve stabilized vision. Nevertheless, they are reviewed at the end of this section.

Optical lever systems

Early stabilized experiments were using large, scleral contact lenses on which a plane mirror was fixed on top of a rod (Ditchburn and Ginsborg, 1952; Riggs and Ratliff, 1952; Riggs et al., 1953). These methods are referred to as *optical lever* methods (Ditchburn, 1973).

An example of an optical lever system is shown in Figure 2·4. A small mirror is

positioned perpendicular to the axis of the lens. A narrow beam of light is projected to the M_1 mirror, reflects on it, passes through an optical system composed of the four mirrors M_2 , M_3 , M_4 , and M_5 , and projects to a screen S situated in front of the subject. When the incident and reflected beams are coplanar with the normal to the mirror, the angle of rotation of the reflected light is twice the angle of rotation of the eye. The optical system is designed to reduce that angle of rotation in order to make it equal to the rotation of the eye. While the first versions of this method could only compensate the azimuth (horizontal) component of eye rotation, the subsequent versions allowed to also compensate the elevation (vertical) component of eye rotation as well as (translational) head movements in all directions.

Several successive refinements were made to the method. Ditchburn and colleagues designed a telescopic system by adding an artificial pupil and a short-focus lens to the device in order to produce a sharply defined image (Clowes and Ditchburn, 1959; Ditchburn and Foley-Fisher, 1986). Riggs and colleagues, on the other hand, attempted to make the contact lens lighter. Instead of being mounted on a rod, the mirror was embedded within the plastic material of which the contact lens was made, so as not to add to the inertia of the contact lens (Riggs and Niehl, 1960). This device was tested in subsequent experiments (Riggs and Schick, 1968).

Many other variations of the contact lens method were developed (Tulunay, 1959; Riggs and Tulunay, 1959; Keeseey, 1960; Koenderink, 1972), in spite of severe critiques made by Barlow (1963), regarding mainly the problem of slippage of the contact lens on the cornea, which could disrupt stabilization in a non negligible way. This slippage issue was later rebutted by Riggs and Schick (1968) who showed that, when properly used, contact lenses offered an accuracy of stabilization of about half an arcminute of visual angle, although Arend and Timberlake (1986a) argued that this may not be sufficient to achieve perfect stabilization (see also the resulting debate between Ditchburn, 1987 and Arend and Timberlake, 1987).

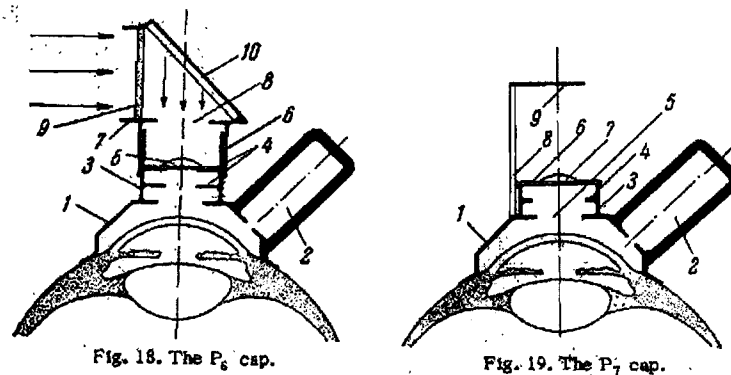


Figure 2.5: Examples of suction caps (from Yarbus, 1967, pages 36–37). These are not scale drawings.

Yarbus's suction cap

The suction cap was invented in the 1950's by Alfred Yarbus, a Russian psychologist whose studies of eye movement patterns have been very influential. The idea behind the suction cap is quite simple: in order to present the subject with a visual stimulus that moves with its eye, one can “glue” it directly on the subject's eye. More precisely, one can build a little cap that fits the sclera and rests on it by suction. The stimulus is positioned directly on the cap, and a short-focus lens located inside the cap brings the image into focus.

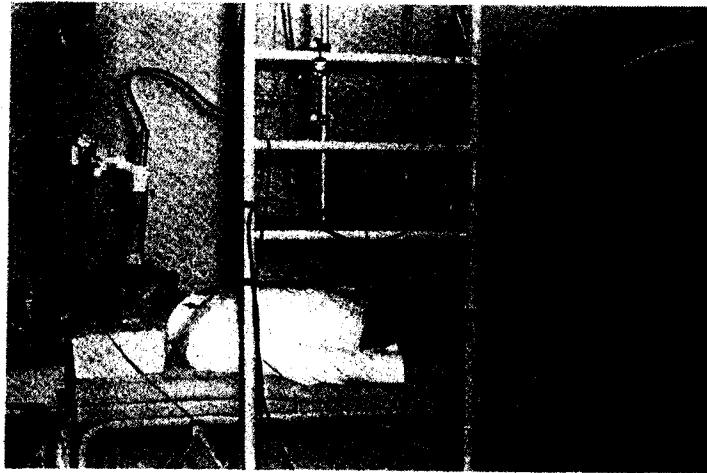
A number of versions of Yarbus's suction cap have been developed, by himself (Yarbus, 1956, 1967) or by others (Barlow, 1963; Gerrits et al., 1966; Gerrits and Vendrick, 1972; Rozhkova et al., 1982b,a, 1985). Examples of suction caps are shown schematically in Figure 2.5. The P_6 cap shown on the left panel consists of a frame (1), a hollow rubber bulb (2), two diaphragms (4), a short-focus lens (5), a round aperture (8), and a mirror (10). In the P_7 cap shown on the right panel, the test field (9) is mounted on top of a round wooden rod (8). Some caps were designed to stabilize the whole vision field (e.g., the P_6 cap shown on the left panel of Figure 2.5) while others allowed the subject to see a superposition of a stabilized image and an unstabilized image (e.g., the P_7 cap shown on the right panel of Figure 2.5). Caps were assembled from several parts that could be made of rubber, duralumin, paper, glass, etc.

Gerrits et al. (1966) developed several versions of the suction cap. In one of them a small electric synchronous motor was mounted on top of the suction cap (Gerrits and Vendrick, 1970). In another version presented in Figure 2·6, the suction cap was modified to receive one end of a flexible optic fiber which allowed to show a reduced TV screen display (Gerrits and Vendrick, 1974). Rozhkova et al. (1982b,a, 1985) made a binocular version of suction caps.

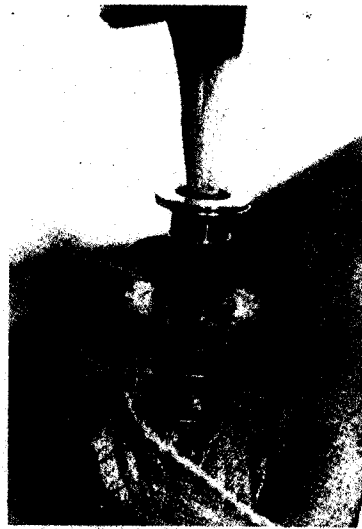
The use of suction caps was particularly delicate since the method is quite invasive. Before placing the cap on the eye, the experimenter had to squeeze the hollow bulb on the side (see Figure 2·5) in order to expel the air. The resulting suction gave the cap a firm fit to the eye. Artificial tears were not needed since the cornea was completely covered by the cap, which retarded its drying out. However, experiments could not exceed five minutes in duration because the cap compressed the blood vessels in the conjunctiva around the cornea. The subject was lying supine (face up) in most experiments to prevent the cap from slipping because of its weight. The eyelids were taped to prevent them from displacing the cap, because such displacement could lead to eye injury. The surface of the eye had to be anesthetized. The suction caused a slight fall of intraocular pressure.

In spite of these drawbacks, Barlow (1963) expressed his preference for suction caps over scleral contact lenses and claimed that the former allowed more precise stabilization. However, this issue was subject to controversies (Riggs and Schick, 1968; Jones et al., 1972) and it now seems that both methods are roughly equivalent (Steinman and Levinson, 1990).

A major advantage of such direct-attachment systems is that they can compensate for all eye and head movements. Optical lever methods allow to display any type of stimuli on the distal screen, but can be used only in a small visual field because the beam of light needs to be narrow enough to hit the mirror on the contact lens without entering the pupil. On the other hand, suction caps can theoretically make use of the whole visual field since they cover the cornea entirely, but the type of stimuli that can be used is quite limited. Lastly, a major drawback of these methods would be that they are invasive and require total cooperation from the subjects, who should do their best to avoid making



(a)



(b)

Figure 2.6: Modified version of a suction cap on which an optic fiber is mounted. (a) The setup used in the experiments (from Gerrits and Vendrick, 1972). The subject looked through the optic fiber to a stimulus on a TV screen. (b) A closeup of the fibers fitting the object holder of the suction cap (from Gerrits and Vendrick, 1974). The fibers move freely with the suction cap and the eye.

saccades (even small ones) or blinking during the experiments. This is why most subjects in early stabilized experiments were the authors themselves, which raises the question of the validity of the results.

Scleral search coil

The *scleral search coil*, originally invented by Robinson (1963), is widely regarded as the gold standard measurement technique for eye movements (Irving et al., 2003). It consists in one or several loops of a conductive wire, defining an electromagnetic coil, that is embedded into a tightly-fitting contact lens or a rubber ring that adheres to the eye. It can also be surgically implanted around the cornea, as commonly performed on macaques. The subject's head is surrounded by a cubic frame, on which three sets of magnetic coils are mounted orthogonally. These coils are driven with high-frequency (e.g., 20 kHz) alternating current in phase quadrature so as to induce currents in the scleral coil. These currents are recorded from two fine wires emanating from the scleral coil. One of these currents is a function of the horizontal position of the eye in its orbit, while the other current is a function of its vertical position. The spatial resolution of the scleral search coil method is about 1' (de Bie, 1985). Scleral coils have been used in human subjects, but they can transiently induce a variety of undesirable effects, including ocular discomfort, hyperemia (blood congestion) of the bulbar conjunctiva, increased intraocular pressure, buckling of the iris, and reduction in visual acuity (Irving et al., 2003).

In order to achieve retinal stabilization, the scleral search coil system needs to be combined with a gaze-contingent display, which is a video display (for example, a computer-driven monitor) refreshed in real-time according to the current position of the eye. Such a system has been used in Max Snodderly's laboratory in various experiments on macaques (Gur and Snodderly, 1987).

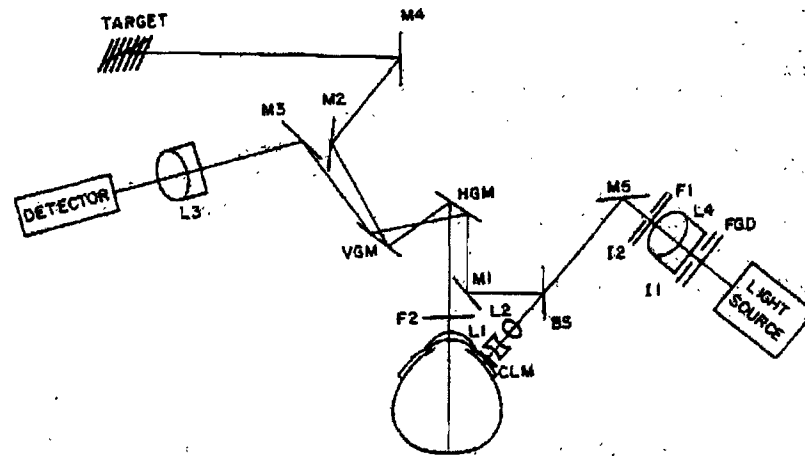


Figure 2·7: Diagram of optical components of Tulunay-Keesey's optical-electronic stabilization system (from Jones et al., 1972). The collimated beam is shown reflected from the contact lens mirror (CLM) through a reversed Galilean telescope (L_1, L_2) to vertical and horizontal galvanometer mirrors (VGM, HGM) which reflect the beam to a detector. The movement of the light beam on the detector is proportional to the difference between eye and galvanometer mirror rotation.

Tulunay-Keesey's optical-electronic active feedback system

Tulunay (a.k.a. Keesey or Tulunay-Keesey) was previously using tightly fitting contact lenses in an optical lever system such as those described above (Tulunay, 1959; Riggs and Tulunay, 1959; Keesey, 1960). Because this kind of system requires the use of lenses in the optical path, the subject's visual field is restricted and spatial resolution is altered. Therefore, Tulunay-Keesey and her colleagues developed an optical-electronic system which no longer required lenses in the optical path, but only mirrors (Jones et al., 1972). Its principle is illustrated in Figure 2·7. A simple feedback system detects eye motion and rotates a mirror through which the target is viewed, to exactly compensate for eye motion. The apparatus stabilizes retinal images by tracking and stabilizing a beam of infrared light reflected from a mirror attached to a tightly fitting contact lens.

According to Jones et al. (1972) this stabilization device has a spatial accuracy of 30 seconds of arc and a frequency response of 75 Hz. The system compensates perfectly for motions with a frequency up to 10 Hz (which include slow drifts and most of the tremor

movements) and adequately for higher frequencies. The response to a typical saccade having a 25 ms duration and an amplitude of 5' causes a maximum stabilization error of 0.45' about 5 ms after the beginning of the saccade, the error becoming essentially zero after 20 ms (Jones and Tulunay-Keesey, 1975).

Overall, Tulunay-Keesey's optical-electronic active feedback system shows many interesting features to achieve retinal stabilization. It allows the use of any kind of stimulus with any display system. The measure of eye position is insensitive to small head movements. However, to ensure that the contact lens mirror does not move out of the light beam, it is necessary to minimize head movements by using a dental bite board molded to each individual subject and rigidly attached to the apparatus bench.

We can think of a few possible drawbacks of Tulunay-Keesey's stabilization system. The first one would be that the tight-fitting contact lens is somehow invasive and tends to slip on the cornea if not correctly fitted, as we saw in our description of optical lever systems. Secondly, the field of view in which the system was able to track the eye was probably quite small. Its extent was not reported, but in most experiments from that laboratory, the display subtended 3.2° vertically and 4° horizontally, or less. Thirdly, the whole apparatus seems to be very delicate and not easy to use. The authors did not comment on the setup procedures nor on their duration. The last publication related to this system dates back ten years ago (Tulunay-Keesey and Olson, 1996), and thus it is not clear whether an implementation of the system still exists.

The Dual-Purkinje-Image eyetracker and stimulus deflector

The Dual-Purkinje-Image Eyetracker (Crane and Steele, 1978) was initially designed "to eliminate artifacts due to eye translation relative to the measuring instrument, which is the most troublesome limitation of other eyetracking instruments" (Crane, 1994).

The principle of the Dual-Purkinje-Image (DPI) Eyetracker is illustrated in Figure 2-8. A beam of infrared light is sent to the subject's eye. Because of the geometry of the eye this beam is reflected at four successive locations. The first and second Purkinje images

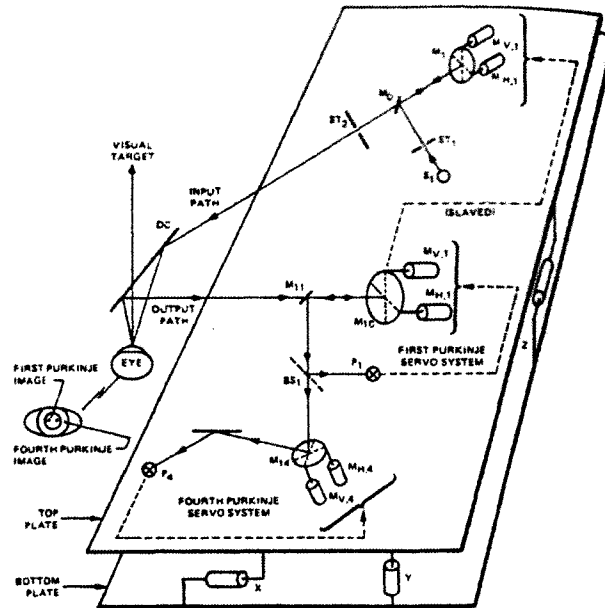


Fig. 2. Simplified schematic of the DPI eyetracker.

Figure 2·8: Simplified schematic of the Dual-Purkinje-Image (DPI) eyetracker (from Crane and Steele, 1985).

are the virtual images formed by the light reflected from the front and rear surfaces of the cornea, respectively; they are almost exactly coincident. The third Purkinje image is a virtual image formed by light reflected from the front surface of the eye's lens; it is formed in a plane far removed from the other images. The fourth Purkinje image is a real image formed by light reflected from the rear surface of the lens acting as a concave mirror. It is formed in almost exactly the same plane as the first Purkinje image.

The DPI eyetracker technology is based on the fact that, if the eye undergoes translation (typically as a result of lateral head movement), the first and fourth Purkinje images move together through exactly the same distance. If the eye rotates in its orbit, however, the two images move through different distances. Hence, the physical separation of these two images yields a measure of the angular orientation of the eye and is uncontaminated by (horizontal and vertical) translational movements.

The DPI eyetracker provides a pair of electrical signals whose magnitudes are proportional to the horizontal and vertical components of the eye rotation in its orbit, as mea-

sured by the spatial difference between the first and fourth Purkinje images (Cornsweet and Crane, 1973).

By itself, the DPI eyetracker can only track eye movements. In order to achieve image stabilization, it has to be coupled to another optical-electronic device called a stimulus deflector (Crane and Clarke, 1978). This device is schematically illustrated in Figure 2·9. It consists in a set of lenses and mirrors, such that when the subject is looking through it, the visible field is constantly kept at the center of the subject's gaze. This is made possible by feeding the two eye position signals coming from the eyetracker, x (for horizontal) and y (for vertical), into two piezo-electric motors driving small mirrors—one moving about a vertical axis, the other about a horizontal axis. These mirrors allow the displayed image to follow the movements of the eye in real time.

There were several successive versions of the DPI eyetracker (six to date). The first production version was Generation III (Crane and Steele, 1978). An automatic focus system was incorporated to also track backward and forward movements of the eye, i.e., translational movements typically due to head movement. This was a very important feature since the apparatus did no longer require the head to be perfectly immobilized, and thus uncomfortable bite boards were no longer necessary for recording eye movements. However, they were still needed in stabilized conditions, because the stimulus deflector only works in 2D (for horizontal and vertical eye movements), and would mistake backward and forward movements for horizontal rotations.

In its current version (Generations 5 and 6), the combination of the DPI eyetracker and the stimulus deflector has a nominal spatial resolution of approximately 1 arcminute, and a total response time of approximately 7 milliseconds (Crane and Steele, 1985; Crane, 1994). Recent experiments using the DPI eyetracker in conjunction with an Adaptive Optics Scanning Laser Ophthalmoscope (AOSLO), described below, confirmed that the spatial resolution of the DPI eyetracker is 1 arcmin or less (Stevenson and Roorda, 2005). The DPI system allows to show any kind of stimuli (including, but not limited to, a CRT display) in a visual field subtending up to 10 degrees. It is not very invasive and rather

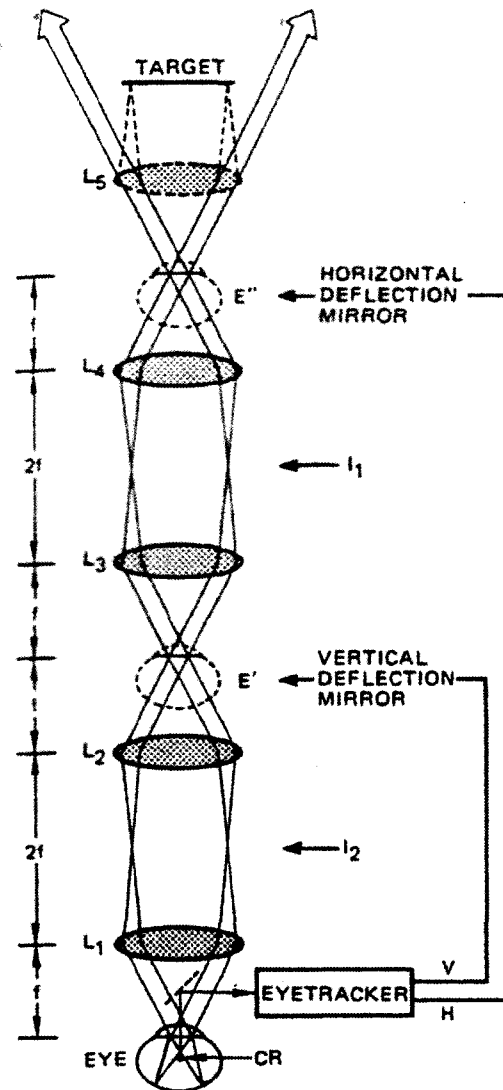


Fig. 14. Two-dimensional image-stabilizing system.

Figure 2.9: Schematic of the stimulus deflector, an optical-electronic device allowing image stabilization (from Crane and Steele, 1985).

easy to use: Preliminary settings take from 2 to 10 minutes in our own experience. In overall, these specifications compare well with Tulunay-Keesey's optical-electronic active feedback system described above.

One significant difference between the DPI eyetracker and other eyetracking methods, however, is that the DPI eyetracker involves measuring the position of the eye-lens by tracking the fourth Purkinje image, which is a reflection on the back of the eye-lens. This feature causes significant differences between the eye position measured with the DPI eyetracker and that measured with a scleral search coil (Deubel and Bridgeman, 1995). In particular, during and shortly after saccades, the acceleration of the eye results in significant deviations of the lens from the optical axis: during the initial acceleration phase of the saccade, the lens lags behind the rest of the eye, while at the end of the saccade, the lens overshoots the final eye position and is pulled back by passive elastic forces. As a result, the DPI eyetracker typically shows a small *undershoot* (or *backshoot*) at the beginning of some saccades, and a more significant *overshoot* at the end of most saccades, compared with simultaneous measurements obtained with the scleral search coil. Deubel and Bridgeman (1995) found that saccadic undershoots and overshoots were more pronounced at near accommodation (22 cm target distance) than at far accommodation (390 cm target distance). The effect was also greatest in young subjects and decreased with age due to the increased stiffness of the accommodative system. Since the DPI eyetracker and the scleral search coil gave identical records of the movements of an artificial eye, the authors concluded that the DPI method captured the undershoots and overshoots of the eye-lens. However, the saccadic overshoots measured with the DPI eyetracker might not be entirely due to movements of the eye-lens, but also to the movements of the whole ocular globe, to some extent. Although Deubel and Bridgeman (1995) did not report overshoots in their scleral search coil records, scleral coil measurements of macaque eye movements can show some degree of overshoot at the end of saccades (D. M. Snodderly, personal communication).

Eyetracking using retinal imaging

The most accurate methods to measure the motion of the eye with respect to the retinal image are those that track the retina itself. The first such system was able to track a blood vessel using an oscilloscope and photomultiplier tube with a resolution of ten arcseconds (Cornsweet, 1958). The development of the Scanning Laser Ophthalmoscope (SLO) allowed to extract eye motion offline by manual marking of blood vessels (Ott and Eckmiller, 1989; Ott et al., 1990; Ott and Daunicht, 1992; Schuchard and Raasch, 1992; Lakshminarayanan et al., 1992), even for high temporal resolution (Stetter et al., 1996).

In the Adaptive Optics Scanning Laser Ophthalmoscope (AOSLO), the image resolution is improved and the magnification has increased, allowing for non-invasive, *in-vivo* imaging of individual photoreceptors (Roorda, 2000). However, the region of interest is so small (1.5 to 2 square degrees in Stevenson and Roorda, 2005) that it may not include large, distinct features such as blood vessel bifurcations. Thus, computational image analysis techniques are necessary to recover motion over a whole frame and to register successive frames with a moving eye. The spatial resolution of AOSLO is about $0.5'$, and it is possible to extract horizontal and vertical eye position with a resolution of $0.125'$ using subpixel registration, although resolution on the torsional axis is lower. The temporal resolution is also very high (16 kHz). As mentioned above, this new, very accurate method allows to validate that the DPI eyetracker has an accuracy of $1'$ (Stevenson and Roorda, 2005).

If tracking eye movements in time is not required, even higher spatial resolution can be achieved. For instance, it is possible to measure the position of a stimulus on the cone mosaic with an error smaller than $0.08'$ ($4.8''$), which is five times smaller than the diameter of the smallest foveal cones. Putnam et al. (2005) used high-resolution retinal imaging with adaptive optics to measure the accuracy of retinal position for repeated visual fixations on the same target. Subjects were required to fixate at the center of a 1° Maltese cross and to press a button when they felt that they were fixating accurately. The high-resolution image of their retina was then acquired during a 4-ms exposure, during which the movement of their eye was negligible in 95% of the trials (the remaining 5% of the trials

that showed some blur in the image were discarded). For each subject, 69 to 199 images were used for analysis. The standard deviation of fixation positions measured in discrete trials ranged from 2.1' to 6.3', with an average of 3.4' (in five subjects), in agreement with previous studies (Ditchburn, 1973; Steinman et al., 1973). Remarkably, the average center of fixation was systematically displaced by about 10' from the fovea (defined as the region of highest cone density), in a direction that depended on the subject, indicating that cone density alone does not drive the location on the retina selected for fixation.

2.1.5 Stabilized vision: major results

The stabilization methods described above were used in a number of laboratories over the world in order to study the effects of retinal stabilization on visual perception. The main findings from the last fifty years of research are summarized in this section. They concern image fading, contrast thresholds elevation, and other effects in motion perception and color vision.

Image fading

The first and most well-known result about stabilized images is that they fade out with time and may eventually disappear (Ditchburn and Ginsborg, 1952; Riggs and Ratliff, 1952; Riggs et al., 1953). Image fading can actually occur even in the absence of any stabilization device, simply by holding relatively still fixation for several seconds and more. Fading of objects in the periphery was reported by Troxler (1804) and has been named the *Troxler effect* (reviewed in Pirenne, 1962; Martinez-Conde et al., 2004). The link between the Troxler effect and the fading of stabilized images was made by Clarke, who attributed both phenomena to neural adaptation (Clarke, 1957, 1960, 1961, 1962).

The time course (and completeness) of fading was especially studied in Ganzfeld experiments. A *Ganzfeld* (“full field” in German) is a completely uniform stimulation of the visual field, which can be achieved by covering one or both eyes with a half ping-pong ball.

The results of Ganzfeld experiments show that fading is faster in low-contrast or low-

luminance environments (reviewed in Avant, 1965). Fading also seems to occur faster with long wavelength light (e.g., red) than with short wavelength light (e.g., blue). For example, on average across four subjects, Gur (1989) found that color disappearance time was 162 s for a 460 nm (blue) stimulus but only 22 s for a 620 nm (red) stimulus with equal luminance.

Another fascinating perceptual phenomenon involving image fading is the case of *entoptic images*, originally described by Purkinje (1825, page 115). Entoptic images are perceptual phenomena that arise from objects within the eye, such as the shadows of retinal blood vessels. For example, a light source applied to the *sclera* (the white outer coating of the eye made of tough fibrin connective tissue) through the closed eyelid will, when moved, elicit a striking image created by the shadows of the larger retinal vessels (Coppola and Purves, 1996). Helmholtz (1866) described entoptic images as the best method to achieve image fading:

When the fixation is sharp and steady, differences of light that are often quite marked will fade out in from 10 to 20 seconds. The way this happens is at first by the brighter parts getting darker, and at the same time the darker parts getting brighter. It is striking too to watch here how sometimes a large mass changes into a faded dark spot, or a bright mass into a pale bright spot, as if the objects were painted with diluted colours and these ran together. Incidentally, the experiment is hard to perform in this way on account of the long steady fixation involving much strain. Every time the eye winks or moves ever so little, the image returns. It is much more convenient and satisfactory to use objects that have fixed positions on the retina itself, such as the retinal vessels . . . What is common to all these methods [of making the retinal vessels visible] consists in letting the shadows of the vessels fall in some unusual direction or in trying to prolong the umbrae of the shadows. But in this case it is also necessary to change continuously the direction of the light that casts the shadow, and only those vessels are visible whose shadows are shifted. As soon as the source of

light is kept steady, the ramifications of the vessels disappear in a few seconds by becoming as bright as the rest of the visual field. They vanish more rapidly and more completely than the images of external objects that are hard to focus; and the weaker the illumination, the more quickly they disappear. (...)

Undoubtedly, in the author's opinion, the rapid disappearance of the shadows of the vessels is exactly the same sort of thing as the disappearance of any objective image with moderate differences of luminosity which is steadily focused by the eye, except that in the former case the difficulties of fixation are absent. [1962 edition, Volume II, pages 280–281.]

Several following studies also experimented on the visibility of the entoptic shadows of the retinal blood capillaries (outside the fovea) and the macular pigment (on the fovea) (Campbell and Robson, 1961; Sharpe, 1972; Drysdale, 1975; Applegate et al., 1990). Coppola and Purves (1996) showed that entoptic images of central retinal capillaries could vanish less than 100 ms after cessation of shadow movements (78 ± 8 ms in five subjects). Previously, Riggs and Schick (1968) had argued that early disappearance of entoptic images could be due to their low contrast and blur, and that it would take a bit longer to have a sharper, more contrasted image disappear. However, the contrast of capillary shadows has been estimated to be between 20 and 40%, depending on the size of the light and its wavelength (Applegate et al., 1990). Considering that the average distance between capillaries is about 20 μm , Coppola and Purves (1996) argued that the entoptic capillary shadows would approximate exoptic grating patterns of 10 cycles/degree, for which the contrast threshold in central vision is about 1%. Therefore, the stimuli provided by the capillary shadows were far above threshold in their experiment.

Fade-out vs. blackout

It is worth noting that there has been some confusion between the “fade-out” and “black-out” phenomena (Gur, 1991). *Fade-out* is a progressive disappearance of the visual stimulus which takes place in both monocular and binocular Ganzfelds as well as in stabilized con-

ditions. As reviewed above, fade-out is affected by light intensity and wavelength, among other parameters. *Blackout*, however, is a sudden disappearance of the visual stimulus which occurs only monocularly and is not affected by light intensity and wavelength. Gur (1991) suggested that fading probably occurred at the retinal stage, as a form of ganglion cells fatigue, while blackout would correspond to some central blocking of input, maybe due to binocular rivalry between the stimulated eye and the occluded eye in monocular experiments.

Contrast sensitivity

In stabilized conditions, contrast sensitivity is impaired and visual perception gradually decreases. The question naturally raises of how to quantify the contrast threshold elevation in stabilized vision. Several attempts were made to determine contrast transfer functions in stabilized conditions. Figure 2.10 summarizes the average contrast transfer functions measured by two different labs.

In the 1970's, Koenderink (1972) was the first experimenter to systematically study spatial contrast transfer functions in stabilized vision. Stabilization was achieved using an optical-lever method (described in section 2.1.4). In his experiments, the subject viewed a uniform field and had to report when it had faded away by pressing a switch that caused a bar pattern to appear. The luminance of the pattern remained identical but its spatial frequency was varied from 2 to 10 cycles per degree. Koenderink found a well-defined threshold for the spatial modulation. Above threshold, subjects perceived a bar pattern that suddenly flashed on, and then rapidly faded. Below threshold the visual field remained empty. The resulting plot of threshold modulation was a low-pass curve.

Subsequently, Kelly (1979a) obtained similar results using a different stabilization method based on the DPI eyetracker (described in section 2.1.4). The eye position data were used to continuously move the stimulus pattern—a stationary sinusoidal grating of spatial frequency ranging from 0.2 to 10 cycles/degree—on a CRT screen. In these experiments, image stabilization dramatically elevated the subject contrast threshold, by a

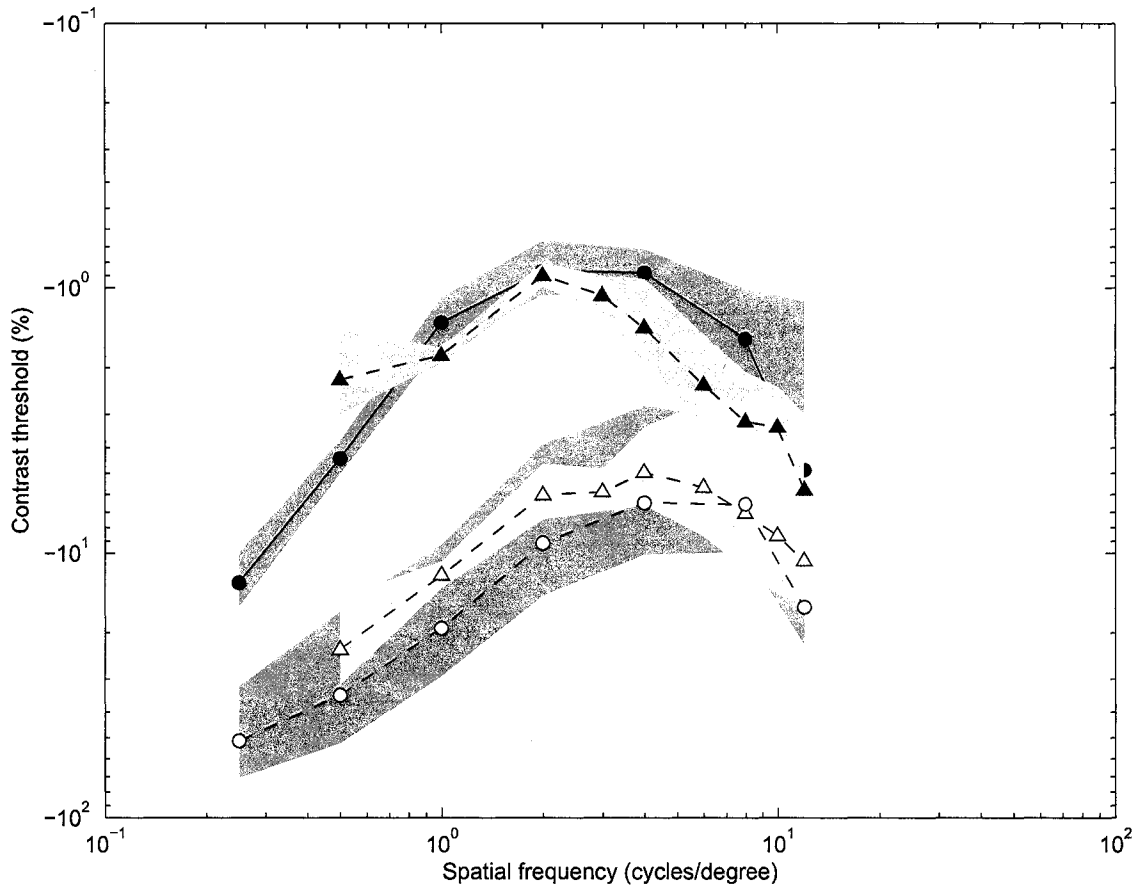


Figure 2.10: Average contrast sensitivity functions obtained in the steady state (after a long period of visual fixation) in Kelly's lab (circles) and Tulunay-Keesey's lab (triangles), plotted on a log-log scale. Kelly's data are means over five datasets, corresponding to the three subjects reported in Kelly (1979a) and the two subjects reported in Burbeck and Kelly (1982). Tulunay-Keesey's data are means over five datasets, corresponding to the two subjects reported in Tulunay-Keesey and Jones (1976) and the three subjects reported in Tulunay-Keesey and Bennis (1979). For each curve, black markers represent stabilized conditions, and white markers represent unstabilized conditions. Grey areas delimit plus and minus one standard deviation around the mean contrast threshold.

factor of about 20. These results, pooled together with those from a subsequent study (Burbeck and Kelly, 1982), are shown in Figure 2·10. Black circles show the average contrast threshold in the stabilized condition, while white circles show the average contrast threshold in the unstabilized condition.

Tulunay-Keesey and Jones (1976) also reported contrast sensitivity functions in stabilized and unstabilized conditions, using their optical-electronic active feedback system (described in section 2.1.4). Image stabilization resulted in a decrease of sensitivity—in a large range of spatial frequencies—only when the target was presented for an indefinite period. That is, for exposure durations ranging from 6 ms to 10 s there was no significant difference between the unstabilized and the stabilized thresholds. Their results obtained in the steady state (after a long period of visual fixation) are shown in Figure 2·10, pooled together with those from a subsequent study (Tulunay-Keesey and Bennis, 1979). Black triangles show the average contrast threshold in the stabilized condition, while white triangles show the average contrast threshold in the unstabilized condition.

Tulunay-Keesey and Jones proposed that the lesser impact of eye movements for short stimulus presentations was probably due to the influence of on-transients in their stimulus presentation. Indeed, Breitmeyer and Julesz (1975) showed that a stimulus presentation having abrupt onsets and offsets, relative to one having gradual onsets and offsets, increased the contrast sensitivity at low spatial frequencies—reinforcing the supposition that transient channels in the visual system (which roughly correspond to the magnocellular pathway) are predominantly tuned to low spatial frequencies (see section 2.2 for more details).

In order to investigate this issue, Tulunay-Keesey and Bennis (1979) designed new experiments in which spatial sinusoidal gratings were presented for longer durations (7.5 s to 10 s) with different temporal envelopes, either gradual (i.e., ramp-like) or sharp (i.e., step-like). As expected, stabilized and unstabilized thresholds were similar in the case of a sharp temporal envelope, but differed by up to 0.3 log unit in the case of a ramp. This last figure is to be considered with caution, however, since Tulunay-Keesey and Bennis

(1979) also showed that stabilized and unstabilized thresholds could be driven close or apart according to the instructions given to the subjects, depending on whether they were allowed to let the image fade to some steady state percept (after 45 s or more) or not. Indeed, allowing for longer periods of fixation magnified the differences between stabilized and unstabilized thresholds. This important finding could explain why Tulunay-Keesey and Bennis (1979) and Tulunay-Keesey and Jones (1980) found less difference between both conditions than Kelly (1979a), who instructed his subjects to wait for the steady state.

This disagreement between Kelly and Tulunay-Keesey was never solved since their respective goals were ultimately different. Tulunay-Keesey's goal was to study stabilization during brief periods comparable with fixation intervals in normal vision, while Kelly advocated steady-state studies arguing that no single presentation envelope could mimic fixational intervals in general (Burbeck and Kelly, 1982).

Color vision

Kelly (1981) investigated chromatic contrast thresholds in similar conditions as achromatic contrast thresholds, using saturated red/green gratings. He obtained a surprising result: in stabilized conditions, saturated chromatic gratings fade out and disappear at 100% contrast. Since he did not control for time, the question remains of how long it took for the stimulus to disappear. In Ganzfeld experiments indeed, color and brightness fade-out are wavelength dependent; as reported above, Gur (1989) found that color disappearance time was 162 s for a 460 nm (blue) stimulus but only 22 s for a 620 nm (red) stimulus with equal luminance.

It is remarkable that so few studies were conducted to investigate the effect of image stabilization on color perception. New experiments are needed to quantify more precisely the time course of fade-out as a function of wavelength, energy, and maybe other parameters such as spatial frequency in the case of grating stimuli. These questions are especially relevant since brain areas involved with processing retinal motion, such as area MT, are

able to signal the direction of motion even for equiluminant color stimuli (reviewed in section 2.2.4).

Motion perception

Kelly (1979b) attempted to quantify the stabilized spatio-temporal threshold surface, which is a generalization of the contrast sensitivity function accounting for retinal velocity as well as spatial fluctuations. He found that, with low velocities in the range of the natural drift motions of the eye (e.g., 0.15 deg/s), the stabilized contrast sensitivity function matched the normal, unstabilized result. At higher velocities, the curve was qualitatively similar but shifted toward lower spatial frequencies. In other words, at low spatial frequencies, the temporal response became nearly independent of spatial frequency, while at low temporal frequencies, the spatial response became independent of temporal frequency. Kelly (1979b) concluded that retinal image motion, especially in the form of the natural drift motions of the eye, was “the *sine qua non* of vision”.

Tulunay-Keesey and VerHoeve (1987) also investigated the role of eye movements in motion detection. A luminous, vertical line was oscillated sinusoidally in the horizontal direction with frequencies varying from 0.5 Hz to 16 Hz, on different backgrounds (blank screen, random dot pattern, or vertical grating). The target bar and the background could be set into motion independently. Results showed that both the absolute value of the threshold and the shape of the motion sensitivity function were affected by both the background and eye movements, particularly over the low temporal frequencies (i.e., below 4 Hz). The main effect of the background—that of increasing motion sensitivity for low frequencies of oscillation—was lost under image stabilization: the visual system detected motion mainly on the basis of velocity regardless of the background. The main effect of eye movements was that of facilitating motion detection, in the case of low frequencies and also when the target moved on a structured background. However, retinal image motion had a detrimental effect when the target moved on a blank background.

More recently, Heidenreich and Turano (1996) studied speed discrimination under sta-

bilized and normal conditions, using a Generation V DPI eyetracker coupled to a stimulus deflector. They estimated the speed discrimination threshold using a two-alternative, forced-choice procedure in which subjects had to report which interval contained the faster moving stimulus as opposed to the reference stimulus. The stimulus was a vertically oriented, 3 cycles/deg sinewave grating subtending a visual angle of 5.6 deg. Heidenreich and Turano found that speed difference thresholds show a general decrease with increasing reference speed, in both stabilized and unstabilized conditions. However, at slow reference speeds ($0.5^\circ/\text{s}$ to $1^\circ/\text{s}$), the stabilized thresholds were significantly higher than the unstabilized thresholds. Further analysis showed that, when plotting these results in terms of retinal image speed instead of distal stimulus speed (by subtracting the average eye drift velocity recorded by the eyetracker), the stabilized thresholds closely matched the normal viewing thresholds. This result suggests that the retinal motion was equally effective, whether it derived from stimulus motion or stimulus motion combined with eye movements.

This might not be true in the particular case of pursuit eye movements. Royden et al. (1992) investigated the perception of heading during pursuit eye movements and found that judgements were more accurate during executed eye movements than simulated eye movements, in the case of eye speeds greater than $1^\circ/\text{s}$, or when there was no horizon serving as a potential cue. They suggested that some extraretinal signal, in the form of an *efferent copy* of the motor command to the eyes or a *proprioceptive signal* from the ocular muscles, may contribute to motion perception under conditions in which motion is ambiguous. However, it should be noted that Royden's experiments were not run in stabilized conditions: subjects were simply asked to fixate a central fixation point while the background was moved according to simulated pursuit eye movements. This procedure may have introduced some artifacts. Heidenreich and Turano's (1996) experiments were better controlled in this respect.

2.1.6 Stabilized vision: Discussion

To summarize, studies that investigated vision under stabilized conditions have shown that images tend to fade over a period of several seconds or minutes in the absence of retinal motion (Ditchburn and Ginsborg, 1952; Riggs and Ratliff, 1952; Riggs et al., 1953; Yarbus, 1967). Although it is still unknown whether perfectly stabilized images disappear completely (Arend and Timberlake, 1986b; Ditchburn, 1987), it is clear that stabilized images tend to fade-out. More precisely, contrast sensitivity is reduced in stabilized conditions with long stimulus presentations, especially at low spatial frequencies (Koenderink, 1972; Kelly, 1979a; Tulunay-Keesey, 1982). However, the precise quantification of the fading phenomenon is still subject to controversies. A number of parameters such as contrast, luminosity, chromaticity, spatial frequency, motion velocity seem to play a role and the time constant can vary from less than 100 ms in the case of low contrast entoptic shadows of retinal vessels (Coppola and Purves, 1996) to several minutes in the cases of high contrast and high luminosity (Kelly, 1979a).

The origins of fading are not clear, either. Some models (described below) suggest that fading is due to some local adaptation process that is also responsible for the formation of “weak” negative afterimages which develop in stabilized conditions at relatively low luminance levels (as opposed to “strong” afterimages due to the bleaching of retinal photopigments). Burbeck and Kelly (1984) proposed an additive model, described below. When an image is stabilized, some local adaptation process occurs which creates a negative afterimage of the stimulus. This afterimage adds to the stimulus itself, contributing to making it fade out and eventually disappear. However, Saleh and Tulunay-Keesey (1986) argued that an additive model could not explain the phenomenon of apparent contrast reversal: When a uniform luminance increment is applied to a stabilized pattern after it has disappeared, the pattern reappears with the reversed phase (Tulunay-Keesey et al., 1987). Hence, Tulunay-Keesey and colleagues proposed successive versions of a multiplicative model for the fading of stabilized images in which the gain, instead of being constant, is inversely proportional to a spatially and temporally filtered version of the stimulus (Saleh

and Tulunay-Keesey, 1986; Tulunay-Keesey et al., 1987; Olson et al., 1993, 1994; Tulunay-Keesey and Olson, 1996). However, neither Burbeck and Kelly's (1984) model nor Saleh and Tulunay-Keesey's (1986) model was defined in neural terms, and it is still unknown which stages of visual processing are responsible for fading.

The fact that vision is so dramatically impaired in stabilized conditions yields to the hypothesis that retinal image motion may be of primary importance at some level of visual processing. The idea is not new; early "dynamic theories" proposed a role for small eye movements given the preponderance of transient neural responses in early vision (Marshall and Talbot, 1942; Arend, 1973). These models later proved to be quantitatively inadequate (Steinman and Levinson, 1990) since they focussed on physiological tremor—the smallest and probably least significant component of eye movements. Nonetheless, the theoretical approach that they advocated could hold for other sorts of movements. The question remains whether the necessary retinal image motion comes from ocular drift and microsaccades, or whether it is simply provided by head and body movements not perfectly compensated for by the vestibulo-ocular reflex (VOR), as suggested by Steinman et al. (1985).

In our laboratory, we hypothesize that fixational instability (whether due to movements of the eyes or the rest of the body) is a crucial component of vision and takes part in the coding of information by neurons in the early visual system. Before presenting this and other theories of neural coding in detail in section 2.4, let us now review the neurophysiological literature regarding early vision and fixational eye movements.

2.2 Brief description of the early visual system

The early visual system is composed of the retina, the dorsal lateral geniculate nucleus (LGN), and the primary visual cortex (V1). Sometimes the definition of the early visual system extends to other cortical areas such as V2, V3, V4, and MT (V5). In this section, we review the current knowledge about some of these areas, from the perspective of their function—along with some basic anatomical facts.

2.2.1 The retina

The following description of human retinal functions is summarized after Oyster (1999, Chapter 14) and Kandel et al. (2000, Chapter 26), unless other references are specified.

The retina is a 200 μm thick layer of cells covering the inside bottom of the eyeball. Light enters the eye through the cornea and passes through the anterior chamber (filled with aqueous humor), the pupil (center of the iris), the lens, the vitreous humor that fills the inside of the ocular globe, and finally lands on the retina. On most regions of the retina, the light has to travel through several layers of neurons before reaching the retinal photoreceptors, located at the outer synaptic layer. However, in the *fovea*, a region of the retina corresponding to the center of the visual field, the cell bodies are shifted to the side so that image distortion is minimized and higher resolution can be achieved.

Most synaptic contacts in the retina are grouped in two plexiform (i.e., “network-like”) layers. The *outer plexiform layer* contains the processes of photoreceptor, bipolar, and horizontal cells, while the *inner plexiform layer* contains the processes of bipolar, amacrine, and ganglion cells. The bipolar cells, having processes in both plexiform layers, bridge between the two. All these cell types are described below.

Photons are absorbed by visual pigments in the *photoreceptors*. There exist two main classes of photoreceptors: *rods* and *cones*. Rods cells are involved with scotopic (dim light) vision, while cone cells are involved with photopic (daylight) vision. In rod cells, the visual pigment is rhodopsin. Various types of cone cells each have a different pigment sensitive to a different color spectrum. Species with three types of cones, such as humans

and Old World primates, are called *trichromats*. It is currently believed that most other mammals are *dichromats* (i.e., have two types of cones), except for sea mammals, which are *monochromats* (only one cone type), and New World monkeys, which show surprising diversity: in most species, males are dichromats and about 60% of females are trichromats, but owl monkeys are all monochromats, and howler monkeys are trichromats.

The three kinds of cones found in humans and Old World primates are sensitive to different wavelengths. L cones are sensitive to “long” wavelengths; their sensitivity curve is centered around 564 nm, which corresponds to red light. Therefore, L cones are sometimes called “red” cones. Similarly, M cones (or “green” cones) are sensitive to “medium” wavelengths centered around 534 nm (green). S cones (or “blue” cones) are sensitive to “small” wavelengths centered around 420 nm (violet). The lens and cornea of the human eye absorb smaller wavelengths, which sets the lower wavelength limit of human-visible light to approximately 380 nm (near “ultraviolet”). Unlike L and M cones, S cones are morphologically distinct and spatially form an independent and nonrandom arrangement across the retina (Dacey, 2000). S cones are absent from the *foveola*, the central region of the fovea (De Valois, 2004). Rods are also absent from the fovea.

In the present review, we focus on *photopic vision*, conveyed by cones only, as opposed to *scotopic vision* (i.e., in dim light, such as moonlight) and *mesopic vision* (intermediate between photopic and scotopic), which involve rods.

A photoreceptor’s signal is proportional to the number of photons that it caught. Differences in signal between neighboring photoreceptors are emphasized by lateral interactions mediated by *horizontal cells*, which project back to the photoreceptors. Horizontal-to-photoreceptor feedback, opposite in sign to the photoreceptor signals, enables contrast enhancement at the photoreceptor level. Photoreceptor signals are then divided into multiple, parallel streams of information conveyed by *bipolar cells*.

Signals reporting increasing and decreasing light intensity are conveyed by separate ON and OFF pathways, starting with ON and OFF bipolar cells. Absorption of light by a cone photoreceptor leads to a decrease in the rate of glutamate release from the cone

terminal, and this change is monitored by several ON and OFF bipolar cells. ON bipolar cells depolarize when light intensity increases, while OFF bipolar cells depolarize when light intensity decreases. The ON and OFF pathways each contain several types of bipolar cells. *Midget bipolar cells* receive inputs from either red (L) or green (M) cones. Hence, there are four types of midget bipolar cells: red-ON, red-OFF, green-ON, and green-OFF. In the central fovea, a midget bipolar cell receives direct input from just one cone. *Diffuse bipolar cells* always receive input from both red and green cones, and they may have some blue cone input as well. The signal from each red or green cone is divided eight times; each cone provides inputs to two midget bipolar cells and six diffuse bipolar cells. Another class of RGCs, *blue cone bipolar cells*, receive input only from blue cones—but always from several of them. Different types of bipolar cells terminate at different levels within the inner plexiform layer, thereby creating functional sublayers.

Information between different streams is then exchanged and compared by *amacrine cells*. These interactions can be made over short (local) to long distances. There exist 25 to 30 anatomically distinct types of amacrine cells in the human retina, using a variety of neurotransmitters, but it is not clear to what extent their functions differ. More generally, the operations of amacrine cells are still poorly understood.

Horizontal, bipolar, and amacrine cells do not generate action potentials (or spikes). Instead, they convey information through the variations in their membrane potential. *Retinal ganglion cells (RGCs)* are the only spiking neurons in the retina, and as such, the first spiking neurons in the visual pathway. While photoreceptors can only signal the amount of photons they received, RGCs are able to signal how light is distributed through space and time. Different types of RGCs convey different types of information. 80% of RGCs are midget or parasol cells. *Midget retinal ganglion cells* receive input from midget bipolar cells. *Parasol retinal ganglion cells* probably receive input from diffuse bipolar cells. ON-center (midget or parasol) RGCs receive input from ON bipolar cells, while OFF-center RGCs receive input from OFF bipolar cells. Another type of RGC, the *bistratified ganglion cells*, constitute 10% of RGCs. Bistratified ganglion cells have dendrites ramifying in both

the ON and OFF layers (hence their name, bistratified), and thus probably receive both ON and OFF inputs. The remaining 10% of RGCs in humans are of 19 or more other types. We will not describe them in this review.

All retinal neurons, including photoreceptors, are only sensitive to light coming from a small region of the world, called their *receptive field* (RF). Charles Sherrington (1906) originally defined the receptive field of a neuron as the region of visual space in which the presence of a stimulus will alter the firing of that neuron. The influence can be positive (+), leading to an increase in firing, or negative (-), leading to a decrease in firing. Another, related way to define the receptive field is as the region of the retina that corresponds in location and angular size to the receptive field in visual space defined above. The traditional way to “map” the receptive field of a cell consists in recording the cell’s response to small light (ON) or dark (OFF) spots flashed at different locations in space.

Bipolar cells and retinal ganglion cells have center-surround receptive fields: a central circular area induces a response of a given polarity (*e.g.*, +) and a concentric, surrounding annular region called *antagonistic surround* induces a response of the opposite polarity (*e.g.*, -). Hence, there exist two different types of center-surround receptive fields: ON-center-OFF-surround (also called ON-center), and OFF-center-ON-surround (also called OFF-center). This spatial structure explains how ganglion cells are sensitive to *contrast*, *i.e.*, the difference in light intensity between the center and surround of their receptive field, rather than to the average light intensity. The origin of the antagonistic surround remains unclear: it could be generated by horizontal cell interactions that become a feature of the bipolar cell signals, or it could be a result of amacrine cell interactions in the inner plexiform layer. The spatial profile of center-surround receptive fields is usually modeled by a Difference-Of-Gaussians (DOG), in which the sensitivity profiles of the center and surround mechanisms are fitted by Gaussian functions of different amplitudes and widths.

The size of a ganglion cell’s receptive field center is closely related to the diameter of its dendritic field. Along the edge of the fovea, dendritic fields of midget ganglion cells are about 10 μm or less in diameter (which corresponds to about $2'$ of visual angle), while the

dendritic fields of parasol cells are three to four times larger. Dendritic field sizes for both types of cells increase with distance (eccentricity) from the fovea. In peripheral retina, they are about 100 μm in diameter (20' of visual angle) for midget ganglion cells and about 300 μm in diameter (1° of visual angle) for parasol cells. Because of the antagonistic surround, the total receptive field is larger than the dendritic field. Strong surround antagonism extends over a region about twice the diameter of the receptive field center. Parasol cells probably have weaker but more extensive surround antagonism, yielding to less contrast enhancement than in midget ganglion cells.

Some types of ganglion cells respond to changes in the spectral component of light. These cells are called *color sensitive*. Bistratified ganglion cells respond to light that becomes increasingly blue (blue-ON) or decreasingly yellow (yellow-OFF), where yellow is the additive combination of red cone and green cone signals. As such, bistratified ganglion cells are a good example of *color opponent* cells without center-surround organization. While midget ganglion cells in peripheral retina are known to lack color opponency, those in central retina have some wavelength information embedded in their signals: they receive input from a single bipolar cell and therefore have a strong excitatory drive from just one cone type. Whether their surround is driven by one or several cone types is still controversial. In other words, it is still unclear whether midget RGCs in central retina exhibit color opponency (Oyster, 1999, Chapter 14).

Parasol cells do not exhibit selectivity for stimulus chromaticity. Nevertheless, the majority of parasol cells can signal chromatic (red/green) contrast by responding to spatial borders defined by red/green contrast, and by responding to temporal changes between red and green. Besides, the red/green luminance balance point—the contrast for which red and green phases of a stimulus elicit responses of equal magnitude—varies across the population of parasol cells. Thus, even at equiluminance, parasol cells as a population can never be truly silenced by heterochromatic stimuli (reviewed in Dobkins and Albright, 2004).

Because a cell's response also depends on the timing of the stimulus, the definition of a receptive field has been generalized from 'space only' to 'space and time'. The *spa-*

spatiotemporal receptive field (STRF) of a cell is a 3D construct consisting of the 2D spatial receptive field as defined above measured at several successive time frames, for a duration corresponding to the neuron's temporal sensitivity window. For example, if a neuron's firing is determined by past events up to 300 ms before the spike occurs, its spatiotemporal receptive field may consist of 30 frames (measured every 10 ms) corresponding to its spatial receptive field at each of these times, from -300 ms to -10 ms. Another way to interpret the STRF is as the "preferred" spatiotemporal stimulus of the neuron, i.e., the stimulus that induces the most activity in the neuron. Yet another way to see it is as a filter through which the ganglion cell perceives the world. This analogy allows to use system identification methods such as reverse correlation (de Boer and Kuyper, 1968; Marmarelis and Marmarelis, 1978) to find the spatiotemporal filter that best describes the STRF. This approach also allows to replicate or predict the output of a cell, given its input and its filter characteristics. For example, the activity of a neuron in the early visual system can be modeled as the temporal convolution of its STRF and its spatiotemporal input (i.e., the "movie" shown in its spatial receptive field). In Chapter 4, we use this method to simulate the activity of retinal ganglion cells when viewing natural images in the presence of eye movements.

Different types of neurons have different temporal properties. Photoreceptors, horizontal cells, and bipolar cells respond to visual stimuli with *sustained* hyperpolarizations or depolarizations. Ganglion cells, however, can have either sustained responses, or *transient* bursts of activity. In primate retina, parasol cells have transient response properties, while midget cells are more sustained. These two types of cells encode different properties of the stimulus. Cells with sustained responses signal the magnitude of an intensity change in the portion of the visual field covered by their receptive field. The larger the change (brightening for ON cells, dimming for OFF cells), the greater the response. Transient cells, on the other hand, report the rate at which light intensity changes, independent of the magnitude of the change. In other words, signals from transient cells reflect the time derivative of their contrast sensitivity function.

The axons of the RGCs form the *optic nerve*. Both optic nerves merge at the *optic chiasm*, where the axons from the nasal half of each retina cross to the opposite side of the brain, while the axons from the temporal hemiretinas do not cross. Thus, the optic chiasm fibers from both retinas are bundled in the left and right optic tracts, such that the axons from the left half of each retina—which carry a complete representation of the right hemifield of vision—project in the left optic tract.

The optic tracts project to three main subcortical targets: the two lateral geniculate nuclei (LGN) of the thalamus, the two superior colliculi (in the dorsal part of the midbrain, called tectum), and the pretectum. The LGN is the main gate for input to the visual cortex; it is described below in further details. The superior colliculus is involved in the control of saccadic eye movements. The pretectum is an area of the midbrain that controls pupillary reflexes.

2.2.2 The lateral geniculate nucleus (LGN)

The two dorsal lateral geniculate nuclei (LGN), one in each thalamus, relay information from the retina to the visual cortex. In humans and monkeys, they are made of 6 main layers (numbered 1–6), intercalated with 6 thinner *koniocellular (K) layers* (numbered K1–K6). To a first approximation, layers 2, 3, 5 and K2, K3, K5 receive inputs from the ipsilateral eye, while layers 1, 4, 6 and K1, K4, K6 receive contralateral inputs. However, at least in macaques, gibbons, chimpanzees—and presumably humans—layer K2 is split into tiers innervated separately by the ipsilateral and contralateral retinae (Hendry and Reid, 2000). Layers 1 and 2 at the bottom of the nucleus contain relatively large cells and are called the *magnocellular (M) layers*. Layers 3–6 contain smaller cells and thus are called *parvocellular (P) layers*. Layer K1, ventral to layer 1, is by far the largest of the koniocellular layers (Hendry and Reid, 2000).

Parvocellular layers receive input from midget retinal ganglion cells. Lesion studies showed that they are involved with color vision and high spatial frequency (i.e., high acuity) vision. They respond mostly to high contrast stimuli.

Magnocellular layers receive input from parasol retinal ganglion cells. They are involved with motion processing and rapid scene identification (Shapley, 1990; Merigan and Maunsell, 1993; Bullier and Nowak, 1995). They are insensitive to color, but respond to lower luminance contrast than P cells.

The input to koniocellular layers is heterogeneous; K layers appear as an amalgam of cells with different properties, and arguably different functions (Hendry and Reid, 2000). K cells have very small somata, resembling grains of sand; hence their name (in Greek, *konio* means sand or dust). K cells are not restricted to K layers; they are also found in M layers and, more frequently, P layers. Layers K3 and K4 receive input from bistratified (or blue-ON-yellow-OFF) ganglion cells, and project to the Cytochrome-Oxidase (CO) *blobs* in V1 (see next section). Therefore, they carry information from S cones and are probably involved with color vision. Layers K1 and K2 are the only regions of the primate LGN innervated by the superior colliculus, and thus might be involved with the reflexive control of eye movements or other functions of the superior colliculus. Layers K5 and K6 relay low-acuity visual information to layer I in primary visual cortex (see next section). Layers K1, K2, K5 and K6 have broad-band responses to visual stimuli, and some cells in K5 and K6 have very large receptive fields compared to M and P cells at the same eccentricity.

ON- and OFF-pathways are propagated from the retina to the LGN. Most retinal receptive field properties are preserved in each layer of the LGN, such as center/surround organization, receptive fields shape (quasi-circular in primates) and size, etc. However, physiological properties of K cells vary much more than those of M and P cells.

Since many LGN studies have been conducted in the cat (including modeling studies from our group), it is worth noting that the P, M, and K pathways in primates are roughly homologous to the X, Y, and W pathways described in cats, although a number of differences exist.

Tonic vs. bursting modes

Thalamic relay cells are known to fire in two possible modes that affect the nature of retinogeniculate transmission: the *tonic* and *burst* modes (reviewed in Sherman, 1996, Sherman and Guillery, 1996, and Sherman and Guillery, 2004). These two modes have also been reported in other brain areas, such as the hippocampus, the cerebellum, and sensory areas in the neocortex (Krahe and Gabbiani, 2004). The tonic mode corresponds to the default mode in which the cell is relatively depolarized. In this mode, an activating input produces a steady stream of unitary action potentials representing tonic firing. In the burst mode, voltage-dependent T-type Ca^{2+} channels get de-inactivated and thus primed for action. Deactivation of the T-channels occurs when the cell has been relatively hyperpolarized for more than 100 ms. The T-channels can then become activated if the cell becomes sufficiently depolarized, e.g., by an excitatory post-synaptic potential. In this case, Ca^{2+} flows into the cell, causing one or more low-threshold spikes occur, separated by 6 ms or less, for up to 100 ms. To summarize, in the burst mode, T-channels are primed by prolonged hyperpolarization, but the Ca^{2+} spikes occur only when triggered by a depolarizing input (reviewed in Perez-Reyes, 2003).

The burst mode occurs most frequently in the form of large-scale synchronized rhythmic activity in the thalamus during slow wave sleep, where cells burst rhythmically at 7–14 Hz. However, in the fully awake animal, thalamic relay cells also show some irregular bursting that is interspersed in tonic activity. In the awake animal, burst spikes comprise 1 to 5% of the total number of spikes.

The possible functions of LGN bursts, and their relevance to vision, are still largely unknown. In the current view, tonic firing provides better signal discrimination, whereas burst firing may improve target detection by increasing the signal-to-noise ratio of neuronal responses (reviewed in Sherman, 1996). Indeed, presynaptic spike bursts can improve the reliability of information transmission across unreliable synapses (reviewed in Lisman, 1997, and Krahe and Gabbiani, 2004). Bursts may also be involved in the detection of specific, behaviorally important events (reviewed in Krahe and Gabbiani, 2004). Bursts outperform

tonic spikes in indicating the occurrence of certain sensory signals (Guido et al., 1995). In the LGN of alert cats, visually evoked bursts occur primarily at the onset of fixation, when the stimulus affects the cell's receptive field for the first time (Guido and Weyand, 1995). In alert macaques, Martinez-Conde et al. (2002) reported that LGN "bursts" correlated more closely than isolated spikes with preceding microsaccades; however, their definition of a "burst" did not match that of Ca^{2+} bursts (see section 2.3). More recent studies have shown that bursts and single spikes in the LGN are triggered by roughly similar visual features, but with some significant differences: Compared to tonic spikes, burst spikes occur with a shorter latency between stimulus and response, have a greater dependence on stimuli with transitions from suppressive to preferred states, and prefer stimuli that provide increased drive to the receptive field center and even greater increased drive to the receptive field surround (reviewed in Alitto and Usrey, 2005).

Control of bursting in the thalamus may have a cortical origin. Sillito and colleagues showed that changes in the strength of corticothalamic feedback can cause shifts in burst probability of thalamic relay cells (reviewed in Sillito and Jones, 2002). The interplay of tonic and bursting modes could represent modulations in the level of vigilance or attention.

If bursts are involved in sensory coding, another question is whether they should be considered as unitary events or whether their internal temporal structure carries additional information (Krahe and Gabbiani, 2004). To our knowledge, this question has never been addressed in the LGN.

To summarize, the LGN is believed to be involved in the dynamic control of the amount and nature of information relayed to cortex (see Casagrande and Norton, 1991, and Sherman and Guillery, 2004, for reviews).

2.2.3 The primary visual cortex (V1)

[Unless otherwise specified, the facts presented in this section are cited from Kandel et al. (2000, Chapter 27).]

The *primary visual cortex* (V1), or striate cortex, corresponds to Brodmann's area 17.

The primary visual cortex in each hemisphere receives information exclusively from the contralateral half of the visual field. In humans and other primates, V1 consists of 6 layers. The principal input from the LGN projects mainly to layer 4, which is further subdivided into 4 sublayers (or sublaminae): 4A, 4B, 4C α and 4C β . Sublayer 4C α receives input primarily from the magnocellular layers of the LGN, while sublayer 4C β receives input mainly from the parvocellular layers. Layers 1–3 receive input from koniocellular layers.

Simple and complex cells

In their seminal contribution to the neurophysiological study of the visual cortex, Hubel and Wiesel (1962) reported that neurons in the input layers of cat V1 had elongated receptive fields, and were more responsive to bars of light of a specific size and orientation than to small spots of light. In Hubel and Wiesel's (1962) original classification, cells passing certain (qualitative) tests were labeled “simple”, while all other cells were called “complex”. More precisely, the receptive fields of simple cells had to satisfy the following four properties: (1) having spatially segregated ON and OFF subregions; (2) exhibiting spatial summation within each region; (3) having antagonistic ON and OFF regions; and (4) the arrangement of these excitatory and inhibitory subregions allowed to predict the neuron's response to any stimulus. In complex cells, the ON and OFF regions overlapped. This classic definition is still considered the most appropriate to classify simple and complex cells. Later, more quantitative metrics were defined (see Hirsch and Martinez, 2006, for a review). First, the *overlap index* measures the spatial separation or overlap between ON and OFF subregions; it is positive when subregions are cospatial, and negative for separated subregions. The distribution of the overlap index is clearly bimodal, being zero or less for simple cells, and significantly positive for complex cells. Second, the *push-pull index* measures the balance of antagonistic responses to stimuli of the opposite contrast within individual subregions, defined as $|P + N|$ where P and N represent synaptic responses to bright and dark stimuli, respectively. The push-pull index is also bimodally distributed; it is around 0 for push-pull (simple) cells, and between 1 and 2 for push-push or pull-pull (complex) cells.

In the context of linear system theory, many investigators started to classify cells based on their spatial linearity (e.g., Movshon et al., 1978a,b; and many more, reviewed in Skottun et al., 1991). Linear neural responses seemed to be restricted to cells whose receptive fields had separate ON and OFF subregions, i.e., simple cells. Therefore, a new definition of simple cells involved the condition of linearity of spatial summation within the receptive field. A convenient measure of linearity was the *relative modulation*, defined as the ratio F_1/F_0 between the amplitude of the first harmonic of the response (F_1) and the mean firing rate (F_0), when the cells were stimulated by drifting gratings. Cells with a small relative modulation were labeled simple cells, while cells with a high relative modulation were considered complex cells. The relative modulation seemed all the more appropriate that it was bimodally distributed over the V1 population, as if supporting the dichotomy between simple and complex cells (Skottun et al., 1991). However, it was later shown that the bimodal distribution of relative modulations in V1 cells was an artifact due to the rectification nonlinearity of spike generation (Mechler and Ringach, 2002). This rectification nonlinearity is further discussed in the description of our neural model in Chapter 4. If the relative modulation is computed from the subthreshold membrane potential instead of the firing rate, it is uniformly distributed—but highly skewed towards complex cells (Priebe et al., 2004).

However, it should not be concluded from Priebe et al. (2004) that there is no distinction between simple and complex cells. The F_1/F_0 ratio, whether computed with subthreshold membrane potentials or with firing rates, is not a good indicator, because linearity is actually not the right criterion to distinguish simple from complex cells (as reviewed in Hirsch and Martinez, 2006). Some cells with complex receptive fields have linear responses (Mechler and Ringach, 2002). Besides, although earlier studies found a correlation between subregion overlap and linearity (reviewed in Skottun et al., 1991), a recent study in awake macaque concluded that the relative modulation was not correlated with subregion overlap (Kagan et al., 2002). When using the overlap index and push-pull index instead, there is a clear dichotomy between simple and complex cells. In an elegant study of cat LGN and V1

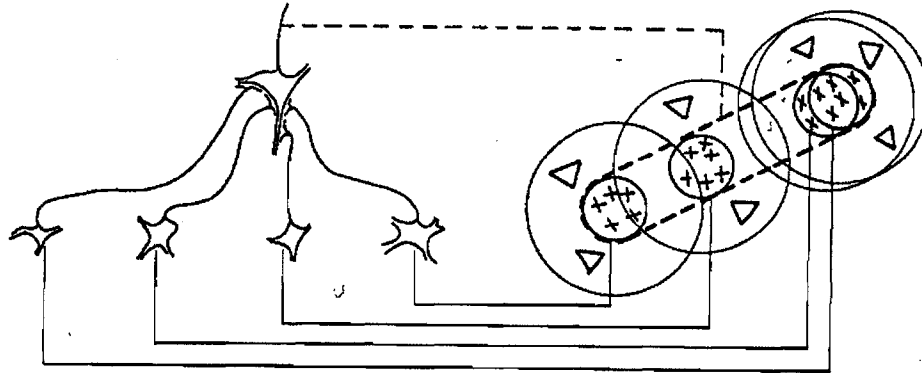


Figure 2.11: “Possible scheme for explaining the organization of simple receptive fields. A large number of lateral geniculate cells, of which four are illustrated in the upper right in the figure, have receptive fields with ‘on’ centers arranged along a straight line on the retina. All of these project upon a single cortical cell, and the synapses are supposed to be excitatory. The receptive field of the cortical cell will then have an elongated ‘on’ center indicated by the interrupted lines in the receptive-field diagram to the left of the figure.” (from Hubel and Wiesel, 1962)

combining *in vivo* intracellular recording with anatomy, Martinez et al. (2005) found that simple cells were exclusively located in layer 4 and upper layer 6, while complex cells were distributed in all layers. These results support the original Hubel and Wiesel proposal that simple cells are an exclusive feature of an earlier stage of visual processing, while complex cells belong to different neural circuits.

According to the well-known mechanistic model proposed by Hubel and Wiesel (1962), the receptive field of a simple cell gets its properties (location, size, and orientation selectivity) from the LGN cells that project to it. Each simple cell samples a specific subset of LGN cells whose center-surround receptive fields are aligned, so that the resulting simple cell receptive field consists of an elongated region flanked by one or more elongated regions of alternating polarities (excitatory/inhibitory), meaning that simple cells have excitatory and inhibitory regions in their receptive fields.

V1 topography

V1 has a topographic organization, comprising orientation columns, ocular dominance columns, and cytochrom-oxidase (CO) blobs.

Each *orientation column* is 30 to 100 μm wide and 2 mm deep, and contains neurons (simple and complex cells) with overlapping receptive fields and the same preferred orientation (as defined above).

Ocular dominance columns represent an arrangement of cells that receive inputs from both eyes with different weights. Binocular cells receive input from both eyes, monocular cells receive input from only one eye, and many cells are in-between, having one dominant input eye but still receiving input from the other eye.

A *hypercolumn* comprised two ocular dominance columns and a complete set of orientation columns, such that all possible orientations are represented for a given location in the visual field. In a hypercolumn, orientation columns are organized in a *pinwheel* fashion, such that adjacent columns have preferred orientations that are only slightly shifted from each other.

Overlapping these columnar systems is another system, composed of peg-shaped patches strongly tainted by cytochrome oxidase (CO) in *ex vivo* preparations, especially in layers 2–3. These regions have been called either *patches* (Horton and Hubel, 1981), or *CO blobs* (Livingstone and Hubel, 1984). They lie centered along ocular dominance columns, to which their long axes are parallel. The neurons within the blobs are not tuned to orientation. Since pinwheel centers of orientation columns are also weakly tuned to orientation, Horton and Hedley-Whyte (1984) hypothesized that blobs are aligned with the pinwheel centers. While Bartfeld and Grinvald (1992) and Maldonado et al. (1997), using optical imaging, argued that blobs and pinwheel centers are not aligned, the spatial resolution of their method was insufficient to accurately locate pinwheel centers and, therefore, the earlier hypothesis that CO blobs and pinwheel centers are coterminous remains the only hypothesis currently supported by reliable observation (Polimeni et al., 2005a). Neurons in the blobs are particularly sensitive to color, and their receptive fields have no orientation,

like those in the retina and LGN. Blobs come in two varieties: blue-yellow and red-green. Blobs in which neurons display a blue-yellow antagonism receive input from layers K3 and K4 in the LGN, while red-green blobs receive input from displaced K cell populations in parvocellular layers 3 and 4 in the LGN (Hendry and Reid, 2000).

2.2.4 Visual area MT

Although not part of the early visual system, area MT is relevant to our study because of its sensitivity to retinal motion, including that due to fixational eye movements.

[The following section is summarized from Britten’s (2004) review, unless otherwise specified.]

Area MT (also called V5) is a small region of primate cortex. Its name, MT, for “medial temporal”, originates from its anatomical location in the owl monkey (a New World primate), although in macaque, area MT is actually located between the occipital and parietal lobes. As reviewed in Born and Bradley (2005), MT receives direct input from V1 (mostly from cells in layer 4B receiving magnocellular input from layer 4C α), the thick CO stripes in V2, V3, the pulvinar complex, but also from LGN koniocellular neurons (Sincich et al., 2004).

MT is part of the *dorsal pathway* of the visual system, which starts with the magnocellular pathway described above. The dorsal pathway is traditionally believed to be involved with processing fast, low-contrast, low-spatial-frequencies visual input, as opposed to the *ventral pathway* involved with high-contrast, detailed, color vision. The ventral pathway is sometimes called the “What” pathway, and the dorsal pathway the “Where” pathway, although it is now understood that these distinctions are too simplistic. Indeed, MT also receives some input from the parvocellular and koniocellular pathways, and MT cells are capable of detecting motion in isoluminant color stimuli, as reviewed below.

MT is organized anatomically as a retinotopic map of the contralateral visual space. MT also displays a columnar organization with respect to direction and disparity. Most MT neurons are directionally selective, meaning that each neuron responds mostly for stimuli

moving in its preferred direction.

Receptive fields of MT cells are large, with diameters about 10 times the diameter of a V1 receptive field at the same eccentricity. However, preferred spatial frequencies of MT cells are comparable to those of V1 cells. About half of MT cells possess antagonistic surrounds, which exert a profound modulatory effect on the response to stimulation in the RF center. The modulation is typically directional and maximally suppresses the response when motion is in the preferred direction. Sometimes, surround stimulation in the anti-preferred direction even facilitates center responses. Antagonistic surrounds are believed to be involved in the segregation of moving objects from their backgrounds (Born et al., 2000).

MT cells have interesting temporal properties. Latencies in MT can be quite short, but span a wide range of values, with a minimum latency of 30 or 35 ms, and a median latency of 90 ms. MT cells are also very sensitive to high temporal frequencies, peaking in the 3–10 Hz range, with cutoff frequencies around 30 or 50 Hz. MT cells show profound adaptation to sustained input. A sudden onset of motion induces an initial transient response typically twice as large as the following sustained response. This initial transient is informative about the acceleration of a moving target and may be useful in guiding pursuit eye movements.

MT cells may also be bandpass tuned for the speed of the stimulus, although this issue is complex and not fully understood. Speed tuning seems to exist only at high stimulus contrast (Liu and Newsome, 2005; Pack et al., 2005, 2006). In any case, preferred speeds in MT cells seem substantially higher than preferred speeds in V1 at comparable eccentricities. The question remains open whether MT inherits its speed tuning from a subset of selected V1 (or V2 or V3) afferents, or performs additional computation.

Several studies have investigated the dual phenomena of motion integration and segregation in MT. Motion integration is complicated by the fact that any local motion detector, such as a cell with a limited receptive field, can measure only the component of motion perpendicular to the local contour seen through that aperture. This *aperture problem* was studied in MT by using *plaid* stimuli consisting of the sum of two sine-wave gratings moving

in different directions. Perceptually, a plaid stimulus often appears as a coherent, single *pattern* which looks like a blurred checkerboard moving in a direction intermediate between the two directions of the *component* gratings. In anesthetized macaques, Movshon et al. (1985) reported that 25% of MT cells responded to the *pattern* motion, 40% responded to the two *component* motions, and the remaining 35% could not be classified, supposedly because of their very broad tuning curves. However, in awake macaques viewing a moving field of small bars, Pack and Born (2001) found that the responses of MT cells changed in time, from bar-orientation-sensitive in the first 60 ms after stimulus onset, to motion-component-sensitive 70–120 ms after stimulus onset, to pattern-sensitive afterwards. This result, although not reproducible in isoflurane-anesthetized monkeys in which most cells remained motion-component sensitive (Pack et al., 2001; Movshon et al., 2003), was later confirmed in Movshon’s lab in opiate-anesthetized macaques presented with plaids: MT population response was initially dominated by component motion signals, and represented pattern motion only 50–75 ms later (Smith et al., 2005).

MT also encodes stereoscopic depth: MT cells are independently tuned for 2D motion and for the depth plane of the stimulus. MT contains an orderly topographic representation for stereo depth, in the form of a “fractured” map: regions of stereo-tuned neurons are interspersed with larger regions where the tuning is weak. There is no relationship between the maps for disparity and the maps for preferred direction (Britten, 2004), and MT neurons are not tuned for motion through 3D space (Born and Bradley, 2005).

While not directly color-selective, MT neurons are able to use information about object color to encode direction of motion (reviewed in Dobkins and Albright, 2004). They are able to signal the direction of moving equiluminant red/green and blue/yellow gratings, although their responses are significantly weaker than for moving luminance gratings. In addition to using chromatic contrast as a cue for motion *correspondence*, MT cells can also use chromatic information for the *integration vs. segmentation* of motion signals in color plaid stimuli made of two component red/green gratings. If the plaid is symmetric (e.g., made of two red-bright/green-dark gratings), MT cells respond to coherent pattern

motion, consistent with perception; however, if the plaid is asymmetric (e.g., made of one red-bright/green-dark and one red-dark/green-bright gratings), MT cells respond to the component motions, again following perception. Finally, chromatic information can be used in some MT cells to improve their performance in a motion discrimination task, when the signal and noise dots were of different colors.

MT receives some extraretinal signals conveying information about eye position and saccadic eye movements, but these effects are modest compared to those in areas above MT, such as MST (Medial Superior Temporal cortex) and LIP (Lateral Intraparietal cortex). There appears to be a general trend in ascending the hierarchy of visual areas, at least in the dorsal stream, for such extraretinal influences to become increasingly powerful (Born and Bradley, 2005).

MT signals play a role in initiating and guiding pursuit eye movements (reviewed in Lisberger et al., 1987). However, if the target is stabilized on the retina, the MT responses disappear (Newsome et al., 1988), suggesting that MT responds to retinal motion itself rather than to extraretinal signals—unlike MST.

2.3 Influence of eye movements on the early visual system

Since the 1990's, extracellular recordings in the brains of alert monkeys have become a routine. Without anesthesia or paralysis, these animals are constantly moving their eyes. Even though monkeys can be trained to maintain steady fixation for long periods of time, fixational eye movements are unavoidable and have usually been regarded as a nuisance as they contribute to the variability of cortical responses (Gur and Snodderly, 1987; Gur et al., 1997, 2005). However, several attempts were made to consider eye movements as an integral part of the experimental design (e.g., Livingstone et al., 1996), and some neurophysiological investigations have focused on studying the effects of these eye movements *per se* (e.g., Gur and Snodderly, 1997; Bair and O'Keefe, 1998; Snodderly et al., 2001).

2.3.1 Modulation by saccades (“Saccadic suppression” and other effects)

The idea that visual perception is suppressed around the time of saccades dates back to the nineteenth century (Erdmann and Dodge, 1898). For a long time it was believed that visual sensitivity is actually reduced during saccades, and this phenomenon was called “saccadic suppression”, although evidence for suppression by saccades was contradictory (reviewed in Ross et al., 2001; Burr and Morrone, 2004). In fact, not all visual functions are suppressed during saccades. Some intrasaccadic perception has been shown to exist in particular experimental conditions (Garcia-Perez and Peli, 2001), and it has been suggested that the apparent loss of perception during saccades is due to visual masking by presaccadic and postsaccadic perception (Campbell and Wurtz, 1978; Corfield et al., 1978). In the current consensus (Ross et al., 2001), saccades trigger two distinct neural processes. First, sensitivity to low spatial frequencies and motion sensitivity are reduced, which suggests that the magnocellular pathway is probably involved (Burr et al., 1994). Second, a gross perceptual distortion of visual space occurs in anticipation of the repositioning of gaze; for example, the perceived position of a flashed target is systematically mislocalized in certain conditions. However, while human psychophysical data clearly suggest an extra-retinal suppression of early (magnocellular) visual activity during saccades, direct physiological evidence is less clear. Saccadic suppression is probably due to a central *corollary discharge* signal (von Holst and Mittelstaedt, 1950) of the oculomotor command, as detailed below.

Saccadic eye movements can modulate visual responses in the LGN, independently of the change in visual input caused by the saccade, as shown by the studies presented below. The origin of this extraretinal signal probably lies in the projection from the brainstem to the thalamus, because this projection is activated when primates make saccades and can modify the temporal properties of LGN relay neurons, and because stimulation of this ascending pathway has been shown to alter the properties of the retinogeniculate synapse, as reviewed in Reppas et al. (2002).

In the LGN of awake cats, Lee and Malpeli (1998) reported a *postsaccadic enhancement* of neural activity, as well as a reduction of response latency by saccades. This postsaccadic

facilitation was substantially stronger in X cells than in Y cells, and was identical in the presence and absence of visual stimulation, i.e., whether the animal was in the dark or was shown large, uniform flashes at various times during and after guided saccades. Besides, in the dark condition, the authors found a suppression of activity starting 200–300 ms before saccade start, peaking 100 ms before saccade start, and smoothly reverting to facilitation by the end of the saccade. This *presaccadic suppression* was similar in X and Y cells. However, the authors “did not see a reason to invoke [perceptual saccadic suppression] as an explanation for the saccade-related gain changes” that they observed.

In the LGN of alert macaques, several experiments were conducted to highlight extraretinal effects of saccades, by presenting spatially uniform (full-field) stimuli that either flickered regularly at 8 Hz (Ramcharan et al., 2001), or were randomly modulated by a temporal white-noise sequence every 7.7 ms (Reppas et al., 2002). In both studies, the monkeys had to perform guided saccades between targets separated by 10° (Ramcharan et al., 2001), 3°, or 12° (Reppas et al., 2002).

In a short study involving a small number of recordings, Ramcharan et al. (2001) found that some M neurons (5/10 cells) showed enhancement during or shortly after a 10° guided saccade—which contradicts the “saccadic suppression” hypothesis. For both M and P neurons, Ca²⁺ bursting was significantly less frequent during and shortly after saccades, suggesting that saccades might contribute to depolarizing LGN neurons.

In a more thorough study, Reppas et al. (2002) found that 90% of magnocellular neurons (42/47 cells) and 21% of parvocellular neurons (5/24 cells) showed a consistent response change around the time of a 12° saccade: weak suppression (starting at or even before the saccade onset), followed by strong enhancement. Furthermore, an analysis of microsaccades and corrective saccades appearing in some trials (with an average amplitude of 1.24°) revealed virtually the same response modulation in M neurons for these small saccades as for the 12° saccades. In magnocellular neurons, saccades also altered the entire temporal profile of the visual responses: visual responses became slightly faster and more transient following a saccade. This finding closely parallels the effects of eye movements on the

perceptual impulse response (Ikeda, 1986); the later phases accelerate significantly soon after saccades, while the early parts show only minimal changes (Burr and Morrone, 1996).

Reppas et al. (2002) also reported saccadic enhancement in more parvocellular neurons when probed with cone-isolating stimuli. The effect was seen in 75% of ON-center neurons ($n = 12/16$), but not in OFF-center neurons ($n = 0/9$). The authors concluded that saccadic modulation is not a fixed physiological property, but depends on the visual stimulus. Their finding underlines the strong dynamic properties of receptive fields in the early visual system, and supports the “magnocellular hypothesis” of saccadic suppression, according to which the visual system makes special efforts to blunt the activity of the magnocellular pathway during saccades (Burr et al., 1994).

In humans, several recent fMRI studies also suggested that activity in both LGN and V1 is strongly modulated by large (35°) saccades. Sylvester et al. (2005) found that LGN and V1 modulation depended on the strength of concurrent visual stimulation: In complete darkness or in the presence of visual stimuli that evoked weak activation, saccades increased the BOLD signal in both LGN and V1 (corrolary discharge), whereas in the presence of strong visual stimulation, saccadic suppression was observed.

2.3.2 Modulation by fixational eye movements

Several studies have investigated the impact of fixational eye movements on neural activity in the early visual system. We review them below.

In the LGN of awake macaques, we saw in section 2.3.1 that fixational saccades modulate neural activity in a similar way as larger saccades: a weak presaccadic suppression is followed by a strong postsaccadic enhancement (Reppas et al., 2002). The influence of other fixational eye movements (such as ocular drifts) on LGN activity has not been investigated, to our knowledge.

Not surprisingly, the primary visual cortex is the area that received the most attention in relation to fixational eye movements. Livingstone et al. (1996) found strong modulations in macaque V1 related to eye movements during free-viewing, including fixational eye

movements. Snodderly and colleagues have been studying V1 neurons in the presence of fixational eye movements in awake macaques. After showing that FEM account for most of the variance in neural responses (Gur et al., 1997), they focused on the differential effects of various types of FEM. They found that different populations of V1 neurons responded selectively to different types of eye movements (Snodderly et al., 2001). “Saccade cells” (27% of the 104 cells) discharged when a fixational saccade moved the center of the receptive field onto the stimulus, off the stimulus, or across the stimulus. “Position/drift cells” (33%) discharged during the intersaccadic (drift) intervals and were not activated by saccades that swept the AR across the stimulus without remaining on it. “Mixed cells” (40%) fired bursts of activity immediately following saccades and continued to fire at a lower rate during intersaccadic intervals. An extraretinal influence accompanying fixational saccades was identified in one of the two monkeys. Like in the LGN, these results in V1 contradict the saccadic suppression theory, according to which the extraretinal effects should be predominantly suppressive (Ross et al., 2001).

In a different laboratory, Martinez-Conde et al. (2000) found that the activity of V1 neurons increased right after the occurrence of a microsaccade (defined as a small saccade of amplitude $3' - 2^\circ$), when an optimally oriented bar was centered over their receptive field. This excitatory effect was reported in 258 cells in 3 monkeys. In a similar study, Martinez-Conde et al. (2002) extended their results to the LGN. In both areas, the increase of neural activity following a microsaccade lasted less than 100 ms and involved 2 to 8 spikes. The authors called these short periods of high firing rate “bursts”, although they clearly differ from the low-threshold Ca^{2+} bursts described in 2.2.2, in which individual spikes are separated by 4 ms or less. According to the authors, microsaccades were better correlated with the occurrence of a “burst” than with either single spikes or instantaneous firing rate.

Leopold and Logothetis (1998) investigated the influence of microsaccades in various visual cortical areas. They re-used data from previous experiments, in which the monkeys had to maintain fixation for extended periods (up to 25 s) and discriminate two circular patches of oriented gratings (one that excited the neuron under study, the other having

little influence on the neuron's firing rate). Leopold and Logothetis reported that, in V1, 37% of the cells (13/35) were suppressed following microsaccades, while 17% (6/35) showed an enhancement, and 46% did not show any significant changes. In V2, 45% of the cells (13/29) were excited after a microsaccade, while the rest of the cells did not show any change. Area V4 showed the most pronounced activity ~ 100 ms after the microsaccade, in 74% (56/76) of the cells. It should be noted that the circular stimulus was generally $< 1^\circ$ in diameter, and that most cells recorded from had receptive fields "nearly always at the center of gaze". Thus, the stimulus was probably larger than the receptive fields in V1, but smaller than the receptive fields in V4, which make the reported effects difficult to compare across visual areas. Other reasons make us think that these results should be interpreted with caution. First, the authors report microsaccadic suppression in V1 in 37% of the cells, while it was not seen in any other study (Martinez-Conde et al., 2000; Snodderly et al., 2001). Second, they did not give their definition of a microsaccade. They simply stated,

Small saccadic movements were extracted offline using an iterative algorithm that relied upon first identifying potential saccades based on eye velocity and then accepting or rejecting each candidate by comparing several of its parameters to the well-known phenomenology of small saccades (Carpenter, 1988; Zuber and Stark, 1965) . . . Corrective saccades were also identified but excluded in the present analysis.

We do not believe that the "phenomenology of small saccades" (as opposed to large saccades) is "well-known": as explained in section 2.1.2, microsaccades and saccades form a continuum which can only be arbitrarily divided into two categories, and Zuber and Stark (1965) actually confirmed that so-called "microsaccades" followed the same "main sequence" (the distribution of saccade velocities vs. saccade amplitudes) as macroscopic saccades. The same concern can be raised for corrective saccades: how were they distinguished from microsaccades in Leopold and Logothetis's analysis?

Using a different experimental paradigm, Gallant et al. (1998) investigated neural ac-

tivity in macaque V1, V2, and V4 during free-viewing of natural images. In V1, they found postsaccadic enhancement in 42% of cells (10/24), postsaccadic suppression in 17% of cells (4/24), and no modulation in the remaining 41% of cells. Postsaccadic enhancement also occurred in 18% of cells (3/17) in V2 and in 45% of cells (9/20) in V4. Of the cells showing modulation in all three areas, most showed substantial variability in activity after each saccade, supporting the view that they were modulated by fixational eye movements.

In macaque area MT, Bair and O'Keefe (1998) reported that saccades and microsaccades elicited changes in the neuronal response that depended upon (1) the average level of stimulus-evoked activity around the time of the saccade, and (2) the direction of the saccade relative to the preferred direction of the neuron. Saccades were able to suppress stimulus-evoked activity when they caused retinal image flow in the neuron's preferred direction. On average, the disturbance lasted 40 ms beginning 40 ms following saccade onset.

The above results show that fixational eye movements influence neural activity in several areas of the early visual system (the retina, LGN, V1, V2, V4, and MT), where neurons are exquisitely sensitive to small fluctuations in the input. In particular, the main effect of microsaccades is excitatory, although some suppression has also been reported in a minority of cells. The influence of microsaccades on neural activity might have three origins: (1) the retinal image displacement; (2) a corollary discharge of the oculomotor command to issue a saccade; or (3) proprioceptive information reporting how the eye has moved.

2.4 Fixational eye movements in neural coding: results from previous modeling studies

Cells in the thalamocortical pathway have spatio-temporal (or dynamic, time-varying) receptive fields. The characteristics of these receptive fields suggest that they are constrained by the need to actively register time-varying stimuli (Ghazanfar and Nicolelis, 2001), in particular in the presence of fixational eye movements. In a series of modeling studies, Rucci and colleagues simulated the activities of LGN and V1 neurons when natural scenes

are scanned by eye movements and found that fixational instability had a strong impact on the correlations among cell activities (Rucci et al., 2000; Rucci and Casile, 2004, 2005; Casile and Rucci, 2006). They proposed that FEM may play an important role in the development, refinement, and maintenance of thalamocortical connectivity, and also that FEM may improve the efficiency of visual representations in the early visual system by reducing correlations among cells. The studies on cortical development are reviewed below, while the studies in coding efficiency are reviewed in more detail in the next section.

2.4.1 FEM and cortical development

Rucci et al. (2000) and Rucci and Casile (2004) simulated neural responses in models of LGN and V1 cells during natural viewing conditions, i.e., when natural scenes were viewed in the presence of eye movements. Geniculate neurons (X cells in the cat LGN) and simple cells in cat V1 were modeled by nonlinear spatiotemporal filters designed on the basis of neurophysiological data. Simulated eye movements replicated the oculomotor activity of the cat and included both large saccades and fixational eye movements. In these simulations, retinal image motion profoundly affected the statistical structure of neural activity despite the brief durations of visual fixation. Fixational instability induced strong synchronous modulations of neural responses in the LGN (Rucci et al., 2000) that were detected and amplified by neurons in the primary visual cortex (Rucci and Casile, 2004).

In the absence of eye movements, when images of natural scenes were presented statically, pairs of LGN cells with the same polarity (ON or OFF) were strongly correlated (i.e., had high levels of covariance) over large distances. This result was a consequence of the broad correlations of natural scenes that provided similar input to cells far from each other (see section 2.4.2). On the contrary, when fixational eye movements occurred, the size of correlated pools of cells was considerably narrower. Figure 2.12 shows the mean dynamics of correlated activity in the LGN predicted by the model when images of natural scenes are presented as input (Rucci, Edelman, and Wray, unpublished data). The differ-

ent curves represent levels of correlated activity between pairs of geniculate cells measured at several delays after the onset of a fixation. In the model, wide pools of cells with the same polarity (i.e., ON-ON or OFF-OFF) and with strongly correlated responses emerged immediately after the end of a saccade. In the presence of fixational instability, the size of these pools became progressively narrower within a fixation. After approximately 200 ms, cells of opposite (ON-OFF) polarities with receptive fields less than 1° apart tended to be modulated synchronously.

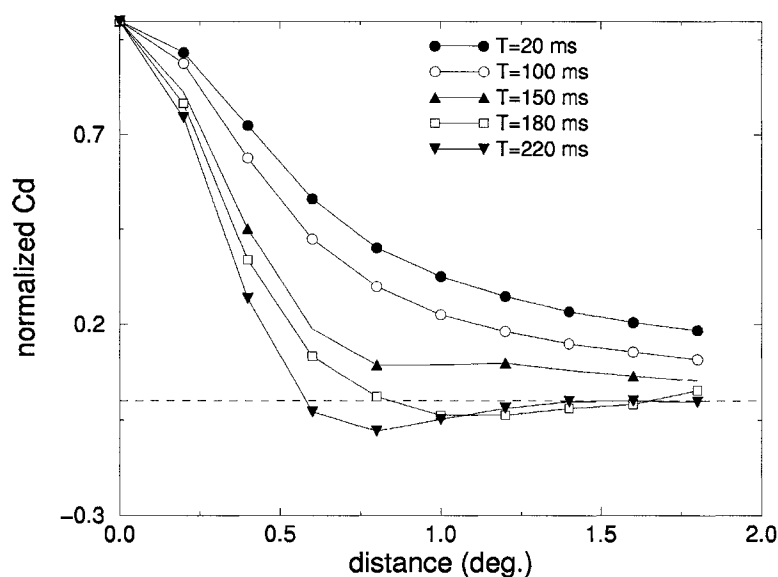


Figure 2.12: Dynamics of correlated activity during visual fixation in a model of the LGN. Levels of correlated activity between pairs of geniculate cells were evaluated at different latencies after the onset of a fixation. The x axis represents the distance between the receptive fields of the two cells. The data are mean values of the correlation difference $C^D(d)$ (the difference between the covariances among cells of the same (ON-ON or OFF-OFF) and opposite (ON-OFF) polarities with receptive fields at distance d from each other: $C^D(d) = C^{\text{same}}(d) - C^{\text{diff}}(d)$). Positive values indicate that on average two cells with receptive fields separated by a distance d will covary more strongly if they are of the same rather than of the opposite polarity. The opposite occurs for negative values (see Rucci et al., 2000, for a detailed description of the methodological procedure).

The results of Rucci et al. (2000) and Rucci and Casile (2004) support the Hebbian hypothesis that the organization of the receptive field of a V1 simple cell depends on the

correlated activity of its thalamic afferents. The Hebbian (or covariance) hypothesis of synaptic plasticity states that the development of segregated subregions in simple cell receptive fields requires synchronous activation (1) among LGN cells of the same type (ON or OFF) with receptive fields located at distances smaller than the width of a simple cell subregion, and (2) among LGN cells of opposite polarity with receptive fields at distances comparable to the separation between adjacent subregions. In other words, the temporal synchrony (or contiguity) of firing patterns is transformed into spatial proximity of synaptic contact (Stent, 1973; Changeux and Danchin, 1976). Such patterns of correlation were found in the simulations, but only in the presence of FEM. Large-scale eye movements alone were not sufficient: Just like a purely static input, they lead to broad correlations among X cells that extended over many degrees of visual field, due to the broad correlations present in natural scenes themselves (see section 2.4.2). The importance of normal eye movements, including FEM, for the development of V1 is in accordance with many experimental studies indicating that, while the initial maturation of orientation selectivity develops before eye opening, visual experience is essential for both refining orientation selectivity and maintaining the normal response properties of cortical neurons (Pettigrew, 1974; Buisseret and Imbert, 1976; Sherk and Stryker, 1976; Fregnac and Imbert, 1978; Albus and Wolf, 1984; Hirsch, 1985; Chapman and Stryker, 1993; Crair et al., 1998). Nevertheless, the precise role of neural activity in the maturation of orientation selectivity remains controversial (see Miller et al., 1999, for a review). Interestingly, very recent results show that visual experience is crucial for the development of direction selectivity in ferret V1 (Li et al., 2006).

The results from Rucci et al. (2000) and Rucci and Casile (2004) suggest that fixational eye movements may affect the second-order statistical structure of neural activity by reducing levels of correlation in the activity of different cells. These studies have raised the hypothesis that fixational eye movements, apart from their impact on cortical development, may also have functional implications in early vision. This aspect was studied in more detail in Rucci and Casile (2005) in the light of the redundancy reduction hypoth-

esis (Attneave, 1954; Barlow, 1961). Because this issue is relevant to our modeling work presented in Chapter 4, we review it in detail in the next section.

2.4.2 A functional role of fixational eye movements

Statistical properties of natural scenes

When video transmission was developed, it was soon realized that real images were highly redundant: on average, they vary little in space and time (Harrison, 1952; Kretzmer, 1952; Oliver, 1952). The development of engineering and statistical methods raised interest in describing natural scenes by their statistical properties. In particular, Fourier analysis soon entered the field of vision science, and it was found that the average *power spectrum* of natural images declines as $1/f^\alpha$ with spatial frequency, with $\alpha \approx 2$ (Field, 1987, 1994; Tolhurst et al., 1992; Ruderman, 1994). It is interesting to note that scale-invariant images have a power spectrum in $1/f^2$, indicating that natural images are roughly scale invariant on average (Field, 1987; Ruderman, 1994). The fact that low spatial frequencies are predominant in natural scenes means that intensity values exhibit broad spatial correlations which typically extend over several degrees of visual field.

Besides, the Fourier transforms of different natural images tend to diverge from each other primarily in terms of their *phase*, and not their amplitude (or power) spectra. Phase is particularly important for edges, since edges require an alignment of the phase of different spatial frequency components. The importance of global phase was demonstrated by Piotrowski and Campbell (1982). In these classic psychophysical experiments, human subjects were presented with images combining the Fourier amplitude of one natural scene with the Fourier phase of another natural scene. Invariably, these mixed images looked much more like the image contributing the phase spectrum, and not like the one contributing the amplitude spectrum. Recent studies have shown that edges, contours and other visually salient features cannot be captured by first- and second-order statistics but must be contained in higher-order statistics (Franz and Scholkopf, 2005).

The redundancy reduction hypothesis

It is a long-standing proposal that one of the tasks of early visual processing is to eliminate some of the redundancy characterizing natural scenes. In the *redundancy reduction hypothesis*, early sensory systems use an *efficient code* to maximize information transfer to higher brain areas (Attneave, 1954; Barlow, 1961).

Since its early formulation—entirely based on theoretical considerations—the redundancy reduction hypothesis has been tested experimentally. It may not hold in cortex, where neural populations are highly redundant (Zohary et al., 1994) and where the number of cells increases in higher areas (Barlow, 2001). However, in early sensory areas, the informational load coming from the sensors is enormous and most of it is irrelevant, due to the redundancy of natural stimuli. For example, the number of optic fibers (the axons of RGCs) leaving the retina is largely inferior to the number of photoreceptors. The existence of this bottleneck in information transmission strongly suggests that information must be compressed somehow.

It is important to realize that there exist two unrelated definitions of redundancy (reviewed in Averbeck et al., 2006). The original one, proposed by Barlow, derives directly from Shannon’s information theory (Shannon and Weaver, 1949). It can be written as

$$1 - \frac{H}{H_{\max}}, \quad (2.1)$$

where H_{\max} , is the maximum entropy of a discrete distribution (subject to constraints) and H is the observed entropy. When extended to continuous distributions (Atick and Redlich, 1990), this redundancy becomes

$$1 - \frac{I}{I_{\max}}, \quad (2.2)$$

where I_{\max} is the channel capacity. The second definition of redundancy is the sum of the information from individual cells minus the total information of the population,

$$\Delta I_{\text{redundancy}} = -\Delta I_{\text{synergy}} = \sum_i I_i - I, \quad (2.3)$$

where I_i is the Shannon information for neuron i and I is the total information (e.g., Gawne and Richmond, 1993; Gawne et al., 1996; Panzeri et al., 1999; Schneidman et al., 2003; Puchalla et al., 2005). Neural codes with negative $\Delta I_{\text{redundancy}}$, or positive $\Delta I_{\text{synergy}}$, are called synergistic codes. *Synergy* means that the population as a whole can encode more information than the sum of its individual neurons. Conversely, neural codes with positive $\Delta I_{\text{redundancy}}$, or negative $\Delta I_{\text{synergy}}$, are called redundant codes. In this case, the population as a whole has less encoding capacity than the sum of its neurons, and the neural code is said to be redundant.

Several information theoretical studies of the early visual (Srinivasan et al., 1982; de Ruyter Van Steveninck et al., 1994; Dan et al., 1996; Baddeley et al., 1997; Vinje and Gallant, 2000, 2002; David et al., 2004) and auditory (Rieke et al., 1995; Chechik et al., 2002) systems have shown that the neural code is matched to the structure of natural stimuli, so that redundancy is reduced as one ascends the sensory pathway.

It is interesting to note that redundancy reduction is not the only way to make a code more efficient. It all depends on which parameter(s) need to be optimized, whether (1) the number of encoding units, or neurons, (2) the number of encoding units which are simultaneously active, (3) the total amount of energy consumed by the system during information transfer and processing (Lennie, 2003) (4) or even, as some suggested, the total length of wires used in brain circuits (Chklovskii et al., 2002). While (3) and (4) are outside the scope of this literature review, we will detail (1) vs. (2) below.

Redundancy reduction corresponds to (1), which is also called *compact coding*. It came directly from the fields of electrical engineering and computer science, in which data compression algorithms are used to reduce the dimensionality of the data (here, the sensory input). In other words, data compression allows a system to encode and transfer information using fewer bits (or other information-bearing units). In computational neuroscience, the idea of using fewer bits was directly translated into using fewer units, or less “neurons”. In a compact neural code, a smaller number of units (“neurons”) should be sufficient to encode a particular subset of all possible inputs—for example, the subset of natural images,

with their particular statistics (reviewed above).

The idea of compact coding was challenged by Field (1987, 1994), who proposed that efficient coding could be achieved in a different way, with a *sparse-distributed* representation of the sensory input. In a sparse-distributed code, the dimensionality of the representation is maintained: the number of cells remains constant or even increases from one processing stage to the next. However, the number of cells responding to any particular instance of the input is minimized, as in (2) above. This coding scheme does not actually reduce redundancy. Rather, high-order redundancy is transformed into redundancy of the firing patterns of the cells. The goal of sparse coding is to maximize the redundancy of the response histograms by minimizing the statistical dependencies between units.

Removing correlations to reduce redundancy

One possible way to decrease redundancy in a given signal is to remove its correlations. This idea was explored first by Srinivasan et al. (1982). In their *predictive coding* theory, the spatial and temporal properties of receptive fields in the early visual system allow neurons to exploit the correlations that exist within natural scenes to achieve redundancy reduction. The idea of predictive coding was initially developed for efficient transmission of video data (Oliver, 1952; Harrison, 1952), by removing predictable, and hence redundant, components. In the spatial domain, center-surround antagonism enables the neuron to use its entire dynamic range to encode a small range of intensities, thus rendering fine detail detectable against intrinsic noise at this and later stages of neural processing. The neuron uses the intensity values in the surrounding regions to generate a statistical estimate of the intensity expected at the center of the receptive field. By subtracting this best estimate from the actual signal entering the center, the amplitude of the transmitted signal is minimized, and Srinivasan et al. (1982) showed in a simplified receptive field model that redundancy is reduced by removing all first-order correlations in the input. However, the authors also point out that, “as one might expect of the simple patterns of inhibition seen in the retina, redundancy is not completely eliminated”. This point is to be remembered when

we describe the work by Atick and colleagues (see below).

Srinivasan et al. (1982) also investigated predictive coding in the temporal domain. They argued that the impulse response of some cells having transient (or phasic) properties could mediate prediction in the time domain, just as center-surround antagonism mediates prediction in the spatial domain. The authors attempted to support their theory quantitatively with preliminary results from the first-order interneurons of the fly's compound eye, analog to bipolar and ganglion cells in the vertebrate retina. They found good agreement between experiment and theory in the temporal domain, but not in the spatial domain. They proposed that the discrepancy in the spatial domain could be due to the assumption of stationary or almost stationary stimuli in their predictive encoding hypothesis, while the fly's interneurons should be "better suited for sampling rapidly moving scenes". In our opinion, this argument also holds in the presence of fixational eye movements. This remarkable insight was, unfortunately, neglected by later studies of the same topic, such as those by Atick and colleagues reviewed below.

In the same trend, van Hateren (1992) proposed a theory of maximizing sensory information, in which redundancy is reduced at high signal-to-noise ratios, but increased at low signal-to-noise ratios to recover from errors in transmission. In the high signal-to-noise scenario, the derived neural filter is high-pass (i.e., sharpening), corresponding in physiology to lateral inhibition and self-inhibition. In the low signal-to-noise scenario, the derived neural filter is low-pass (i.e., smoothing), which corresponds to spatial pooling and temporal summation.

In accordance with Srinivasan et al. (1982), several studies have shown that temporal decorrelation of the signal takes place at the level of a single neuron. Dan et al. (1996) showed that individual neurons in the Lateral Geniculate Nucleus whitened their input, i.e., removed the temporal autocorrelations in the visual input. However, the proposal that the early visual system is able to decorrelate natural stimuli has been less successful in the spatial domain than in the temporal domain. Atick (1992) suggested that the response characteristics of LGN cells may be particularly well designed to remove broad

spatial correlations present in natural scenes. Like van Hateren, Atick (1992) and Atick and Redlich (1992) predicted that RGCs spatial filters would be band-pass or high-pass at high signal-to-noise ratios, and low-pass at low signal-to-noise ratios.

Atick and Redlich (1992) also designed a model for spatial kernels suited to achieve decorrelation of natural images. In a noise-free situation, these kernels were simply whitening kernels $K(f) \sim |f|$, fit to the $1/f$ distribution of amplitudes in natural images. In the presence of noise, these kernels were modeled as a linear filter composed of a series of three filters: the optical modulation function of the eye, a low-pass filter (to eliminate the noise), and a whitening filter K as in the noise-free case. Plotting these filters as contrast sensitivity functions of spatial frequency beared a strong resemblance to human psychophysical contrast sensitivity functions. The authors used this resemblance as evidence that their filters had to be good descriptors of actual retinal filters.

However, Atick and Redlich's prediction is challenged by neurophysiological measurements showing a large variability in the frequency responses of lateral geniculate neurons and retinal ganglion cells. Both in the cat (So and Shapley, 1981; Linsenmeier et al., 1982; Cheng et al., 1995) and in the monkey (Derrington and Lennie, 1984; Croner and Kaplan, 1995), many cells do not exhibit a dependence on spatial frequency proportional to f^2 . Even for those cells that do exhibit an f^2 response, this relationship tends to be valid only within a limited range of frequencies.

Furthermore, Atick's theory neglects the fact that during natural vision, the spatiotemporal structure of the signals entering the eyes depends not only on the visual scene, but also on the movement performed by the animal during the acquisition of visual information. Eye movements, in particular, since they are always present during natural vision, may have a strong influence on the structure of neural activity.

Changes in the second-order statistics are also important with respect to theories that propose a role for synchronous modulations in transmitting visual information, such as the binding-by-synchrony or temporal-correlation hypothesis (Singer and Gray, 1995; Singer, 1999). In the LGN, nearby cells tend to exhibit correlated spiking (Alonso et al., 1996),

a feature that has been proposed to contribute to the transmission of information (Dan et al., 1998).

To investigate the contribution of FEM to the correlations among LGN cells in natural vision—when natural scenes are browsed by eye movements, Rucci and Casile (2005) developed a mathematical formulation of the impact of FEM on the second-order statistics of the LGN input and output. The modeled LGN cells were nonlinear spatiotemporal filters designed on the basis of neurophysiological data in cat X cells which, as explained above, do not have optimal spatial characteristics for decorrelating their correlated input, because of their significant departure from linearity in the low spatial frequency range. For mathematical convenience, Rucci and Casile simulated fixational eye movements as an ergodic process with zero moments of the first order and uncorrelated components along the horizontal and vertical axes, and Gaussian temporal and spatial correlations. In the simulations of LGN activity, wide pools of cells were strongly correlated when natural images were presented statically in the absence of retinal motion, while in the presence of fixational eye movements, spatial correlations in the input had little influence on the correlations among cells: the same patterns of output correlations were obtained for (highly correlated) natural images as for (uncorrelated) white noise input.

Rucci and Casile (2005) showed that two main elements contributed to decorrelating the responses of LGN cells in the presence of FEM. The first element was the introduction of a spatially decorrelated component to the input signal, due to the occurrence of FEM. A new dynamic component $R_{\bar{f}\bar{f}}$ was added to the power spectrum of the input. This term lacked spatial correlations even when the cells viewed a natural image, or any image with a power spectrum declining as $1/f^2$ (or steeper) with spatial frequency f . The small jitter caused by fixational eye movements creates temporal fluctuations in the retinal input which depend on the local changes in intensity, i.e., on the first spatial derivative of the image. Since spatial differentiation corresponds to multiplication by f in the spatial frequency domain, any image with a $1/f^2$ power spectrum (or steeper), corresponding to a $1/f$ (or steeper) distribution of amplitudes, has a first spatial derivative with a flat power spectrum.

Thus, the first derivative of a natural image (corresponding to small fluctuations on the image) is spatially uncorrelated.

It is important to note that, in Rucci and Casile (2005), the only source of correlation was in the input itself. Other sources of correlation among cells (reviewed in Usrey and Reid, 1999) were not considered, and would require *in vivo* experiments or more sophisticated neural network models.

The analysis of Rucci and Casile (2005) assumed a steady state corresponding to an indefinitely long fixation. In other words, these simulations strictly applied to a later period of visual fixation, the period following the initial 150 ms transitory interval when neural responses have adjusted to the stimulus brought in by the saccade. Rucci and Casile predicted that initially correlated neural responses would become progressively less correlated during a period of visual fixation. This prediction led to the design of our modeling work described in Chapter 4.

2.4.3 Fixational eye movements as part of the neural code

The idea that fixational eye movements are an integral part of vision began with theories about visual acuity. This history, which dates back to Helmholtz (1866), is reviewed by Steinman and Levinson (1990). While *static theories* emphasized intensity discrimination as a limiting factor for acuity, *dynamic theories* emphasized the role of eye movements. Since then, other ideas have been proposed for a possible role of fixational eye movements, including improvement of feature estimation (Greschner et al., 2002) and figure/ground segregation (Ölveczky et al., 2003) in the retina.

Below we review one original contribution explaining how FEM might be involved in a temporal neural code.

“Figuring space by time”

Ahissar and Arieli (2001) drew a parallel between the early visual system and the somatosensory system in the rat, which consists of sensors (the whiskers), the somatosensory

cortex—in particular its layer 4, called *barrel cortex*, and two parallel pathways ascending to the barrel cortex: the lemniscal pathway and the paralemniscal pathway, going through two different areas of the thalamus. Ahissar and Arieli (2001) underlined that, in *spatial coding*, the information was assumed to be coded by the identity of the activated cells, while in *temporal (latency) coding*, information was coded in the relative timing of firing in the neurons. Ahissar and Arieli (2001) proposed that a temporal encoding-decoding scheme is utilized for processing fine spatial details in relative coordinates, while a spatial encoding-decoding scheme is utilized for processing coarse spatial details in absolute coordinates. The retinal temporal encoding proposed by Ahissar and Arieli (2001) is acknowledgely an implementation of the idea of “differential amplifier” suggested by Westheimer to explain hyperacuity (Westheimer, 1990). An example of hyperacuity is vernier acuity, the ability to detect a fracture in a bar, but without being able to precisely tell where the fracture is located. Samely, in Ahissar and Arieli’s theory, the differential nature of temporal encoding entails an inability to resolve absolute location. Fine image analysis would be based on temporal coding, while global image analysis would be based on spatial coding, in absolute coordinates.

The ideas proposed by Ahissar and Arieli (2001) differ from the older “dynamic theories” described earlier. These models focused on the high-frequency tremor, and assumed integration of the temporally encoded outputs of the retina (e.g., Arend, 1973; Marshall and Talbot, 1942). Instead, Ahissar and Arieli’s model relies on the entire spectrum of FEM and does not assume integration. As explained above, the fine temporal information embedded in the retinal output has a hyperacuity resolution, which would be lost by an integration process. Moreover, Ahissar and Arieli favor an active control of fixational eye movements, reminiscent of the rat’s whiskers system. An active control of fixational eye movements remains to be tested experimentally.

Chapter 3

Psychophysical experiments: Contributions of fixational eye movements to the discrimination of briefly presented stimuli

3.1 Introduction

As reviewed in Section 2.1, early experiments in stabilized vision focused on conditions of sustained fixation, in which stimuli were presented for long periods of time. Few studies have examined the consequence of eliminating FEM during brief stimulus presentations similar to those that occur during natural viewing conditions. These studies selectively focused on visual acuity and contrast sensitivity, and reported either no significant effect of image stabilization (Keeseey, 1960; Tulunay-Keeseey and Jones, 1976), or an improvement of performances under stabilized conditions with brief stimulus exposures (Riggs et al., 1953).

No previous study has investigated the effect of brief retinal stabilization on stimulus discrimination. As reviewed in the previous chapter, however, the results of more recent psychophysical, neurophysiological, and computational studies argue in favor of an important role of fixational instability even during the brief periods of visual fixation. For example, it has been observed that entoptic images generated by casting shadows of the foveal capillaries onto the retina tend to disappear in less than 80 ms (Coppola and Purves, 1996), an interval that correlates well with the rapid decay of neuronal responses in the monkey's primary visual cortex (V1) with unchanging stimuli (Ringach et al., 1997; Mazer et al., 2002). Neurophysiological recordings with awake monkeys have shown that fixational eye movements strongly modulate the responses of neurons in different cortical areas (Gur et al., 1997; Leopold and Logothetis, 1998; Martinez-Conde et al., 2000). In particular,

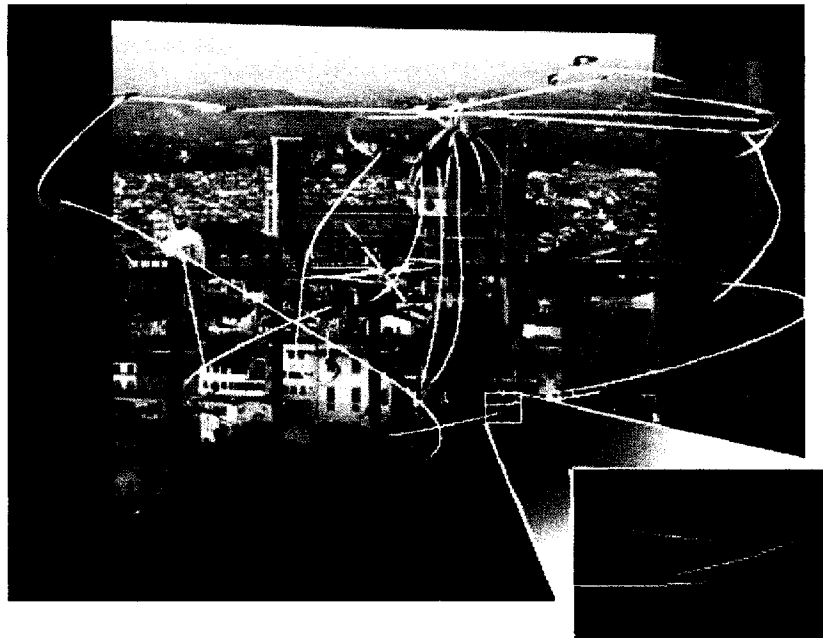


Figure 3.1: An example of macroscopic and microscopic eye movements. A recorded trace of eye movements is shown superimposed on the original image. The panel on the bottom right shows a zoomed portion of the trace in which small fixational eye movements are present. The color of the trace represents the velocity of eye movements (red: slow movements; yellow: fast movements). Blue segments mark periods of blink.

in area V1 of the macaque different populations of neurons respond selectively to the two main components of fixational eye movements: small saccades and drifts (Snodderly et al., 2001). Furthermore, large-scale computer simulations of neuronal responses in the early visual system during oculomotor activity suggest that fixational instability profoundly alters the structure of correlated activity. In these simulations, fixational eye movements induced synchronous modulations of neuronal responses in the Lateral Geniculate Nucleus (Rucci et al., 2000) that were detected and amplified by neurons in the primary visual cortex (Rucci and Casile, 2004).

This body of literature raises the hypothesis that previous experiments on stabilized vision, with their focus on evaluating visual acuity or contrast sensitivity, may have not explored conditions adequate to unveil possible effects of fixational instability in the presence of brief stimulus presentations. In this chapter, we report the results of a forced-choice discrimination task that was designed on the basis of our recent modeling work to enhance the effect of fixational instability on the structure of correlated activity. We show that in this task subjects perform differently under stabilized and unstabilized conditions, even when stimuli were presented for only 500 ms. This psychophysical study was published in Rucci and Desbordes (2003).

3.2 Methods

3.2.1 Subjects

Four subjects with normal vision participated in the experiments. Three subjects were naive about the purposes of the experiments and were paid to participate. A fourth subject was one of the authors. Informed consent was obtained from all subjects following the procedures approved by the Boston University Charles River Campus Institutional Review Board.

3.2.2 Apparatus

Stimuli were generated on a Millennium G550 graphics card (Matrox Graphics Inc., Dorval, Qc, Canada) and displayed on a 21" Trinitron CRT at a resolution of 800×600 pixels and vertical refresh rate of 75 Hz. Subjects were kept at a fixed distance of 110 cm from the monitor by means of a dental imprint bite bar and a head rest that prevented movements of the head.

Eye movements were monitored and recorded by a Generation 6 Dual-Purkinje-Image (DPI) eyetracker (Fourward Technologies Inc., Buena Vista, VA) originally designed by Crane and Steele (1978), as described in section 2.1.4. The nominal resolution of this eyetracker is about $1'$ with a time delay of approximately 0.25 ms (Crane and Steele, 1985). Vertical and horizontal eye position data were sampled at 1 kHz, digitally low-pass filtered (Butterworth filter with 100 Hz cutoff frequency), and recorded for subsequent analysis. To determine the synchronism between traces of eye movements and the stimulus, a small square was periodically flashed at one of the corners of the screen, and the voltage of a photocell covering the square was simultaneously sampled and recorded. Subjects gave their responses by pressing one of two keys on a joystick.

Image stabilization was maintained by a stimulus deflector coupled to the DPI eyetracker (Crane and Steele, 1978). When properly calibrated, this optical-electronic device shifts the image in the opposite direction and by the same amount as the eye movements with a total response time of approximately 6 ms and a spatial resolution of approximately $10''$. Stimuli were always viewed through the deflector in both stabilized and unstabilized conditions.

3.2.3 Stimuli

Visual stimuli were designed on the basis of our recent modeling work to enhance the possible impact of fixational eye movements in visual discrimination. Each stimulus consisted of a 30×4 pixel light gray bar (approximately $30'$ of visual angle) embedded in a 42×42 pixel gray square. In each trial, the bar was tilted by $+45^\circ$ or -45° with equal probability

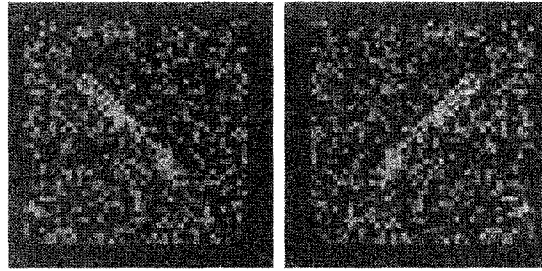


Figure 3.2: Examples of stimuli used in the experiments. Left: $+45^\circ$ bar. Right: -45° bar.

(angles are measured counterclockwise from the vertical axis). Results from our simulations have indicated that modulations in neuronal responses due to small eye movements may become particularly relevant in the presence of noisy stimuli. Noise was added to the stimulus according to the following algorithm: Each pixel of the square matrix had a fixed probability (the noise density) of being affected by noise. The intensity values of noisy pixels were replaced with random values selected from a uniform distribution between 0 and 255. In all experiments, a noise density of 80% was used. Stimuli were displayed on a gray background of uniform luminance equal to the mean luminance of the stimulus (22.2 cd/m^2). Figure 3.2 shows typical examples of the stimuli. Contrast levels were individually adjusted for each subject so that performances in the presence of the normally moving retinal image were around 70–80% (see section 3.2.4: “Procedure”). Different contrasts were used in Experiment 1 and Experiment 2. Contrast levels ranged from 2.0% to 4.3% in Experiment 1 and from 3.7% to 4.9% in Experiment 2. The screen background was kept isoluminant at a fixed value of 22.2 cd/m^2 . It should be noted that the luminance experienced by subjects was attenuated by the stimulus deflector.

3.2.4 Procedure

Each subject participated in several experimental sessions of approximately 30 min each. Each experimental session started with preliminary setup operations that lasted between 10 and 15 min and allowed the subject to adapt to the low level of light in the room. These preliminary operations included positioning the subject optimally and comfortably in the

apparatus; tuning the eyetracker until successful tracking was achieved; calibrating the stimulus deflector until successful stabilization (see below); and running a brief procedure that allowed conversion of the eyetracker output voltages into degrees of visual angle. This conversion was achieved by performing a quadratic regression on the basis of nine points for which spatial positions and output voltages were known.

Calibration of the stimulus deflector, a critical step for achieving accurate stabilization, was performed following the afterimage method described by Kelly (1979a). In this procedure, the subject is responsible for adjusting the offsets and gains of the deflector. These parameters depend on several factors, including the morphology of the eye. In a preliminary coarse calibration, subjects adjusted the deflector settings by comparing the movement of a stabilized dot to crosshair landmarks that were displayed in the unstabilized field. In the successive fine-tuning phase, a small, bright bar was displayed on a dark background. Subjects used the negative afterimage that developed from fixating the bar for 30 s to refine stabilization while performing a number of small saccades along the horizontal and vertical axes. After a saccade, the displayed bar moved farther than its dark afterimage if the gain was set too high, whereas it moved short of the afterimage if the gain was set too low. Using a vernier potentiometer, the subject finely adjusted the gains so that the afterimage always remained hidden behind the bar during eye movements.

After these preliminary setup operations, subjects were presented with blocks of 25 experimental trials. A brief break between two consecutive blocks allowed the subjects to relax and occasionally check the accuracy of stabilization by repeating the calibration routine. Overall, subjects were never constrained in the experimental setup for more than 30 minutes in a row.

In the experimental trials, subjects reported in a forced-choice procedure whether the stimulus bar was tilted by $+45^\circ$ or -45° . Three experiments were run. Stimuli were presented for 2 s in Experiment 1 and for 500 ms in Experiments 2 and 3. In all experiments, blocks of 25 trials alternated between two different conditions: stabilized and unstabilized. As shown in Figure 3, the temporal sequence of events in an unstabilized trial consisted in

(a) presenting an initial fixation dot at the center of the screen for 1.57 s; (b) at the offset of the fixation dot, cueing the location of stimulus. Cueing was performed by four arc segments that surrounded the chosen position for 240 ms; (c) after an interval of 240 ms, displaying the stimulus at the cued location for a fixed duration of either 2 s (Experiment 1) or 500 ms (Experiments 2 and 3); (d) masking the stimulus by a high-energy mask that was displayed for 1.33 s. In the unstabilized trials of Experiments 1 and 2, to allow the normal fixational instability that occurs after saccades in natural viewing conditions, the stimulus was presented at a fixed distance from the fixation dot and the subject was required to make a saccade toward it. Stimuli were displayed 240 ms after the cue to ensure that subjects would fixate the cued location at the time of stimulus appearance. This interval was selected on the basis of preliminary experiments that evaluated subject saccadic and reaction times. In the control experiment (Experiment 3), stimuli were cued and displayed at the center of fixation.

In the stabilized condition, the stimulus deflector eliminated retinal image motion by compensating for the subject eye movements. In this case, the stimulus always appeared immobile at the center of the fovea. As illustrated in the right panel of Figure 3.3, the sequence of events in the stabilized condition was similar to that of the unstabilized condition. The main differences were the absence of the saccade (which, in this case, would have disrupted retinal stabilization) and, in Experiments 1 and 2, the absence of the saccade cue, which was eliminated to avoid the annoying afterimages that develop with repetitive presentation of identical visual stimulation in the same retinal location. In Experiment 3, stabilized and unstabilized conditions were identical and included a lower intensity cue at the center of fixation (and thus no saccade).

To compensate for individual differences in contrast sensitivity, contrast levels for each subject were determined in a preliminary session, in which we systematically varied stimulus contrast. Contrast levels were chosen so that percentages of correct discrimination were between 70% and 80% correct in the unstabilized condition.

Contrast sensitivity functions were also determined for each subject in three different

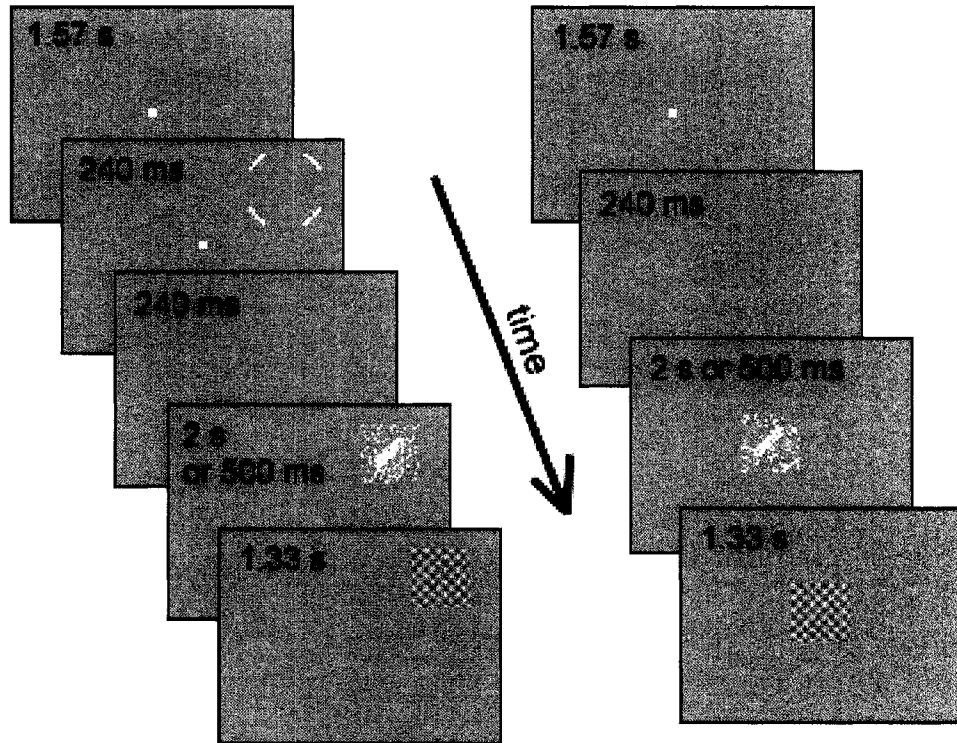


Figure 3.3: Main experimental procedure (Experiments 1 and 2). Subjects were required to detect the orientation of a noisy bar that was displayed for either 2 s (Experiment 1) or 500 ms (Experiment 2). Performances in two conditions, stabilized and unstabilized (i.e., with the normally moving retinal image), were compared. Left: unstabilized trials. Right: stabilized trials. In the control experiment (Experiment 3), the procedure was identical in both stabilized and unstabilized trials; the cue and stimulus were always presented at the center of fixation.

conditions: stabilized with a 2-s presentation; stabilized with a 500-ms presentation; and unstabilized with a 500-ms presentation. Consistent with previous reports (Tulunay-Keesey and Jones, 1976), visual stabilization had little or no effect on the sensitivity thresholds obtained with these brief stimulus durations. The contrast sensitivity functions measured under visual stabilization were similar to those obtained in unstabilized conditions, and the curves measured with stabilized exposures of 2 s and 500 ms were almost identical to each other. An example of contrast sensitivity functions measured for one subject in the various conditions is given in Figure 3-4.

3.3 Results

3.3.1 Experiment 1

In the first experiment, we examined the effect of visual stabilization with a stimulus presentation of 2 s. Although longer than the typical durations of visual fixation, a 2-s period of observation provides a good reference point for experiments with shorter durations, as it allows a relatively long interval for fixational instability to exert its possible influence on neural activity. Figure 3-5 shows the percentages of correct discrimination obtained in Experiment 1. The individual subject data as well as their overall means are shown in separate graphs. Each graph compares performances in the stabilized and unstabilized conditions. In the unstabilized condition, following the preliminary contrast selection procedure (see section 3.2: "Methods"), percentages of correct discrimination were 72% for BE ($N = 164$), 69% for TC ($N = 97$), and 76% for GD ($N = 74$). The mean percentage of correct discrimination over all subjects was 72%. Percentages of correct discrimination dropped to chance level for all subjects when the image was stabilized on the retina. Under stabilized conditions, percentages of correct discrimination were 51% for BE ($N = 82$), 53% for TC ($N = 51$) and 47% for GD ($N = 59$). In this case, the mean percentage of correct discrimination over all subjects was 51%. One-tail z tests of the differences in the percentages of correct discrimination under stabilized and unstabilized conditions were all significant at the 0.05 levels (BE: $z = 3.21$, $p < .05$; TC: $z = 1.94$, $p < .05$; GD: $z = 3.35$,

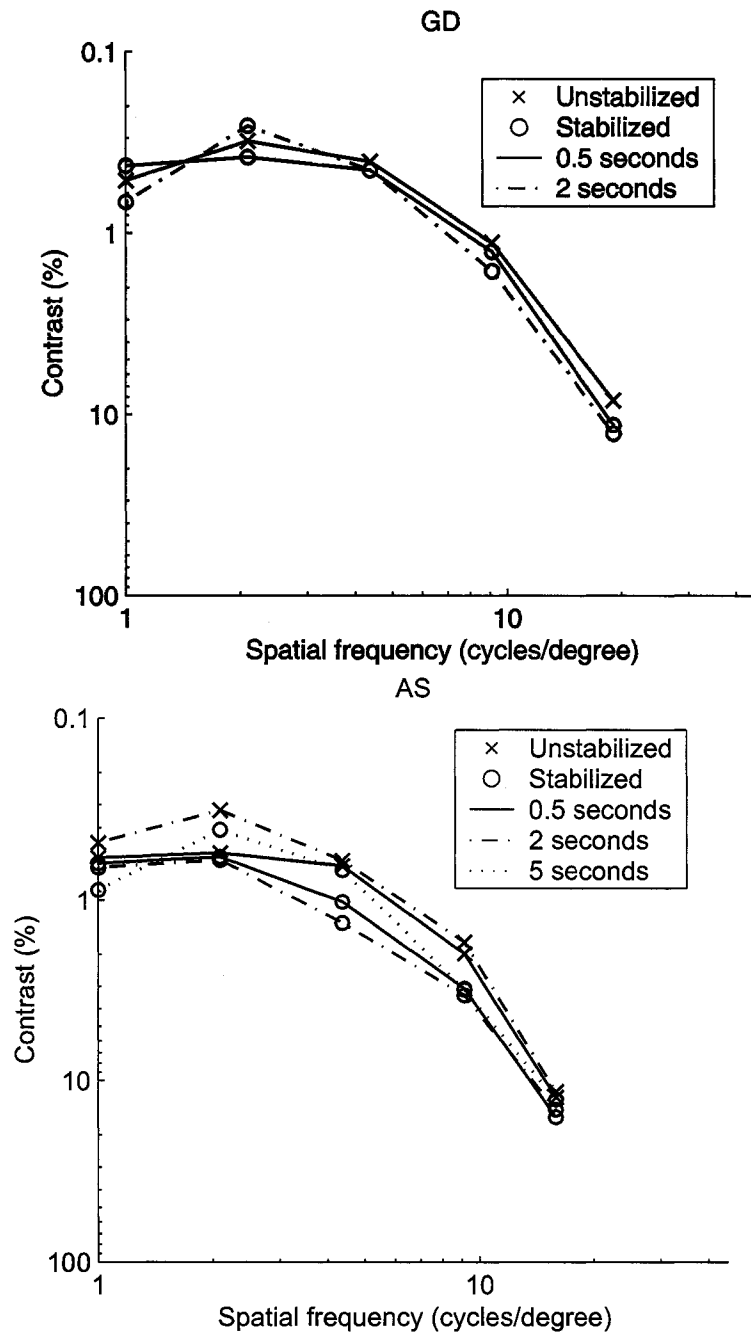


Figure 3.4: Contrast sensitivity functions for subjects GD and AS, measured in different experimental conditions.

$p < .05$).

3.3.2 Experiment 2

While substantially shorter than the durations of stimulus presentation used by most previous experiments with stabilized vision, 2 s is still a long interval compared to the periods of visual fixation that occur during natural viewing conditions. In order to investigate whether a similar impairment in visual discrimination is also present with shorter exposures, in Experiment 2 the stimulus exposure was reduced to 500 ms. A period of approximately 500 ms has been reported as the average duration of visual fixation for free-viewing of simple patterns stimuli similar to the ones used in our experiments (Harris et al., 1988; Andrews and Coppola, 1999).

Figure 3·6 shows the percentages of correct discrimination obtained with this shorter stimulus duration. As in Figure 3·5, performances in the stabilized and unstabilized conditions are compared in different graphs for the three subjects. In the unstabilized condition, percentages of correct discrimination were 72% for BE ($N = 249$), 80% for TC ($N = 143$), and 83% for GD ($N = 98$). The mean percentage of correct discrimination over all subjects was 76%. Similar to Experiment 1, lower percentages of correct discrimination were found for all subjects when the image was stabilized on the retina. In the stabilized condition, percentages of correct discrimination with 500-ms exposure duration were 62% for BE ($N = 221$), 66% for TC ($N = 119$), and 66% for GD ($N = 80$). The mean percentage of correct discrimination over all subjects was 64%. One-tail z tests of the differences in the percentages of correct discrimination under stabilized and unstabilized conditions were all significant at the 0.05 levels (BE: $z = 2.18$, $p < .05$; TC: $z = 2.44$, $p < .05$; GD: $z = 2.52$, $p < .05$). It is interesting that in the unstabilized condition all subjects required higher levels of stimulus contrast to produce levels of performance similar to those obtained in Experiment 1. Because corresponding reductions in contrast sensitivity thresholds were not observed when measuring contrast sensitivity functions (see Figure 3·4), it appears that this impairment occurred specifically in the discrimination

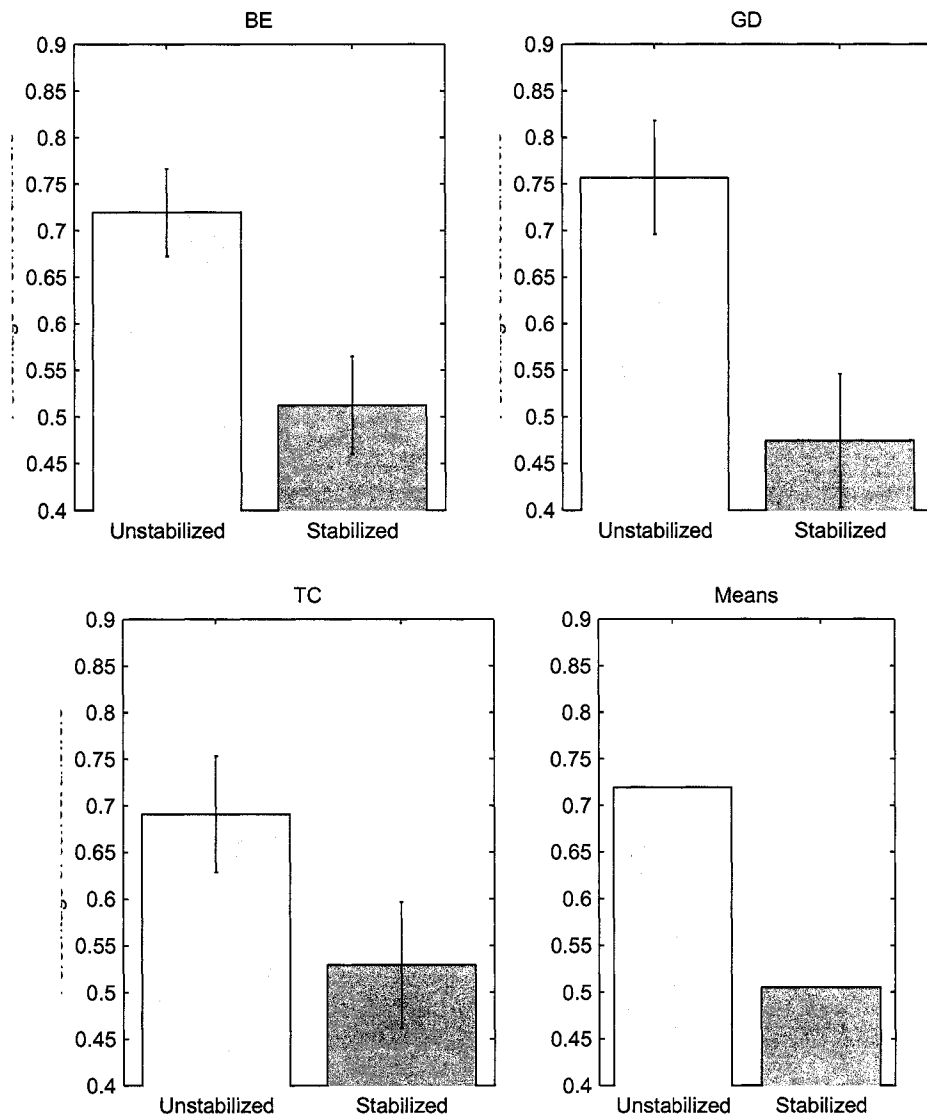


Figure 3.5: Percentages of correct discrimination obtained in Experiment 1 when the stimulus was presented for 2 s. The results for each subject as well as the overall means are shown. The two bars illustrate the results obtained under stabilized and unstabilized conditions. Error bars at the 0.05 significance levels are shown.

experiments. It should also be noted that although direct comparison of Figures 3·5 and 3·6 suggests that percentages of correct discrimination were more severely affected by image stabilization in Experiment 1 (with a 2-s stimulus exposure) than in Experiment 2 (with a 500-ms stimulus exposure), a quantitative analysis is complicated by the fact that contrast levels could not be finely tuned to exactly match the percentages of correct discrimination in the unstabilized conditions of the two experiments.

Previous experiments on stabilized vision have reported a reduction in contrast sensitivity with prolonged exposure to stabilized stimuli. With the brief stimulus presentations of our experiments, contrast sensitivity functions measured in the absence or presence of retinal image motion (i.e., stabilized or unstabilized conditions) produced similar thresholds (e.g., see Figure 3·4). Nevertheless, it is still possible that some degree of image fading occurred due to the continuous presence of a uniform background during and in between trials. In Experiment 1, subjects occasionally reported a partial fading of the image toward the end of a block of trials (the trials in which this occurred were removed from data analysis). In Experiment 2, image fading was never experienced. Nonetheless, to test if a decrement in contrast sensitivity could account for the impairment in discrimination performances under stabilized conditions, data were analyzed to distinguish early trials (the first 10 trials in each block of 25 consecutive trials) from late trials (the last 10 trials in each block). The results of this analysis are shown in Figure 3·7. In the stabilized condition, only TC exhibited slightly better performances in the first part of a block of trials. Percentages of correct discrimination for TC were 73% in the first 10 trials and 66% in the last 10 trials. However, this difference was well within the range of statistical variability ($z = 0.95, p > .05$). The other subjects performed almost identically in early and late trials. Percentages of correct discrimination in the stabilized condition were 62% in the first 10 trials and 62% in the last 10 trials for BE, and 68% in the first 10 trials and 66% in the last 10 trials for GD. For all subjects, no statistically significant differences were found between early and late trials, neither in the unstabilized nor in the stabilized conditions. Thus, the reduction in percentages of correct discrimination measured in Experiment 2 was

not due to a corresponding long-term fading of the image.

3.3.3 Experiment 3

In the previous experiments, unstabilized and stabilized trials differed not only in retinal image motion but also in the procedure of stimulus presentation. To allow the normal instability of visual fixation, in the unstabilized trials, subjects performed a saccade toward a cued location at which the stimulus was presented. In contrast, to ensure a high quality of retinal stabilization, in the stabilized condition, stimuli were presented at the center of the screen while the subject maintained fixation.

To examine the possible influence of this procedural difference, in Experiment 3, we matched the conditions of stimulus presentation in stabilized and unstabilized trials. In this control experiment, the stimulus was always preceded by a cue (also in stabilized trials) and presented at the center of fixation in both stabilized and unstabilized trials.

It is known that under conditions of sustained fixation subjects tend to show a lower degree of fixational instability than in natural viewing conditions (Steinman et al., 1967; Kapoula et al., 1986b). In Experiment 3, two subjects (GD and TC) exhibited a clear reduction of fixational instability, whereas the third subject (AS) remained at approximately the same level. While for GD, fixational instability decreased of a factor of two with respect to Experiment 2 (1.7 arcmin² vs. 3.4 arcmin², in correct trials), TC exhibited a more pronounced reduction to about 1/4, as shown in Figure 3·10 (2.5 arcmin² vs. 9.0 arcmin², in correct trials).

Figure 3·8 shows subject performances in Experiment 3. The two subjects with little or no reduction in fixational instability maintained a statistically significant difference between stabilized and unstabilized conditions. Percentages of correct discrimination dropped from 75% ($N = 177$) in the unstabilized condition to 68% ($N = 162$) in the stabilized condition for GD, and from 76% ($N = 148$) to 67% ($N = 98$) for AS. Both differences were significant at the 0.05 levels according to one-tail z tests (AS: $z = 1.87$, $p < .05$; GD: $z = 1.68$, $p < .05$). In contrast, TC, who exhibited a substantial reduction in fixational instability, performed

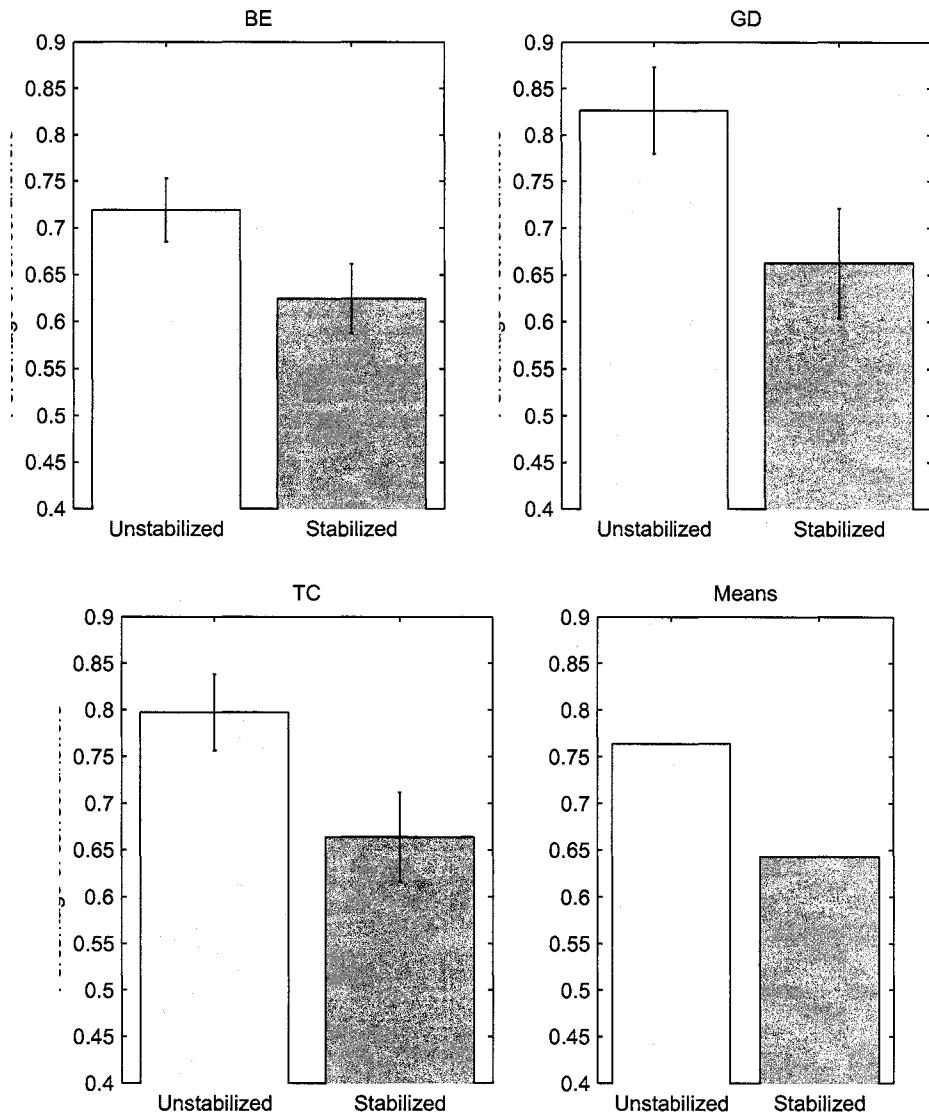


Figure 3.6: Percentages of correct discrimination obtained in Experiment 2 when the stimulus was presented for 0.5 s. The results for each subject as well as the overall means are shown. The two bars illustrate the results obtained under stabilized and unstabilized visual conditions. Error bars at the 0.05 significance levels are shown.

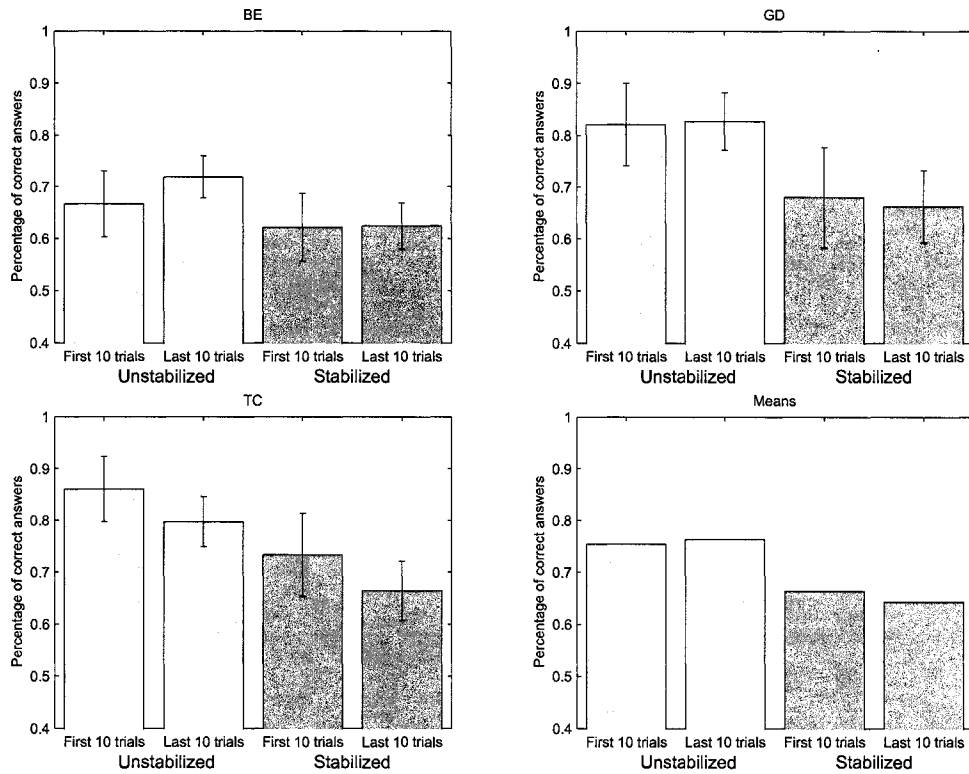


Figure 3.7: Percentages of correct discrimination in early and late trials of Experiment 2. The results for each subject as well as the overall means are shown. Percentages of correct discrimination obtained in the first 10 trials of each block of 25 consecutive trials are compared to those obtained in the last 10 trials. Bars of different intensity illustrate the results obtained under stabilized and unstabilized conditions. Error bars at the 0.05 significance levels are shown.

at an equally low level in both conditions: 66% ($N = 95$) in the unstabilized condition and 64% ($N = 91$) in the stabilized condition ($z = 0.25$, $p > .05$).

Thus, the difference in performance that was found between unstabilized and stabilized conditions in Experiments 1 and 2 was still visible under sustained fixation in Experiment 3, for the two subjects who maintained a substantial degree of fixational instability.

3.3.4 Oculomotor activity

During free-viewing, when the head is not restrained and movements of the eye combine with movements of the head and body, a considerable degree of retinal image motion occurs during the periods of visual fixation. In our main experiments (Experiments 1 and 2), to approximate free-viewing conditions and enhance fixational instability, stimulus presentation was preceded by a saccade. Table 3.1 summarizes oculomotor activity in the unstabilized condition (i.e., when subjects were free to move their eyes on the stimulus) of Experiments 1 and 2. To estimate fixational instability during a trial, we measured the spatial amplitude of drift periods and the amplitude of fixational saccades. Drift amplitude was defined as the length of the segment joining the initial and final positions of the eye during a fixation. Saccades were detected by a velocity threshold of $10^\circ/\text{s}$. Although individual differences were present, all subjects exhibited a significant degree of fixational instability with both drift and saccades: On average, the amplitude of drift was $7.7'$ in Experiment 1 and $4.5'$ in Experiment 2. The mean amplitude of saccades was $27'$ in both Experiments 1 and 2. Not surprisingly, subjects executed more saccades during the longer stimulus presentation of Experiment 1 (2 s) than in Experiment 2 (500 ms). The mean number of saccades was 3.0 in Experiment 1 and 0.2 in Experiment 2.

Although fixational saccades appeared to improve performance, they were not sufficient to account for the difference between percentages of correct discrimination in the stabilized and unstabilized conditions. In Figure 3·9, the unstabilized trials were classified depending on whether or not they included a fixational saccade. The presence of a fixational saccade clearly enhanced performance for all three subjects. However, a significant difference was

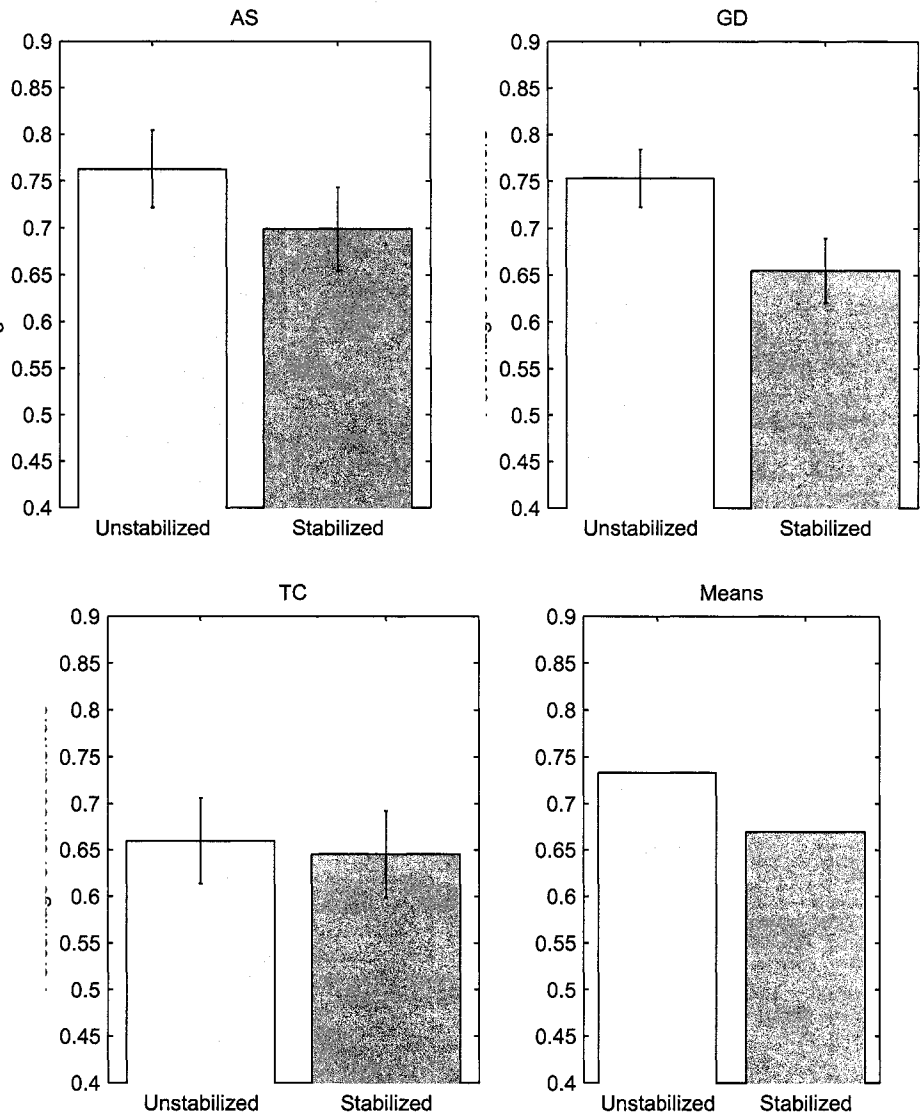


Figure 3·8: Percentages of correct discrimination obtained in Experiment 3. The results for each subject as well as the overall means are shown. The two bars illustrate the results obtained under stabilized and unstabilized visual conditions. Error bars at the 0.05 significance levels are shown.

Experiment 1 (2 s)	BE	TC	GD	Means
Average number of saccades	4.5	1.9	2.5	3.0
Average saccade amplitude	24.8	38.3	17.8	27.0
Average drift amplitude	8.7	7.8	6.5	7.7
Experiment 2 (500 ms)	BE	TC	GD	Means
Average number of saccades	0.3	0.1	0.3	0.2
Average saccade amplitude	24.8	39.6	17.9	27.4
Average drift amplitude	5.3	4.9	3.4	4.5

Table 3.1: Subject oculomotor activity in the unstabilized conditions of Experiments 1 And 2.

still present between stabilized trials and unstabilized trials in which no saccade occurred.

To estimate the overall spatial extent of fixational instability, we also evaluated the area of the rectangle defined by the SDs of the vertical and horizontal components of the eye position. Figure 10 shows the average area covered by fixational instability for GD and TC, the two subjects who participated in all three experiments. The mean area covered by fixational eye movements was 15 arc min² in Experiment 1 and 2.8 arcmin² in Experiment 2 for GD, and 76 arcmin² in Experiment 1 and 7 arcmin² in Experiment 2 for TC. In Figure 3·10, trials are sorted according to the subject’s response (i.e., whether the subject correctly or incorrectly reported the orientation of the target). Not surprisingly, the spatial span of fixational eye movements was much larger in Experiment 1 (with 2-s trials) than in Experiments 2 and 3 (with 500-ms trials). More interestingly, the average span of fixation was larger in correct trials than in incorrect trials. The only exception was TC in Experiment 3, the only case among all subjects and experiments in which the difference between percentages of correct discrimination in stabilized and unstabilized conditions was not statistically significant. A larger fixational instability in successful trials is consistent with the hypothesis of a contribution of fixational eye movements in visual discrimination.

3.4 Discussion

During visual fixation, small movements of the eyes and the head keep the projections of the scene onto the retina in constant motion. It is unclear whether this fixational insta-

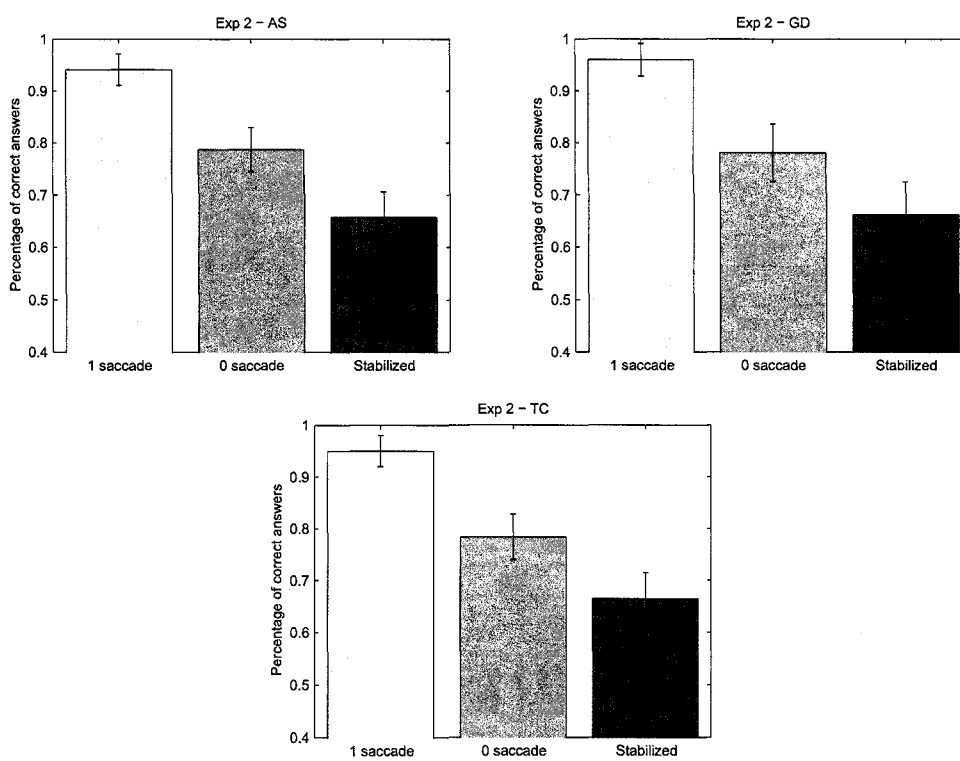


Figure 3.9: Percentages of correct discrimination in unstabilized trials that included one fixational saccade (left) and no fixational saccade (center), and in stabilized trials (right).

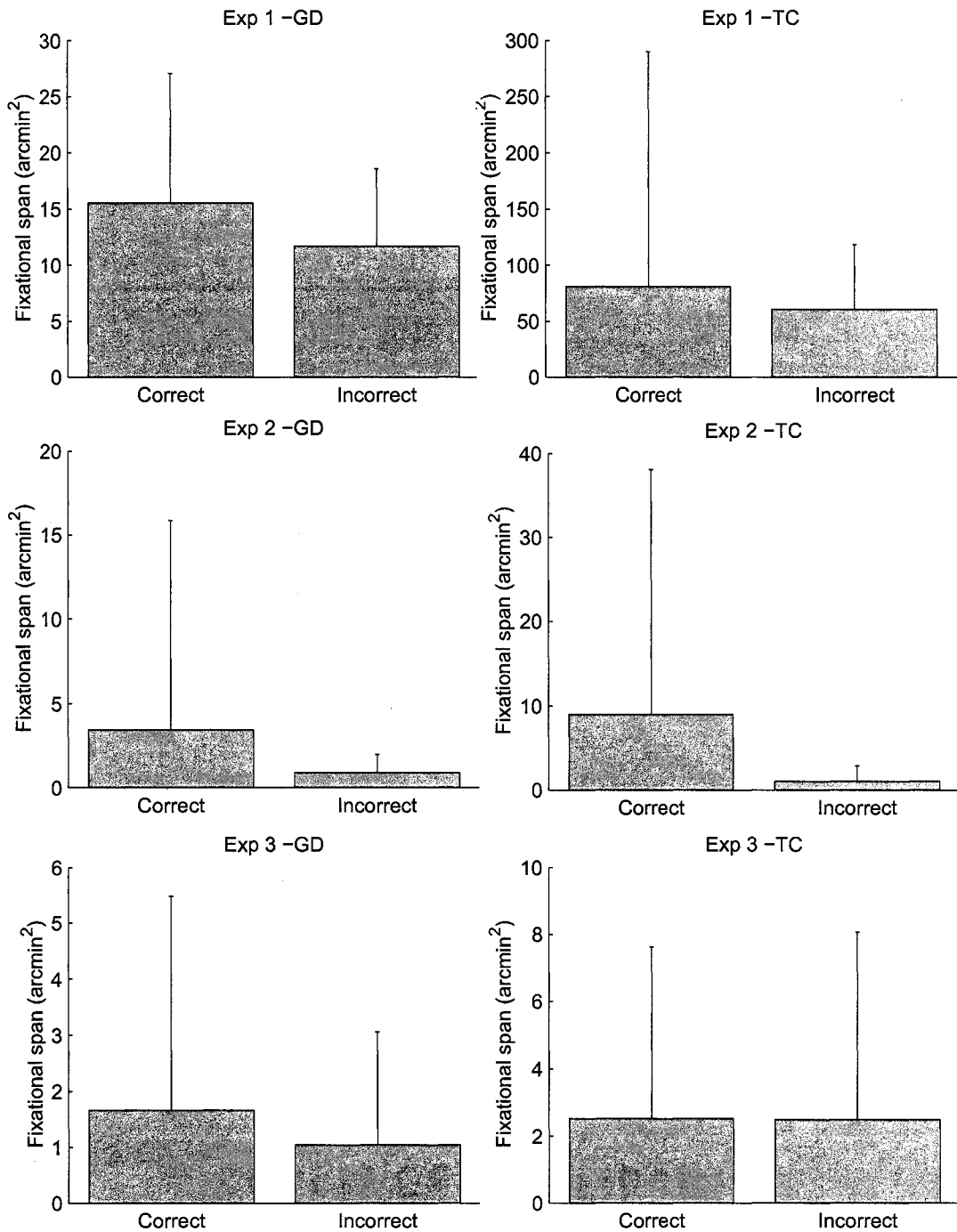


Figure 3.10: Mean area covered by fixational eye movements in unstabilized trials as a function of the subject response (correct or incorrect) for GD and TC, who took part in all three experiments.

bility serves a useful purpose in natural viewing conditions, when fixation typically lasts a few hundreds milliseconds. By showing an impairment in visual discrimination of briefly presented stimuli, the results of our experiments are consistent with the hypothesis that the motion of the image on the retina plays a role in refreshing, and possibly structuring, neural activity during the brief periods of visual fixation.

3.4.1 Stabilization of briefly presented stimuli

The analysis of visual performances in the presence of stabilized retinal images dates back more than half a century. Initial studies were stimulated by dynamic theories of visual acuity, which argued for a role of the motion of the eye in hyperacuity (Averill and Weymouth, 1925; Marshall and Talbot, 1942). These theories were disproved by the first pioneering efforts in eliminating fixational eye movements (Riggs et al., 1953; Keeseey, 1960). Interest in stabilized vision was then renewed by the discovery that images tend to fade away in the absence of motion on the retina. While many experiments have investigated image fading when stimuli are presented for various durations ranging from tens of seconds to minutes (Riggs and Ratliff, 1952; Ditchburn and Ginsborg, 1952; Barlow, 1963; Evans, 1965; Gerrits et al., 1966; Yarbus, 1967; Keeseey, 1969; Koenderink, 1972; Kelly, 1979a), few studies have considered fixational instability within the context of the brief interval of natural visual fixation.

Previous experiments on stabilization of briefly presented stimuli have found no significant differences with respect to the case in which normal retinal motion occurs. Indeed, it has been reported that acuity for such diverse targets as black lines, vernier displacements, and gratings improves as a function of exposure duration in a similar way for the stabilized and the normally moving retinal image, and similar absolute values of acuity were obtained in both cases (Keeseey, 1960). Furthermore, similar thresholds were found for detecting stabilized and unstabilized gratings with exposure duration ranging from a few milliseconds to 4 s (Tulunay-Keeseey and Jones, 1976). These previous findings are in agreement with our measurements of contrast sensitivity functions, which produced very

similar thresholds with stimulus exposures of 500 ms and 2 s in stabilized and unstabilized conditions. However, they are in sharp contrast with the results of our discrimination experiments in which the absence of retinal image motion significantly impaired subject performances. This different effect of retinal stabilization in contrast sensitivity and orientation discrimination may originate from a number of sources: The experiments differed not only in the task, but also in the stimuli and procedure.

A first important difference was the level of stimulus noise. Whereas contrast sensitivity was measured by means of noise-free gratings at different spatial frequencies, a high level of noise corrupted the stimuli of our discrimination experiments. As described in the second part of the Discussion, stimulus noise may enhance the impact of modulations of neural responses due to fixational eye movements. This is consistent with the results of some preliminary experiments with different noise densities (data not shown), which showed a more significant impact of stabilization with higher levels of noise.

A second important difference was the degree of fixational instability. In previous studies (Keeseey, 1960; Tulunay-Keeseey and Jones, 1976), subjects maintained fixation during presentation of gratings. It is known that eye movements are reduced in this condition of sustained fixation (Steinman et al., 1967; Kapoula et al., 1986a). It is possible that a reduction in the amount of fixational instability attenuated the difference between stabilized and unstabilized contrast sensitivity thresholds. In our main experiments (Experiments 1 and 2), to approximate the fixational instability that occurs during natural viewing, subjects were required to perform a saccade toward a cued location in the unstabilized trials.

Despite the brief durations of stimulus presentation, the retinal image moved considerably in the unstabilized trials. Both small saccades and drifts contributed to move the stimulus. All subjects made small saccades in both Experiment 1 and 2. No systematic relationship could be seen between subject performances and the shifts in fixation point operated by these saccades. Given the small size of the bar, which could be comfortably seen with a single fixation, it is unlikely that saccades were used to redirect the fovea to different regions of the stimulus. Similarly, the opposite hypothesis (i.e., that saccades

were performed in an attempt to move the fovea away from the stimulus, thus low-pass filtering the image by means of the lower resolution of the visual periphery) is also unlikely given the small size of saccades. We did not attempt to distinguish between possible contributions of different types of small eye movements for two main reasons. First, during natural vision, eye movements combine with other movements of the head and body, and it becomes difficult to extrapolate data obtained with a constrained head to more natural viewing conditions. Second, the results of our computer simulations suggest that if a sufficient degree of retinal image motion is present, different types of eye movement have a similar effect on the second-order structure of neural activity, as long as they occur within a spatial window of comparable size.

As in any study involving retinal stabilization, one may question the accuracy with which retinal motion was eliminated. In our experiments, particular care was taken in eliminating movements of the head, calibrating the stimulus deflector individually for each subject, and minimizing possible sources of noise. Image stabilization was achieved by means of a stimulus deflector directly coupled to the DPI eyetracker, a device with a response time of 6 ms and spatial resolution of 10'' (Crane and Steele, 1978). While perfect retinal stabilization of exoptic images is not possible, both the disappearance of afterimages during the calibration phase and the different levels of subject performance measured in the stabilized and unstabilized conditions argue for a high quality of retinal stabilization.

3.4.2 Predictions from neural modeling

The discrimination experiment described in this work was designed on the basis of our recent computational work on modeling neuronal responses during oculomotor activity. Neurophysiological investigations of the visual cortex of the macaque, a species with visual and oculomotor characteristics similar to those of humans, have shown that neurons in the striate cortex respond to small changes in the visual signals produced by fixational saccades and ocular drift (Gur et al., 1997; Leopold and Logothetis, 1998; Martinez-Conde et al., 2000; Snodderly et al., 2001). Our simulations of Lateral Geniculate Nucleus and V1

neuronal responses during eye movements indicate that the jittering of the image on the retina contributes to shaping the second-order statistics of thalamic and thalamo-cortical neural activity during visual fixation (Rucci et al., 2000; Rucci and Casile, 2004). The second-order statistical structure of neural activity acquires particular importance in the light of theories that propose a role for synchronous modulations of neural activity in transmitting visual information (Singer and Gray, 1995; Singer, 1999).

Figure 11 illustrates the putative effect of fixational instability on the statistical structure of neural activity for the task considered in this work. The receptive fields of three geniculate cells are shown: Cells A and B are centered on the stimulus bar (a -45° bar), while the receptive field of cell C is located on the background in a position that would be covered by a bar of opposite orientation (a $+45^\circ$ bar). Due to the noise in the stimulus pattern, it is assumed that cells A and C possess a high mean level of activity, whereas cell B settles on a lower level. During visual fixation, the motion of the retinal image modulates the activity of the three cells in different ways. Fixational modulations tend to be synchronous in cells A and B that are activated by the stimulus bar, and occur with independent temporal dynamics in cell C. The results of our modeling work suggest that these short-lived modulations of thalamic responses are effective in activating cortical cells and may thus help disambiguate confusing input signals. For the stimulus configuration of Figure 11, the emerging prediction is that subjects are more likely to report the presence of a -45° bar (covering the receptive fields of cells A and B) under normal visual conditions, and a $+45^\circ$ bar (covering the receptive fields of cells A and C) under stabilized conditions when, in the absence of fixational modulations, the mean levels of neural responses have a stronger influence on the activity of postsynaptic neurons.

Mathematically, the prediction of our model can be characterized in terms of a different influence of the levels of correlation (the mean of the product of two signals) and covariance (the mean of the product of two signals with their averages removed) of cell responses. Due to the high average level of activity, cells A and C are more strongly correlated than cells A and B. Cells A and B, however, possess a higher level of covariance during the normal

jittering of visual fixation, because their responses tend to be modulated synchronously by fixational eye movements. Our model predicts that responses of neurons at later stages in the visual hierarchy are more strongly affected by patterns of correlated activity during stabilized vision and by levels of covariance during normal vision.

3.5 Conclusion

Both the impairment in visual discrimination observed under retinal stabilization and the higher degree of fixational instability observed in successful trials are consistent with the hypothesis that fixational instability plays a role in structuring neural activity during the brief periods of visual fixation. In addition, a comparison of the results of Experiments 1 and 2 suggests that the difference in performance between stabilized and unstabilized conditions is larger with a 2-s stimulus duration. This is also consistent with the predictions of the model that a longer presentation of the stimulus should result in an improvement in discrimination performances by allowing both a more prolonged period for affecting the statistical structure of neural activity and a larger instability of visual fixation.

Regardless of the actual sources of instability, small saccades, ocular drifts, and/or combinations of movements of the eye and the head, a substantial degree of retinal image motion occurs during natural vision. In addition to humans, fixational instability has been observed in every species for which eye movements have been recorded, including the monkey (Skavenski et al., 1975b; Motter and Poggio, 1984; Snodderly and Kurtz, 1985; Snodderly, 1987), the cat (Pritchard and Heron, 1960; Hebbard and Marg, 1960; Winterson and Robinson, 1975; Conway et al., 1981b), the rabbit (Collewijn and van der Mark, 1972), the turtle (Greschner et al., 2002) and even the owl (Steinbach and Money, 1973), a species whose eyes are often considered immobile. The results of this work provide support to the hypothesis that this jittering plays a role even within the brief periods of visual fixation. Further studies are needed to determine the precise nature of this role and its relevance in the presence of more natural visual stimulation.

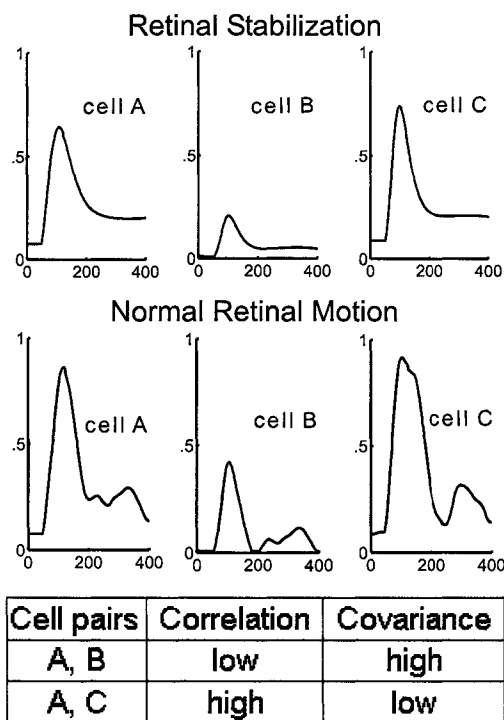
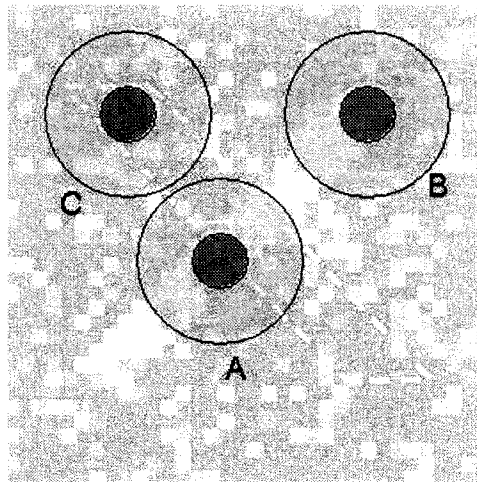


Figure 3.11: The rationale leading to the design of the experiments. The receptive fields of three ON-center geniculate cells are shown overlapped on the bar stimulus. The graphs illustrate the response of each cell during a stabilized and an unstabilized trial. The table shows the levels of correlation and covariance of activity.

Chapter 4

Fast decorrelation across primate retinal ganglion cells due to fixational eye movements

4.1 Introduction

In this chapter, we report a neural modeling project investigating the influence of fixational eye movements on the spatial and temporal structure of correlated activity in populations of retinal ganglion cells. The responses of primate retinal ganglion cells were simulated while their receptive fields scanned natural images following pre-recorded eye movements patterns. These eye movements were recorded in humans using the DPI eyetracker described in section 2.1.4. The experimental conditions were analogous to those described in Chapter 3, except that the subjects were freely viewing images of natural scenes. The use of macaque cells in conjunction with human eye movements is justified by the similarity of eye movements patterns across both species (Skavenski et al., 1975a; Motter and Poggio, 1984; Snodderly and Kurtz, 1985; Snodderly, 1987).

Firing synchrony, and more generally, neural dynamics are crucial to understanding how the brain processes sensory information. Although the specific mechanisms are still debated, it is now widely acknowledged that spatiotemporal patterns of neural activity carry information in the nervous system (Abeles, 1991; Arieli et al., 1995; Singer and Gray, 1995; Diesmann et al., 1999; Usrey and Reid, 1999; Ikegaya et al., 2004; Kerr et al., 2005). In fact, some have argued that precise temporal correlation could be used as an additional information channel (Dan et al., 1998). Similarly, bursts of spikes in single neurons (Martinez-Conde et al., 2000) could correspond to highly synchronous activity in the ensemble, and might provide a “reset” signal for temporal coding mechanisms (Usrey

and Reid, 1999; Gaarder, 1968).

In the visual system, stimulus-dependent synchrony is an important source of correlation in cell activities (Usrey and Reid, 1999). Common input as well as shared circuitry can induce synchronous spiking in neighboring retinal ganglion cells (RGCs) (Puchalla et al., 2005). Correlations due to common input might signal the presence of important features in the visual scene, such as an edge or an object (Singer and Gray, 1995). Synchronous spiking of neighboring retinal ganglion cells (RGCs) has been described in mammals, among others (Rodieck, 1967; Arnett and Spraker, 1981; Mastronarde, 1983a,b, 1989; Meister et al., 1995; Meister, 1996; Brivanlou et al., 1998). However, synchrony can also come from spurious correlations in the visual input, particularly in the presence of highly correlated images such as natural scenes. The intensity values of the pixels representing a natural image tend to be highly correlated both in space and in time (Field, 1987). A visual system relying on spikes should discard these “uninteresting” correlations so as not to confound them with relevant correlations that convey important information. Information theoretic considerations proposed that a redundancy reduction mechanism is needed to compensate for the information bottleneck created by the optic nerve (Attneave, 1954; Barlow, 1961). One possible way to reduce redundancy is to eliminate pairwise correlations among neurons. Spatial decorrelation in the retina has been proposed, but never conclusively demonstrated. Theoretically, natural images can be decorrelated by center-surround spatial filters qualitatively similar to the receptive fields of RGCs (Srinivasan et al., 1982; Atick and Redlich, 1990, 1992; van Hateren, 1992), but these theoretically-derived filters do not agree quantitatively with neurophysiological measurements which show that real RGCs are significantly more sensitive to low spatial frequencies than the ideal, decorrelating spatial filter (e.g., Croner and Kaplan, 1995). Early theories of neural decorrelation focused on spatial receptive fields and did not consider cell sensitivity to time-varying input. Although these theories were later extended to the temporal domain (Dong and Atick, 1995a,b; Dan et al., 1996), they only considered temporal variations in the visual scene itself. They did not account for the most important source of retinal motion, which is self-motion.

Previous modeling studies from our lab suggest that fixational eye movements might play an important role in the correlational structure of neural activity (Rucci et al., 2000; Rucci and Casile, 2004, 2005; Casile and Rucci, 2006). These studies examined the long-term influence of fixational eye movements on correlated activity in models of cat LGN and V1 neurons. The initial transient response following a saccade was discarded to focus on the steady-state case corresponding to the end of a period of fixation, and synthetic eye movements were generated from random processes.

The present study differs in two important ways. First, we investigated the typical temporal evolution of correlation among RGCs during the time course of short periods of fixation, to distinguish how the influence of oculomotor activity differs at various times with respect to the occurrence of saccades. Second, we simulated primate retinal ganglion cells in the presence of real patterns of eye movements. We modeled the two main types of primate RGCs, magnocellular-projecting parasol (M) cells and parvocellular-projecting midget (P) cells, which are known to have substantially different response properties: M cells are transient, while P cells have sustained responses. The receptive fields of populations of RGCs scanned natural images following eye movements patterns previously recorded in human subjects. We found striking differences in the dynamics of spatial patterns of synchronous activity among cells, depending on their type (M or P). These results suggest that fixational eye movements might contribute to a neural encoding scheme in which different properties of the stimulus are represented at different periods during visual fixation.

4.2 Methods

Visual stimulation

To replicate the spatiotemporal input to the retina that occurs under natural viewing conditions, the responses of macaque RGCs were simulated as their receptive fields followed the trajectories of recorded eye movements. In the main simulations of this study, the visual inputs consisted in 20 gray-scale photographs of natural scenes chosen from a public

domain database (van Hateren and van der Schaaf, 1998). The average power spectrum of these images was best fit by $1/f^{2.02}$, which is consistent with other measurements of the power spectrum of natural images (Field, 1987; Ruderman, 1994). In these images one pixel corresponded to $1'$ of visual angle, and each image spanned a visual field of 17×17 square degrees.

In control simulations we used three sets of 20 artificially generated images consisting of noise with predefined power spectra varying as $1/f^2$, $1/f^3$ and $1/f^4$ with spatial frequency f . These images were generated by filtering white noise patterns with appropriate spatial kernels.

The spatiotemporal input to simulated retinal neurons, $I(\mathbf{x}, t)$, was produced by moving the receptive fields of modeled cells following trajectories of eye movements. These traces were recorded from four human observers with normal vision during free-viewing of the same 20 natural images used in the neural simulations. The use of human eye movements to simulate neural responses in the macaque retina is justified by the similarity of human and macaque eye movements (Snodderly and Kurtz, 1985; Snodderly, 1987). Eye movements were recorded with a Generation 6 Dual-Purkinje-Image eyetracker (Fourward Technologies Inc., Buena Vista, VA). This device has a nominal time delay of approximately 0.25 ms and a spatial resolution of $1'$ (Crane and Steele, 1985; Stevenson and Roorda, 2005) and therefore enables to record the fine eye movements that occur during visual fixation. A dental imprint bite bar and a forehead rest prevented movements of the head. Vertical and horizontal eye position data were sampled at 1 kHz and low-pass filtered at a 100-Hz cutoff frequency. Informed consent was obtained from all subjects following the procedures approved by the Boston University Charles River Campus Institutional Review Board.

In control simulations, to study the influence of the amplitude of eye movements, we used synthetic fixational eye movements modeled as random walks with various step sizes. Two symmetric random walks simulated horizontal and vertical eye position, respectively. We drew 30 random locations on each of the 20 images as starting points for fixation, and for each of these 600 fixations, we generated 300-ms sequences of synthetic fixational eye

movements, as follows. For each of the two random walks, the initial pixel position was drawn from a uniform distribution on the image, and thereafter a new step was drawn every 1 ms from a normal distribution with zero mean and standard deviation σ in the range $0.3'$ – $6'$. To evaluate the spatial extent of the region covered by these 300-ms synthetic fixations, we measured the “angular span” of each fixation path by computing the maximum distance from the centroid of the path to each of its points. The average angular span depended on σ . In our simulations, we used $\sigma = 0.3', 3', 6'$, which corresponded to average spans of $5.7', 57'$, and $115'$, respectively.

Modeling neuronal responses

The responses of RGCs were simulated using spatiotemporal kernels as in Enroth-Cugell et al.’s (1983) classical model. Following convention, we term magnocellular-projecting parasol ganglion cells, “M cells” and parvocellular-projecting midget ganglion cells, “P cells”. We modeled populations of ON-center M and P cells using receptive field parameter values taken from two categories: parafoveal (0 – 5° eccentricity) and peripheral (20 – 30° eccentricity). Parameter values for each of the four types of cells (“Parafoveal M”, “Parafoveal P”, “Peripheral M”, “Peripheral P”) were taken from corresponding neurophysiological measurements of macaque RGCs (Croner and Kaplan, 1995; Benardete and Kaplan, 1997a, 1999a,b). For each population, we simulated 305 cells arranged on a pattern composed of 19 concentric circles with 16 cells on each circle and one cell at the center of the population. The radii of the circles varied from $5'$ to $95'$ in steps of $5'$.

The response of a model cell to visual stimulation was defined as the deviation in the instantaneous firing rate with respect to the level of spontaneous activity. The visual response at time t of a cell at location $\mathbf{z} = (x, y)$ in the retina, $\alpha_{\mathbf{z}}(t)$, was computed as the temporal convolution between the spatiotemporal stimulus $I(\mathbf{x}, t)$ —the movie obtained by sampling the image following eye movements—and the cell spatiotemporal kernel $h_{\alpha}(c, \mathbf{x}, t)$,

followed by rectification, such that

$$\alpha_{\mathbf{z}}(t) = \left[\int_{S_z} \int_{-\infty}^t h_{\alpha}(c, \mathbf{x}', t') I(\mathbf{x}', t - t') d\mathbf{x}' dt' \right]_{\beta} \quad (4.1)$$

where c parametrizes the local level of contrast, S_z is the area of the retina spanned by the cell's receptive field, and the operator $[\cdot]_{\beta}$ indicates rectification with threshold β , *i.e.*, a threshold-linear static nonlinearity such that $[z]_{\beta} = z - \beta$ if $z > \beta$, and $[z]_{\beta} = 0$ if $z \leq \beta$. Time was discretized in 1-ms steps.

RGC kernels measured physiologically are not space-time separable because the response elicited by stimulation of the surround is delayed relative to the response to stimulation of the center (Enroth-Cugell et al., 1983; Dawis et al., 1984). In order to account for this center-surround delay, the spatiotemporal kernel $h_{\alpha}(c, \mathbf{x}, t)$ was modeled as in Cai et al. (1997) by the sum of two space-time separable terms representing the contributions from the center and surround of the receptive field, respectively, as in

$$h_{\alpha}(c, \mathbf{x}, t) = h_{\text{cnt}}(c, \mathbf{x}, t) + h_{\text{srn}}(c, \mathbf{x}, t) = g_{\text{cnt}}(c, t) f_{\text{cnt}}(\mathbf{x}) + g_{\text{srn}}(c, t) f_{\text{srn}}(\mathbf{x}) \quad (4.2)$$

where g_{cnt} and f_{cnt} are the temporal and spatial components of the center, and g_{srn} and f_{srn} those of the surround. The spatial kernels $f_{\text{cnt}}(\mathbf{x})$ and $f_{\text{srn}}(\mathbf{x})$ were modeled as two-dimensional Gaussian functions with amplitudes A_{cnt} and A_{srn} and standard deviations σ_{cnt} and σ_{srn} . Spatial parameters were set to median values measured in macaque RGCs in the parafoveal and peripheral regions of the visual field (Croner and Kaplan, 1995).

Following the model introduced by Victor (1987) for cat RGCs, the temporal profile of the receptive field center, $g_{\text{cnt}}(c, t)$, was computed as the inverse Fourier transform of the temporal-frequency response $K(c, \omega)$ to a sine-wave grating whose contrast c was modulated at temporal frequency ω . This model, described below, has been successfully applied to fit data from macaque RGCs (Benardete et al., 1992; Benardete and Kaplan, 1997a, 1999a,b). The temporal-frequency response $K(c, \omega)$ was modeled by the series of a

set of low-pass filters and a high-pass stage in the form of

$$K(c, \omega) = Ae^{-i\omega D} \left(1 - \frac{H_S}{1 + i\omega\tau_S} \right) \left(\frac{1}{1 + i\omega\tau_L} \right)^{N_L} \quad (4.3)$$

where D represents the initial delay of transmission from the optic chiasm to the retina; A , the overall gain; H_S , the strength of the subtractive stage; τ_S , the time constant of the high-pass stage; τ_L , the time constant of the low-pass stages; and N_L , the number of low-pass stages (Victor, 1987; Benardete et al., 1992). As with spatial parameters, temporal parameters of the model were set to median values measured in macaque RGCs (P cells: Benardete and Kaplan, 1997a; M cells: Benardete and Kaplan, 1999a). The temporal profile of the surround, $g_{\text{srn}}(c, t)$, was similar to that of the center, except for a center-surround delay τ_{CS} , such that

$$g_{\text{srn}}(c, t) = g_{\text{cnt}}(c, t - \tau_{\text{CS}}).$$

The value of τ_{CS} was generally set to 3 ms. Control simulations examined the effect of varying τ_{CS} between 0 and 10 ms, which is the range of center-surround delays measured in neurophysiological studies of RGCs and lateral geniculate nucleus neurons in macaque (Smith et al., 1992; Benardete and Kaplan, 1997a, 1999b; Reid and Shapley, 2002).

In the case of P cells, the stimulus contrast c is known to have little influence on the receptive field properties (Smith et al., 1992; Lee, 1996; Benardete and Kaplan, 1997a, 1999b). M cells, however, exhibit a mechanism of contrast gain control by which the temporal profile changes with stimulus contrast (Shapley and Victor, 1978, 1979; Kaplan and Shapley, 1986; Benardete et al., 1992; Lee et al., 1994; Benardete and Kaplan, 1999a). In the model of M cells, the value of τ_S in (4.3) varied as a function of contrast c such that

$$\tau_S(c) = \frac{T_0}{1 + \left(\frac{c}{C_{1/2}} \right)^2}, \quad (4.4)$$

where T_0 is the time constant at zero contrast and $C_{1/2}$ represents the contrast at which τ_S is half its initial value (Victor, 1987; Benardete and Kaplan, 1999a). In this study,

the average contrast was 12%, except in control simulations. This value is consistent with estimates of the average contrast in natural scenes (Ruderman, 1994; Brady and Field, 2000).

Since activity in the model was defined as the variation around the spontaneous firing rate, a positive response means that the current firing rate is higher than the spontaneous firing rate, while a negative response corresponds to a firing rate lower than the spontaneous firing rate. Rectification was present in the model to account for the asymmetry between the possible ranges of negative and positive responses. Real firing rates can increase largely above the spontaneous firing rate but they cannot go below zero. In the simulations, the rectification level was defined as the percentage of the range of negative activity that rectification eliminated from the linear model (*i.e.*, the model without rectification). Unless otherwise specified, we used 50% rectification, meaning that half of the range of negative activity of the unrectified model was eliminated.

Statistical analysis of simulated neural activity

We examined the temporal evolution of spatial patterns of correlated activity during a 300-ms period of fixation, which is the typical duration of intersaccadic intervals (Harris et al., 1988; Andrews and Coppola, 1999). The correlation between the responses $\alpha_{\mathbf{x}_i}(t)$ and $\alpha_{\mathbf{x}_j}(t)$ of a pair of cells located at positions \mathbf{x}_i and \mathbf{x}_j was evaluated at several times t_k following fixation onset. At each time t_k , levels of correlation were computed over a time interval of duration T centered at t_k , as in

$$r_{\mathbf{x}_i\mathbf{x}_j}(t_k) = \langle \alpha_{\mathbf{x}_i}(t) \alpha_{\mathbf{x}_j}(t) \rangle_{[t_k - \frac{T}{2}, t_k + \frac{T}{2}]} = \frac{1}{T} \int_{t_k - \frac{T}{2}}^{t_k + \frac{T}{2}} \alpha_{\mathbf{x}_i}(t) \alpha_{\mathbf{x}_j}(t) dt. \quad (4.5)$$

Levels of correlation $r_{\mathbf{x}_i\mathbf{x}_j}(t_k)$ were averaged over all pairs of simulated cells whose receptive fields were separated by the same distance d , and averaged over a large set of fixations \mathcal{F}

on the database of natural images, giving the spatial correlation function

$$r(d, t_k) = \left\langle \left\langle r_{\mathbf{x}_i \mathbf{x}_j}(t_k) \right\rangle_{|\mathbf{x}_j - \mathbf{x}_i| = d} \right\rangle_{\mathcal{F}}.$$

In the main simulations, we used a total of $n = 522$ fixations, each with a different pattern of recorded eye movements. In control simulations using synthetic fixational eye movements, we used 30 fixations on each image, for a total of $n = 600$ fixations.

In the rest of this chapter we use the term “correlation” to refer to a normalized version of the spatial correlation function, such that a cell auto-correlation (*i.e.*, the correlation for a receptive field separation $d = 0$) had unit amplitude. We focused on two time intervals: the first 100 ms after fixation onset, which we call Early Fixation, and the 200–300 ms interval after onset, referred to as Late Fixation. The procedure for measuring correlation is illustrated by the example in Figure 4·1.

4.3 Results

In this study we examined the temporal evolution, during visual fixation, of the spatial structure of correlated activity in retinal ganglion cells. Figure 4·1 explains the procedure followed to measure levels of correlation between the responses of pairs of cells. As illustrated in Figure 4·1*a*, to replicate the spatiotemporal input to the retina during natural viewing, the receptive fields of populations of modeled RGCs scanned natural images following sequences of recorded eye movements. Figure 4·1*b* shows the responses of three cells during a 300-ms period of visual fixation. After an initial burst of activity at fixation onset, the responses of the simulated cells were strongly modulated by the occurrence of fixational eye movements, as can be seen in the 100–300 ms interval.

As described in the Methods, the degree of coactivation of pairs of RGCs was quantified by the correlation across their responses at zero time delay. Levels of correlation were evaluated at several times during the course of a 300-ms fixation. They were averaged over a large number of fixations on different images, and also averaged over all pairs of simulated cells whose receptive fields were separated by the same distance d . The resulting pattern

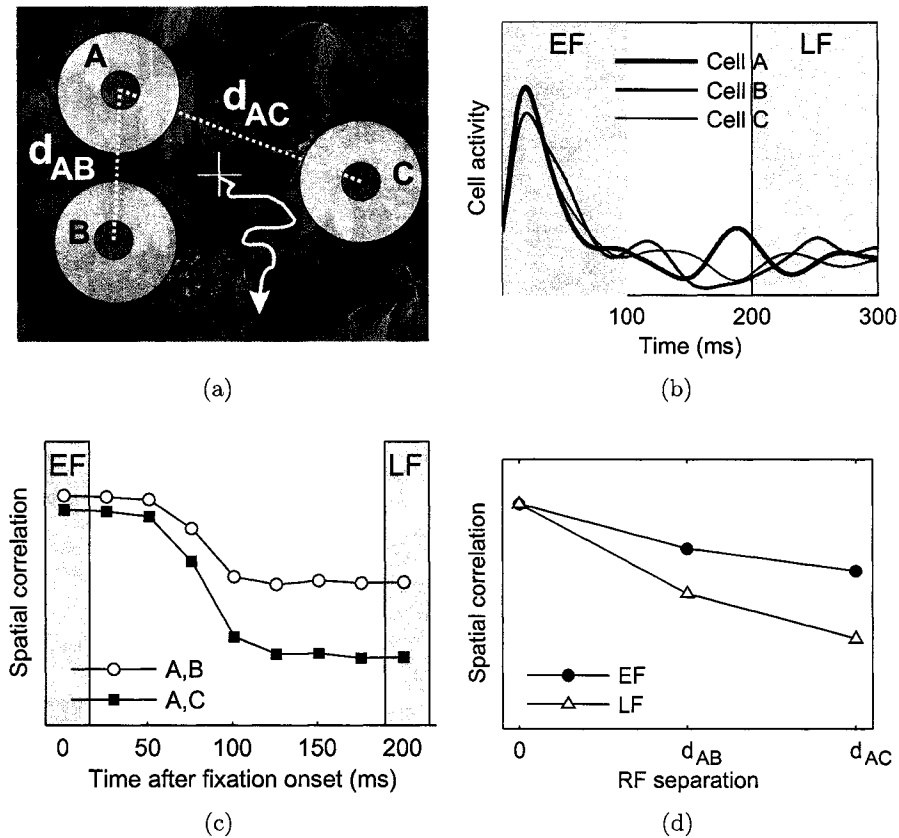


Figure 4-1: Procedure for measuring the dynamics of patterns of correlated activity in populations of model RGCs. (a) Cell responses were simulated while their receptive fields scanned images of natural scenes following sequences of recorded eye movements. The white arrow represents the motion of the gaze during a period of fixation. For clarity, only three cells, A , B , and C , are shown here; d_{AB} and d_{AC} represent the distances between the receptive field centers of the two pairs of cells (A, B) and (A, C), respectively. (b) Example of simulated neural responses during a 300-ms period of visual fixation. Two intervals of interest, Early Fixation (EF) and Late Fixation (LF), are highlighted in gray. (c) Correlation as a function of time after fixation onset for the two pairs of cells (A, B) and (A, C). (d) Correlation as a function of receptive field separation, plotted separately for the two periods of Early Fixation and Late Fixation.

of correlation was a function of two variables: t , the time relative to fixation onset at which correlation was evaluated, and d , the distance between the centers of two receptive fields. Figure 4·1*c* shows the time course of correlation during fixation, for the two pairs of cells of Figure 4·1*a*. In both curves, a data point at t represents the mean level of correlation evaluated over the 100-ms interval centered at t . In Figure 4·1*d*, the same data as in Figure 4·1*c* are replotted as a function of the separation between the receptive fields of the two cells. The two curves in this graph represent correlation during two different time intervals: 0–100 ms (Early Fixation) and 200–300 ms (Late Fixation).

The main results of our simulations are reported in Figure 4·2, which shows the typical evolution of correlated activity over the time course of a short period of fixation, as explained in Figure 4·1*c*. Each panel in Figure 4·2 shows the results of one of the four simulated neuronal populations: Parafoveal M cells, Parafoveal P cells, Peripheral M cells, and Peripheral P cells. In each panel, different curves represent mean levels of correlation between pairs of cells with receptive fields at different separations. At the onset of fixation, the sudden change in visual input resulted in wide pools of synchronously active cells in all simulated neuronal populations. As explained later in this section, this pattern of activity was a consequence of the broad spatial correlations present in natural images. In populations of P cells, both in the parafovea (Figure 4·2*a*) and in the periphery (Figure 4·2*b*), correlation changed little during the course of fixation. On the contrary, fixational eye movements strongly influenced levels of correlation in pairs of M cells. As shown in Figure 4·2*c,d*, levels of correlation sharply decreased soon after the onset of visual fixation in pairs of M cells with receptive fields separated by more than 5' in the parafovea, or 25' in the periphery. That is, in the presence of the normal instability of visual fixation, the spatial structure of correlated activity in populations of M cells quickly became unaffected by the broad correlations of natural scenes.

Levels of correlation in Figure 4·2 were evaluated over a temporal window of duration $T = 100$ ms. To achieve a finer temporal resolution, in Figure 4·3 we used windows of shorter durations. As shown by these data, levels of correlation started to decrease

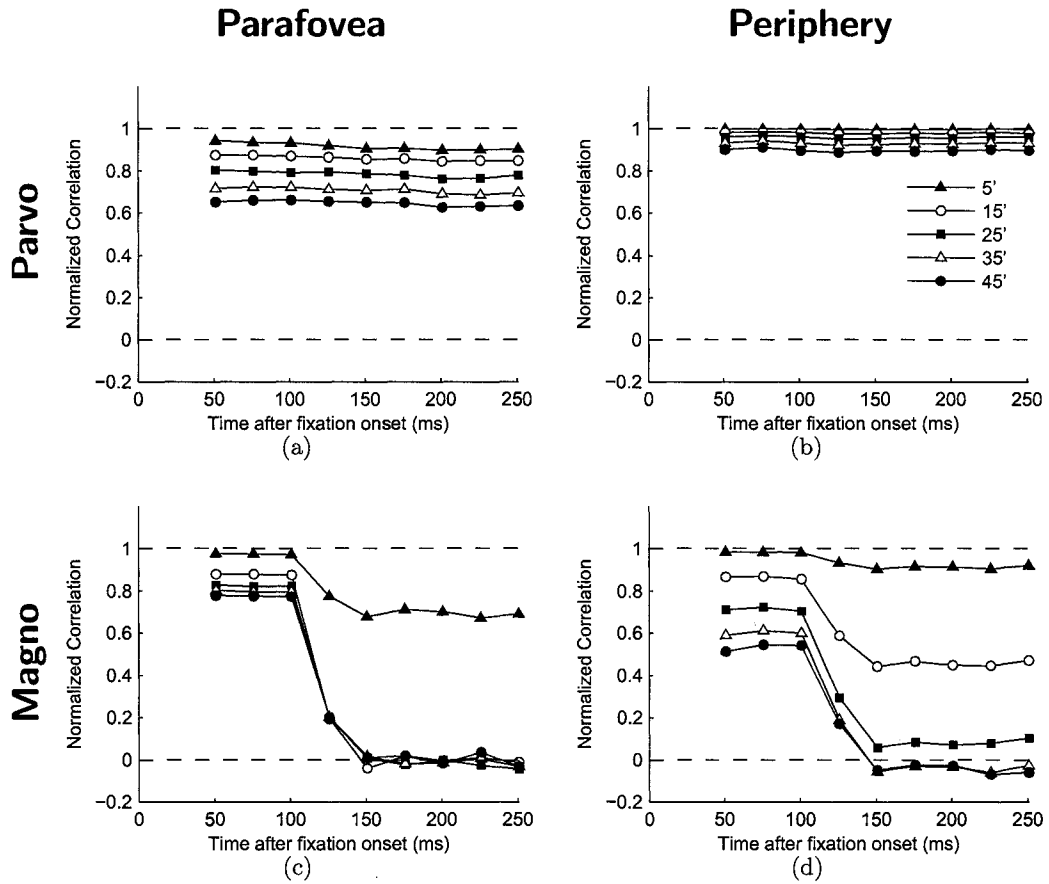


Figure 4.2: Dynamics of correlated retinal activity during visual fixation on natural images. Each panel shows the temporal evolution of the patterns of correlated activity in a given population of neurons: (a) parafoveal P cells, (b) peripheral P cells, (c) parafoveal M cells, (d) peripheral M cells. Each curve represents the dynamics of correlation between pairs of cells with receptive fields separated by a given distance in the range 5'–45'. A data point at time t represents pairwise correlation averaged over the $[t-50, t+50]$ interval and averaged over $n = 522$ periods of fixation on 20 different natural images. In this and the following figures (unless otherwise specified), the model parameter values were: 3-ms center-surround delay, 50% rectification, and 12% contrast level.

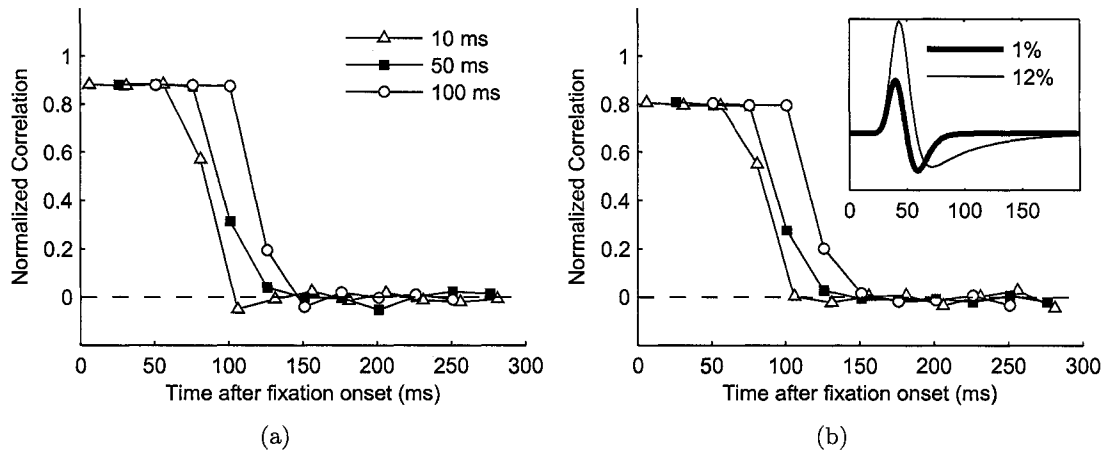


Figure 4.3: Influence of the duration of the correlation window on the dynamics of correlated activity in pairs of parafoveal M cells. Each curve represents levels of correlation evaluated over intervals of different durations T (see Eq. 4.5 in Methods) during the course of visual fixation. The two panels show the temporal evolution of correlated retinal activity for pairs of retinal ganglion cells with receptive fields centers separated by $15'$ (a) and $35'$ (b). The insert in (b) shows the temporal impulse responses of simulated M cells, for two different levels of contrast: 1% and 12%.

approximately 50 ms after the onset of fixation, and decorrelation was virtually completed by 100 ms after the onset of fixation. As shown in the insert in Figure 4.3(b), 50 ms correspond to the duration of the positive lobe of the temporal impulse response of M cells, while 100 ms is its entire duration. That is, cells became progressively uncorrelated as soon as they lost memory of the previous fixation.

In Figure 4.4, the same data as in Figure 4.2 are plotted again, this time as a function of the separation between receptive field centers. Only the correlation levels computed during the two time intervals of Early Fixation and Late Fixation are shown in this figure. During Early Fixation, correlation extended over several degrees of visual field, that is, even pairs of cells with little or no spatial overlap in their receptive fields were strongly correlated at the onset of visual fixation. In the case of P cells, fixational eye movements had little impact on levels of correlation: as shown in Figure 4.4a,b, the spatial structure of correlated activity during the period of Late Fixation was very similar to that present

during Early Fixation, independent of the visual eccentricity of cell receptive fields. The situation differed in the case of M cells, for which levels of correlation changed considerably during the course of visual fixation. For these cells, the spatial extent of correlated activity was considerably narrower during the period of Late Fixation than during Early Fixation. As shown in Figure 4·4c, in the parafoveal region, the responses of M cells with receptive fields as close as 15' became virtually uncorrelated in the presence of fixational eye movements. This distance was determined by the diameter of the receptive field center, which was 12' for parafoveal M cells in our model. Indeed, as shown in Figure 4·4d, the spatial extent of correlation was slightly broader across peripheral cells, which had larger receptive field centers (28'). Hence, when viewing natural images in the presence of fixational eye movements, the responses of pairs of M cells with non-overlapping receptive field centers became progressively less correlated during the time course of a typical fixation.

The dynamic decorrelation of M cell responses during visual fixation critically depended on three main factors: the sensitivity of M cells for luminance changes in their receptive fields, the small spatial region covered by fixational eye movements, and the second-order statistics of natural images. Figure 4·5 examines the impact of separately manipulating each of these factors.

To examine the relative contributions of spatial and temporal characteristics of cell responses to the dynamics of correlation, in control simulations we modified the temporal response characteristics of M cells to make them less transient, by substituting the impulse response of an M cell with that of a P cell. Therefore, the resulting modeled neurons were hybrid cells combining the spatial profile of a parafoveal M cell with the temporal sensitivity of a P cell. As shown in Figure 4·5a, levels of correlation among these cells remained high during the course of visual fixation, like in the case of P cells. Conversely, Figure 4·5b shows levels of correlation measured across hybrid cells which combined the spatial profile of a parafoveal P cell with the temporal sensitivity of an M cell. In this case, decorrelation occurred as in normal M cells. These results show that *it is the temporal properties of M cells, and not their spatial characteristics, that are responsible for the dynamic decorrelation*

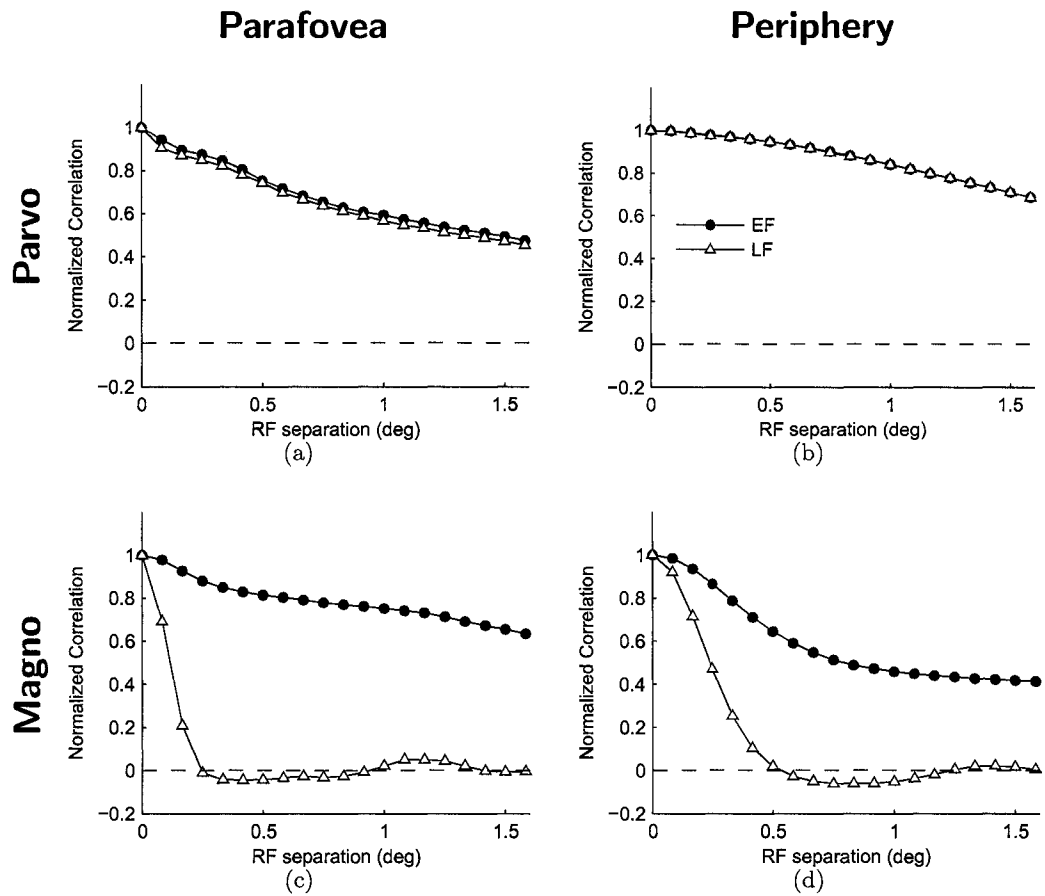


Figure 4.4: Spatial structure of correlated retinal activity during visual fixation on natural images. Data are the same as in Figure 4.2, but plotted as a function of the distance between receptive field centers. Only two time intervals are shown: Early Fixation (0–100 ms) and Late Fixation (200–300 ms).

found when natural images are viewed in the presence of fixational eye movements.

To study the influence of the spatial scale of fixational eye movements on the dynamics of correlated activity, we examined the structure of correlated activity obtained with synthetic fixational eye movements of various amplitudes. As explained in the Methods, these sequences of eye movements were generated as random walks with various step sizes. We used 5 different step sizes which, for 300 ms of fixation, corresponded to average angular spans of $0.6'$, $5.7'$, $29'$, $57'$, and $115'$, respectively. For each amplitude, we simulated a total of 600 fixations, randomly localized on the 20 natural images of our database. As shown in Figure 4·5b, decorrelation was more pronounced for eye movements smaller than 1° than for larger ones. This result explains why decorrelation between the responses of M cells occurs during small eye movements of fixation, but not in the presence of larger eye movements such as saccades.

To examine the influence of the second-order statistics of natural images on the dynamic decorrelation of M cells responses, we examined the patterns of correlated activity during viewing of artificial images with various power spectra. As explained in the Methods, images with power spectra varying as $1/f^2$, $1/f^3$, and $1/f^4$ with spatial frequency f were created by filtering white noise images with appropriate spatial kernels. The power spectra of natural images decline as $1/f^2$ (Field, 1987, 1994; Tolhurst et al., 1992; Ruderman, 1994). Images with power spectra that decline faster than $1/f^2$, for example $1/f^3$ and $1/f^4$, have even broader spatial correlations than natural images. For each pre-defined power spectrum, levels of correlations were estimated over 20 artificial images, using 30 randomly selected fixations on each image. The results in Figure 4·5c show that fixational eye movements decorrelated the responses of M cells only in the presence of images with a $1/f^2$ power spectrum, like natural images. Neither $1/f^3$, nor $1/f^4$ images led to decorrelated responses by the end of a 300-ms period of fixation. This specificity of dynamic decorrelation for images with a $1/f^2$ power spectrum is explained later in this section.

Whereas the factors described in Figure 4·5 were critical for the dynamic decorrelation of M cell responses, our results were largely unaffected by the precise choice of model

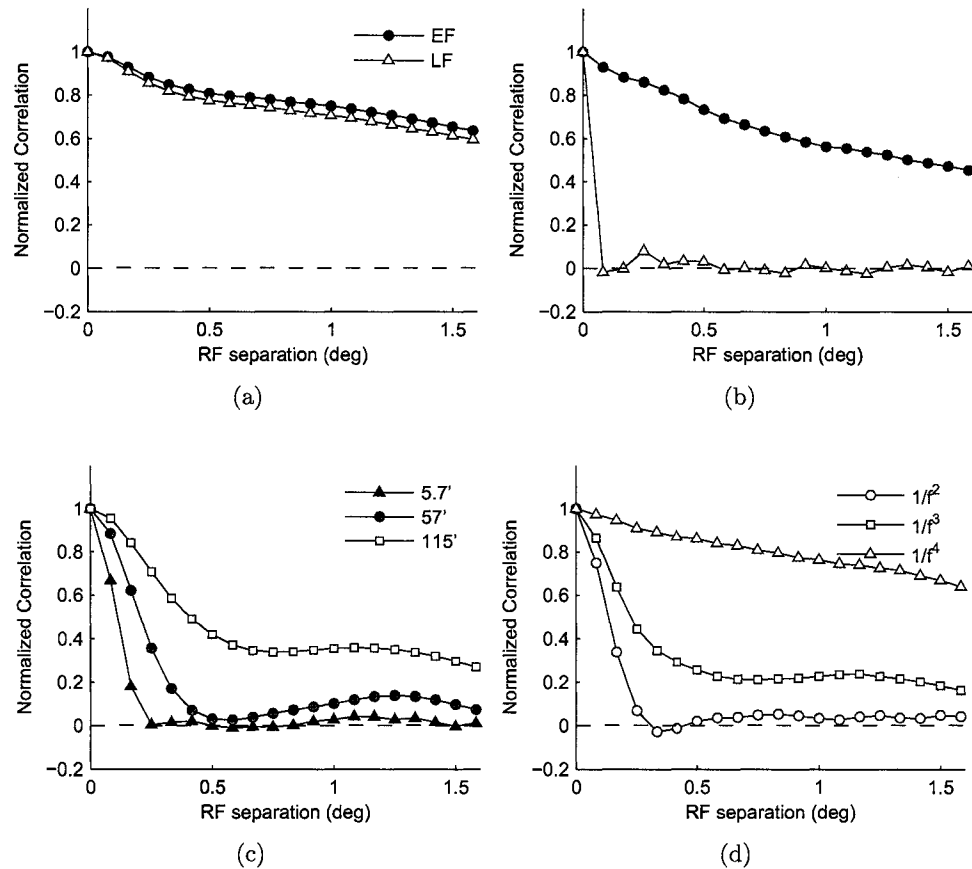


Figure 4.5: Main factors contributing to the dynamic decorrelation in pairs of M cells. (a) Spatial extent of correlated activity in a model of a hypothetical cell which combines the spatial receptive field of a parafoveal M cell with the temporal sensitivity of a P cell. Correlation in these cells is identical to correlation in P cells (see Figure 4.4a). (b) Spatial extent of correlated activity in a model of a hypothetical cell which combines the spatial receptive field of a parafoveal P cell with the temporal sensitivity of an M cell. Correlation in these cells is identical to correlation in M cells (see Figure 4.4b). (c) Importance of the small amplitude of fixational eye movements: Spatial extent of correlated activity across pairs of parafoveal M cells in Late Fixation, when fixational eye movements of various amplitudes were simulated as discrete random walks. (d) Importance of the power spectrum of the input image: Spatial extent of correlated activity across pairs of parafoveal M cells in Late Fixation, during presentation of stimuli with various power spectra.

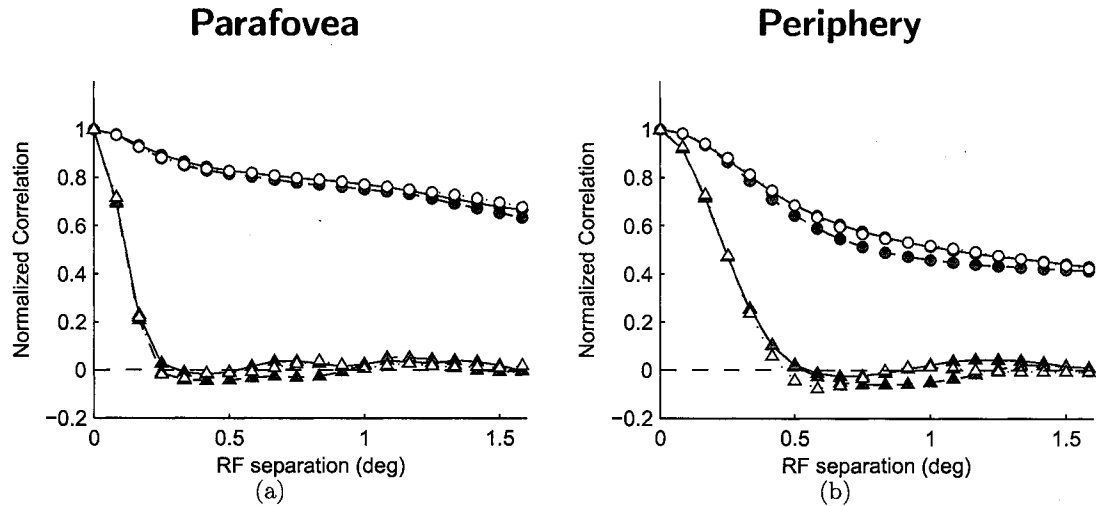


Figure 4.6: Influence of rectification on the dynamics of correlated activity in M cells. The left column shows results for parafoveal cells ($0\text{--}5^\circ$ eccentricity). The right column shows results for peripheral cells ($20\text{--}30^\circ$ eccentricity). Circles denote Early Fixation ($0\text{--}100$ ms), triangles represent Late Fixation ($200\text{--}300$ ms). Rectification level was varied from 0% (continuous lines, black symbols) to 50% (dashed lines, gray symbols) to 100% (dotted lines, white symbols).

parameters. To test the robustness of decorrelation, in a further series of simulations, we systematically modified the values of several model parameters. These simulations examined the impact of the two sources of nonlinearity present in our M cell model, rectification and contrast gain control, as well as the influence of the degree of space-time inseparability of modeled receptive fields. The results of these simulations are shown in Figures 4.6, 4.7, and 4.8.

Rectification in the model accounts for the fact that real firing rates cannot be negative. Figure 4.6a,b shows that patterns of correlated activities, as well as their dynamics, were virtually unaffected by the degree of rectification used in the simulations. Even for 100% rectification, *i.e.*, when rectification eliminated the full range of negative activity that would have been otherwise present, the structure of correlated activity was highly similar to that observed in the absence of rectification.

The second source of nonlinearity present in the model of M cells was a mechanism of

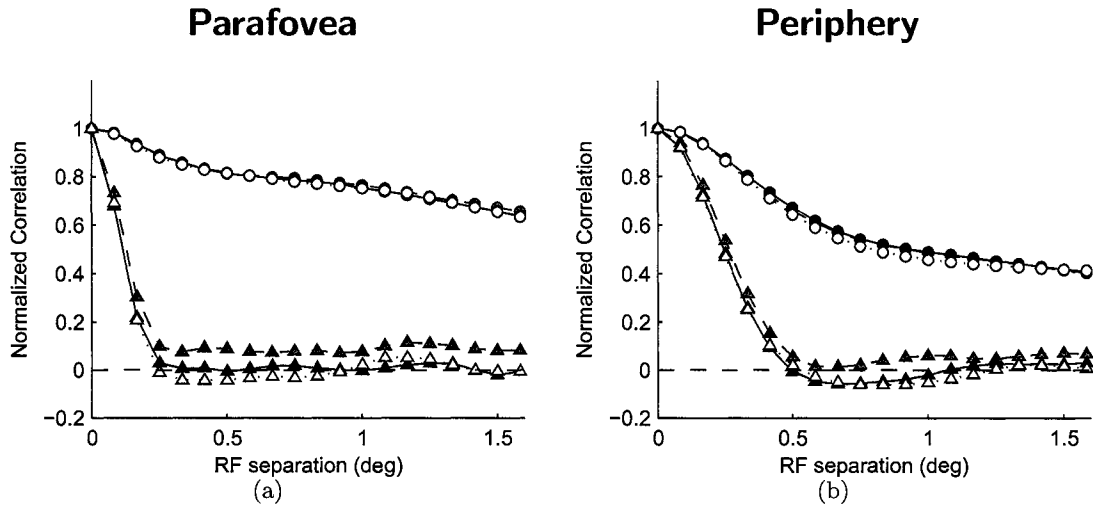


Figure 4.7: Influence of contrast on the dynamics of correlated activity in M cells. Circles denote Early Fixation (0–100 ms), triangles represent Late Fixation (200–300 ms). Contrast level was varied from 1% (dashed lines, gray symbols) to 5% (continuous lines, black symbols) to 12% (dotted lines, white symbols). (e,f) Effect of center-surround delay. Center-surround delay was varied from 0 ms (continuous lines, black symbols) to 3 ms (dashed lines, gray symbols) to 10 ms (dotted lines, white symbols).

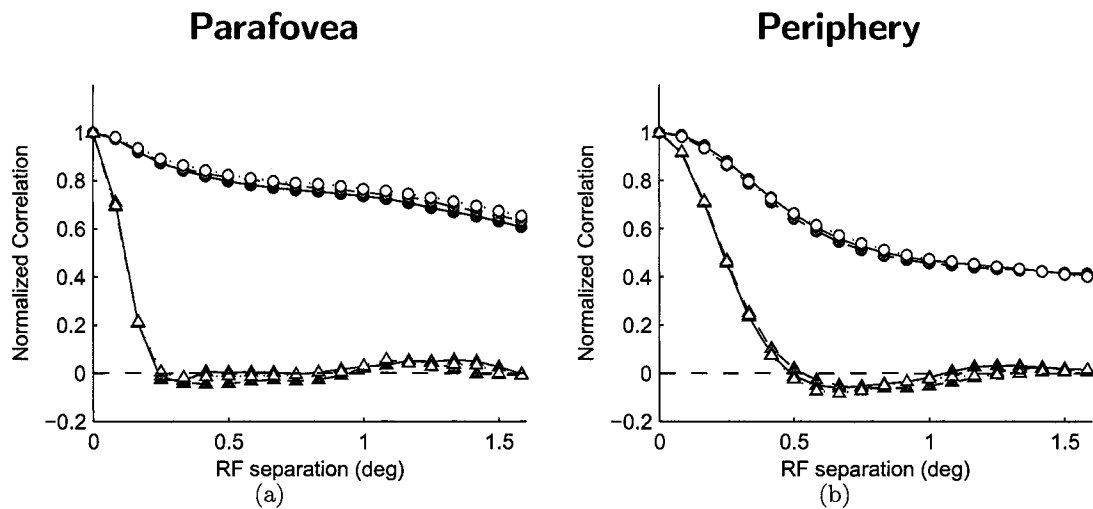


Figure 4.8: Influence of center-surround delay on the dynamics of correlated activity in M cells. Circles denote Early Fixation (0–100 ms), triangles represent Late Fixation (200–300 ms). Center-surround delay was varied from 0 ms (continuous lines, black symbols) to 3 ms (dashed lines, gray symbols) to 10 ms (dotted lines, white symbols).

contrast gain control (Shapley and Victor, 1978, 1979; Benardete et al., 1992). Whereas P cells are well approximated by linear models for a wide range of contrast levels (Smith et al., 1992; Lee, 1996; Benardete and Kaplan, 1997a,b), macaque M cells can be described by a linear model only for small luminance signals around a fixed contrast (Kremers et al., 1993; Lee et al., 1994). As explained in the Methods, our model accounts for contrast gain control by the contrast parameter c in Eq. (4.4), which modifies the temporal impulse response of M cells according to the level of contrast (Benardete and Kaplan, 1999a). Figure 4·7a,b shows the spatial structure of correlated activity in M cells for three different levels of contrast: 1%, 5%, and 12%. The responses of M cells tend to saturate beyond a contrast level of 12% (Lee et al., 1990). As shown by these data, the results obtained at different contrast levels were almost indistinguishable.

In a third set of control simulations we examined the influence of the degree of space-time inseparability in the receptive fields of M cell. Again, the data in Figure 4·8a,b show that varying the center-surround delay τ_{CS} from 0 to 10 ms, the range of values found in macaque RGCs (Smith et al., 1992; Benardete and Kaplan, 1997a, 1999b), had negligible influence on the observed patterns of correlation.

These control simulations show that the dynamic decorrelation between M cell responses that occurred in the presence of natural images and small fixational eye movements was a robust phenomenon. Decorrelation was little influenced by the visual eccentricity of the cell receptive fields, the percentage of rectification, contrast gain control, and the degree of space-time separability of the cell kernels.

What are the origins of the decorrelation of M cell responses during visual fixation on a natural image? Figure 4·9 provides an intuitive explanation. This example illustrated a period of visual fixation following a large saccade (see Figure 4·9a). Both cases of a pair of P cells and a pair of M cells are examined.

Figure 4·9b shows the spatiotemporal input to each cell resulting from the occurrence of eye movements. Input luminance signals varied as the movements of the eye changed the position of the two receptive fields on the image. Before the saccade, both cells received low-

luminance input because their receptive fields were located on a dark region of the scene. The average input luminance, \bar{I}_A and \bar{I}_B , increased after the saccade, as the receptive fields of the two cells were now located on a brighter region. During fixation, fixational eye movements kept the retinal image in motion, therefore producing fluctuations ΔI_A and ΔI_B in the input luminance.

Figure 4.9c shows simulated neural responses during the period of fixation following the saccade, for the two pairs of P cells (top panel) and M cells (bottom panel). The time course of correlated activity for the two pairs of cells is shown in Figure 4.9d. Following the saccade, P cells fired vigorously and their responses were correspondingly highly correlated. This high initial correlation was a consequence of the similar input received by both cells which, in turn, was due to the broad correlations of natural scenes. In natural images, intensity values tend to be correlated over large distances (Field, 1987). Therefore, during viewing of natural scenes, pairs of cells with non-overlapping receptive fields often receive similar input, as in the example of Figure 4.9. Because of their sustained temporal responses, P cells remained strongly sensitive to the average values of luminance \bar{I}_A and \bar{I}_B during the course of fixation. Therefore, their level of correlation remained high throughout fixation, as shown in Figure 4.9d.

The broad correlations of natural images were also responsible for the strong correlations across M cells in the period immediately following the saccade. However, M cells are characterized by transient temporal responses and are highly sensitive to the way that the stimulus present in their receptive field changes with time. Thus, the transient nature of M cells contributed to establish two regimes of activity. In the initial period of fixation, M cells were strongly influenced by the average luminance values \bar{I}_A , \bar{I}_B and how these values changed with respect to the previous fixations. Later, during the course of visual fixation, the responses of M cells were modulated by the changes of luminance ΔI_A and ΔI_B resulting from fixational eye movements. These two input regimes have substantially different second-order statistics. Average values of luminance in natural images are correlated over large distances. Conversely, it can be shown that local fluctuations in luminance tend to

be spatially uncorrelated (see Appendix). These properties of natural images are a direct consequence of their average power spectrum declining as $1/f^2$ with spatial frequency (Field, 1987, 1994; Tolhurst et al., 1992; Ruderman, 1994). For small eye movements, the local changes in luminance experienced in the receptive fields approximate the first-order spatial derivative of the image. Since the operation of differentiation corresponds to multiplication by frequency in the Fourier domain, any image with a $1/f^2$ power spectrum has a first spatial derivative with a flat power spectrum, i.e., it is spatially uncorrelated. It is this transition from (i) a temporal sensitivity to a broadly correlated input to (ii) a temporal sensitivity to spatially uncorrelated input which was responsible for the decorrelation across pairs of M cells that occurred during the course of visual fixation. Therefore the dynamic decorrelation observed in our simulations of M cells only depended on the three main factors examined in Figure 4.5: the dynamics of M cell responses, the small amplitude of fixational eye movements, and the $1/f^2$ power spectra of natural images.

4.4 Discussion

4.4.1 Summary of simulation results

In this study, a model of macaque RGCs was used to simulate neural responses when natural scenes are scanned by recorded sequences of human eye movements. We examined the dynamics of patterns of spatially correlated activity, at zero time difference, in pairs of cells whose receptive fields were separated by various distances. At the onset of fixation, broad pools of coactive cells were present. Independently of the cell type (M or P), cell responses were strongly correlated over several degrees of visual field, an area much larger than their receptive fields. Following this initial period, whereas correlation remained approximately constant among P cells, the responses of M cells with non-overlapping receptive field centers became, on average, uncorrelated by the end of a typical 300-ms fixation.

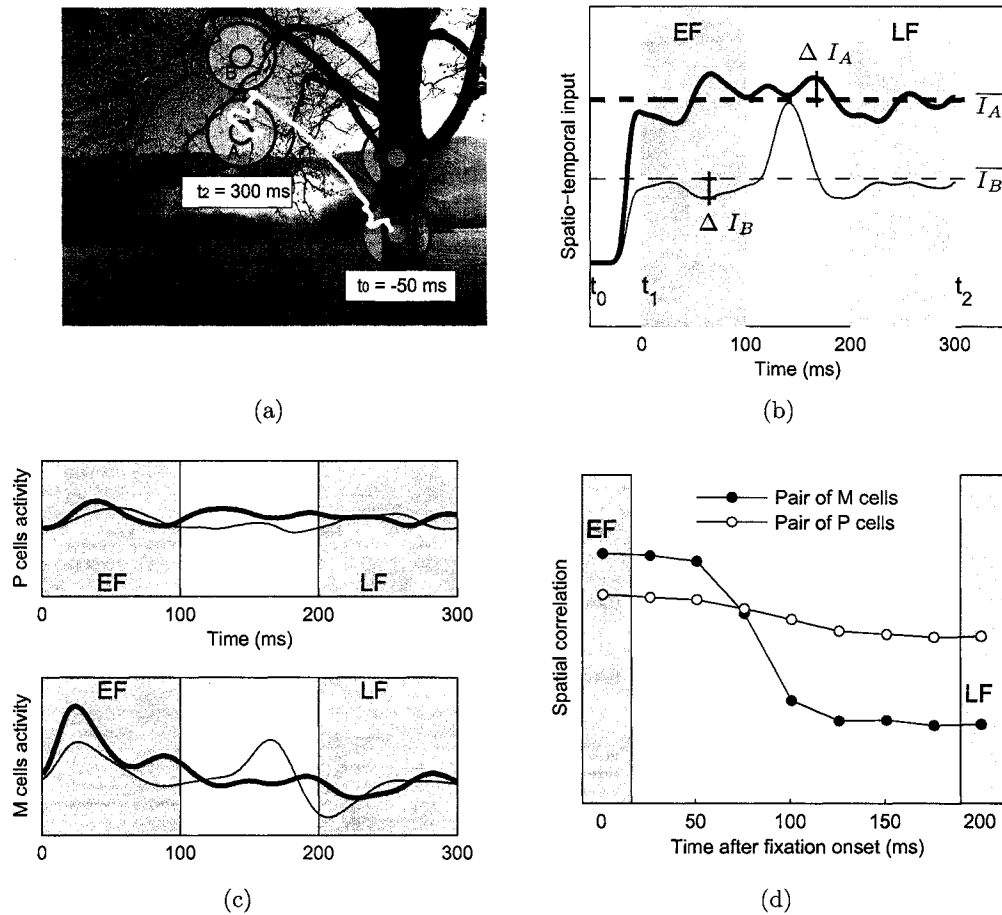


Figure 4.9: Example of the dynamics of correlated activity during a single fixation. (a) A natural scene is scanned by a sequence of eye movements (white arrow) that includes a saccade followed by a fixation. The saccade starts at $t_0 = -50$ ms. Fixational eye movements occur following the saccade, between $t_1 = 0$ and $t_2 = 300$ ms. (b) Spatiotemporal input to the two cells during the 350-ms interval starting from saccade onset. The two curves show the temporal evolution of the input to the two receptive fields. Luminance varies as the receptive fields move. (c) Responses of a pair of P cells (top panel) and a pair of M cells (bottom panel) during the fixation period occurring after the saccade. (d) Pairwise correlation between the responses of M cells (black circles) and between the responses of P cells (white circles) as a function of time. While correlation remains high between P cells, in M cells it decreases to 0.

4.4.2 Validity of the result

In this work we tried to remain as close as possible to original experimental data by using published model parameters for macaque RGCs (Croner and Kaplan, 1995) and real patterns of human eye movements recorded in our laboratory. Several factors were not considered in the model, including sources of correlated activity other than shared visual stimulation (Usrey and Reid, 1999), and slow adaptation of neural responses to luminance (Barlow and Levick, 1969) and contrast (Smirnakis et al., 1997; Chander and Chichilnisky, 2001). While our results need to be confirmed with *in vivo* experiments, they were remarkably robust in computer simulations. Levels of correlation in the model were virtually unaffected by wide ranges of model parameters, including the size of receptive fields (which are smaller in the central visual field than in the periphery), the amount of rectificative nonlinearity, the level of contrast, and the center-surround delay (see Figures 4·6, 4·7, and 4·8). In retrospect, it is not surprising that decorrelation was so robust, given that the dynamic decorrelation among model M cells originated from such fundamental properties as the second-order statistics of natural images, the small spatial scale of fixational eye movements, and the transient nature of M cells.

Second-order statistics of natural images

As explained above, the distribution of intensity values in natural scenes declines as $1/f$ with spatial frequency (Field, 1987, 1994; Tolhurst et al., 1992; Ruderman, 1994). Small fluctuations in natural images, corresponding to the first derivative in spatial coordinates, thus have a flat distribution in the frequency domain (because derivation in the space domain corresponds to multiplication by f in the frequency domain). Hence, local intensity changes in natural images are not correlated (Rucci and Casile, 2005). This property explains why, in our simulations, decorrelation only happened for images with the same power spectrum as natural images, as illustrated in Figure 4·5*d*.

Amplitude of eye movements

During natural viewing, eye movements sample the visual input at two different scales. Macroscopic saccades move the gaze to distant regions of the natural scene, which tend to be broadly correlated on average. On a smaller scale, fixational eye movements cause fluctuations approximating the first derivative of the image. Importantly, decorrelation of M cell responses occurred only for a small jitter of the eye around the point of fixation. Larger movements, such as macroscopic saccades, correspond to larger spatial fluctuations on the natural image which are not well approximated by the first spatial derivative of the image. Control simulations using randomly generated eye movements, reported in Figure 4·5*c*, clearly showed that decorrelation was stronger for small-amplitude eye movements and that decorrelation did not occur for eye movements of large amplitude.

Temporal transience of M cells

In control simulations reported in Figures 4·5*a* and 4·5*b*, we switched the temporal and spatial characteristics of M and P cells. The results confirmed that it was the temporal transience of M cells that was responsible for the observed dynamic decorrelation of cell responses.

Decorrelation has fundamental origins and is very robust

To summarize, the dynamic decorrelation among modeled cells follows from the combined effect of several factors: (1) the spatial frequency content of the spatiotemporal input to the retina, which is due to the spectrum of the image as well as to the small amplitude of fixational instability; and (2) the transient property of M retinal ganglion cells.

4.4.3 Decorrelation and the redundancy reduction hypothesis

What could be gained from spatial decorrelation of cell responses in the retina? A first advantage is a more efficient encoding of visual information, obtained by redundancy reduction (Attneave, 1954; Barlow, 1961). Natural images are highly redundant: on average,

they vary little in space and time (Field, 1987). Elimination of the correlations present in natural input has been proposed as a way to reduce redundancy (Srinivasan et al., 1982; Atick and Redlich, 1990, 1992; van Hateren, 1992). These proposals argued that spatial filters qualitatively similar to the receptive fields of cells in the retina and LGN were sufficient to discard the broad correlations present in natural images. However, data from neurophysiological recordings do not support these theories. Many cells in the early visual system are strongly sensitive to low spatial frequencies (e.g., Croner and Kaplan, 1995) in a way that is not compatible with the psychophysical contrast sensitivity functions used by Atick and Redlich (1992) to approximate the responses of individual cells. The responses of true cells such as those that we modeled are not decorrelated in the presence of static natural images: Simulated RGC responses were all highly correlated at the onset of fixation, before eye movements could have any effect, and in the case of P cells, correlation remained high throughout fixation.

These previous theories, however, implicitly assumed the visual scene to be statically projected onto the retina. They ignored the fact that, during natural viewing, incessant small eye movements alter the spatiotemporal structure of the input signal. The present study shows that, even if M cells are sensitive to low spatial frequencies, the responses of a population of M cells become spatially decorrelated when these cells are presented with the visual input produced by fixational eye movements. Contrary to the above theories, we propose that the decorrelation of neural responses originates not from the spatial characteristics of their receptive fields, but from their temporal sensitivity. Cells with transient responses, such as M cells, are especially sensitive to changes in their input. During the course of fixation they continuously respond to the uncorrelated, dynamic component introduced by fixational eye movements, which explains why their responses become uncorrelated by the end of a normal period of fixation. This effect does not occur for cells with more sustained responses, such as P cells, which are mostly sensitive to the static, broadly correlated component of the visual input, and remain correlated over an entire fixation. Control simulations shown in Figures 4.5a and 4.5b confirm that it is the temporal

profile of the cells, and not their spatial profile, that lead to the observed dynamic spatial decorrelation of neuronal activities. It is important to note that spatial decorrelation across simultaneous cell activities does not come at the expense of increased correlations in the temporal domain. The cross-correlation function of pairs of cells whose receptive field centers are non-overlapping is flat (data not shown), which means that cell activities are not temporally correlated.

4.4.4 A dynamic, multiplexing neural code

A second consequence of a dynamic decorrelation of neural responses is the possibility of sequentially encoding different features of the visual scene during the course of visual fixation. In our model, patterns of correlated activity among M cells changed with time. These changes underlie the possibility of a temporal multiplexing of visual information, in which visual features at various spatial scales are encoded at different times during a period of fixation. This multiplexing encoding would work as follows in a population of cells. At the onset of fixation, when cells are correlated over large distances, they would convey information about the low spatial frequencies, i.e., the global structure of the visual scene. At a later period, however, the decorrelated structure of retinal activity would be ideally suited to signal local, high-spatial-frequency changes in the input to the cell receptive fields. In other words, the end of the fixation period (200–300 ms after fixation onset) provides a second input channel that enhances high spatial frequencies, whose power is low in static natural images but higher in the presence of retinal jitter.

This dynamic code would be in agreement with the “global precedence effect” (Navon, 1977), or coarse-to-fine integration of visual information, observed both in psychophysics and in neurophysiological recordings. Human perception exhibits a coarse-to-fine time course (Parker et al., 1992; Schyns and Oliva, 1994; Parker and Costen, 1999), although it remains controversial whether this processing scheme occurs at the perceptual level or at higher cognitive levels which are out of the scope of this dissertation (Morrison and Schyns, 2001). Nevertheless, there is evidence in anesthetized macaque V1 that the preferred spatial

frequency of cells shifts from low to high frequencies during the time course of a 200-ms fixation (Frazor et al., 2004). This is consistent with our proposal that the upstream population of RGCs encodes low frequencies before high frequencies. In isolated retinas, Smirnakis et al. (1997) proposed that spatial scale decomposition exists at the level of the RGC, as two input pathways (undergoing independent adaptation): one (H, “high-pass”) integrating the stimulus with a spatially antagonistic receptive field; the other one (L, “low-pass”) having a broad receptive field. The H pathway could be implemented by bipolar cells, the L pathway by wide-field amacrine cells. However, Smirnakis et al. (1997) did not report different time scales for both pathways. More research is needed to investigate the evolution of spatial frequency sensitivity in retinal ganglion cells.

A dynamic neural code would require the existence of a reference time. For example, decoding should be synchronized with the onset of visual fixation. A reset signal might be provided by the efference copy of the saccade motor command, indicating when a new fixation period starts (Gaarder, 1968; Usrey and Reid, 1999). Alternatively, the reset could be triggered in a bottom-up fashion by the sudden change in the structure of correlated activity in the retina.

Decorrelation is an important feature of this dynamic neural code. Because cell responses are, on average, spatially uncorrelated in the earliest stage of visual processing, this code could advantageously emphasize pertinent correlations such as those signaling the presence of an edge. In this case, M cells would not only be involved with encoding motion, as is currently believed, but may also contribute to detailed spatial vision, a role usually solely attributed to the parvocellular pathway.

The idea of a multiplexing neural code in the retina was also proposed by Meister et al. (1995), but in the form of a combinatorial code for vision whose elementary symbols are multineuronal firing patterns rather than single action potentials from individual cells. In our case, multiplexing would occur at the scale of each single neuron. In both proposals, multiplexing is parsimonious in that it uses a minimal number of neurons: The same cells can represent different types of visual information.

4.4.5 An alternative explanation for the role of FEM in natural vision

Visual perception is an active process which should not be studied in isolation of behavior, but instead in “ecological” conditions (Gibson, 1979). In this study, we demonstrated that the combination of natural images and FEM gave remarkable properties to the retinal input. In the current view, the role of FEM is to prevent visual percepts from fading (Martinez-Conde et al., 2004, 2006). As reviewed in section 2.1, this explanation is insufficient. Fading occurs after several seconds to minutes, a duration much longer than that of natural fixations (Harris et al., 1988; Andrews and Coppola, 1999). It is not even clear whether visual percepts would ultimately disappear in the prolonged absence of FEM (Arend and Timberlake, 1986b; Ditchburn, 1987; Arend and Timberlake, 1987). Besides, our own psychophysical experiments (reported in Chapter 3) suggested that discrimination performance could be impaired in the absence of FEM for stimulus presentations as short as 500 ms, during which fading is not experienced (Rucci and Desbordes, 2003). Several other roles of fixational eye movements have been proposed, in hyperacuity (Averill and Weymouth, 1925; Marshall and Talbot, 1942; Arend, 1973), in retinal feature estimation (Greschner et al., 2002), and in retinal segregation of object and background motion (Ölveczky et al., 2003), as reviewed in section 2.2. The present study supports an alternative explanation, in which fixational eye movements provide a critical mechanism for structuring neural activity in the early visual system into a more compact, multiplexing format.

4.4.6 Concluding remarks about natural vision and decorrelation

To conclude, this study contributes to unveil the role of retinal jitter in neural encoding of visual stimuli. In normal conditions, fixational instability does not only consist of fixational eye movements such as small saccades and ocular drifts, but also of other body movements not perfectly compensated by the vestibulo-ocular reflex (Steinman et al., 1985). Further work is needed to generalize the present result to other sources of motion. Statistics of natural time-varying images have only been studied in the absence of eye (and body)

movements (Dong and Atick, 1995a; van Hateren and Ruderman, 1998). In addition, we believe that decorrelation would also occur in a model accounting for luminance and contrast adaptation (e.g., van Hateren et al., 2002). We recommend that all future studies of the early visual system using natural images also account for FEM, since we showed that the spatial power spectrum of the visual input can be strongly affected by the occurrence of retinal jitter.

Chapter 5

Conclusion

To conclude this dissertation, we summarize our results below and provide future directions related to the study of fixational eye movements in natural viewing conditions.

5.1 Summary of results

This work consisted of two studies based on the integration of several fields, including visual psychophysics, computational modeling, image processing, and natural image statistics.

In the first study we used a high-resolution eyetracker and stabilization device to analyze the effect of retinal stabilization on discriminating the orientation of a low-contrast and noisy small bar that was displayed for either 500 ms or 2 s. The bar was randomly tilted by 45° either clockwise or counterclockwise. For both exposure durations, percentages of correct discrimination were significantly lower under conditions of visual stabilization than in the presence of the normally moving retinal image. These results are consistent with the predictions of previous computational models from our lab that simulated neuronal responses in the early visual system during oculomotor activity, and support the hypothesis that fixational eye movements are critical for visual processing.

In the second study we examined the influence of fixational eye movements on the temporal evolution of spatial patterns of synchronously active retinal ganglion cells. Parvocellular (P) and magnocellular (M) neurons in both the central and peripheral visual fields were modeled by spatiotemporal receptive fields matched to macaque neurophysiological data. The responses of cells were simulated while their receptive fields scanned natural images following patterns of recorded eye movements. At the onset of fixation, the responses of cells separated by up to several degrees were highly correlated, because of the broad cor-

relations present in natural images. Whereas levels of correlation remained approximately constant among P cells, the responses of M cells with non-overlapping receptive field centers became uncorrelated by the end of a typical 300-ms fixation. Therefore, populations of M cells were able to discard the broad spatial correlations present in natural images. We showed that this dynamic spatial decorrelation was a highly robust phenomenon originating from the interaction of the second-order statistics of natural images, the retinal image motion introduced by fixational eye movements, and the temporal transience of M cells.

Overall, these results indicate that fixational eye movements play an important role in vision, even during short periods of fixation that last only a few hundreds of milliseconds. These periods characterize active, unconstrained vision in humans and other primates. Our work suggests two conclusions. First, in the absence of fixational instability, the ability to discriminate low-contrast, noisy targets is impaired. Second, these small eye movements seem to compensate for the overwhelmingly dominant low spatial frequencies present in all natural images, by enhancing the higher-frequency components that compose edges and contours.

5.2 Future directions

More experiments, both psychophysical and neurophysiological, need to be done in stabilized conditions to investigate the role of fixational eye movements. However, the standard method for stabilizing the retinal image used in the present work has some limitations that prevent the execution of other important experiments. A first limitation is that stabilization can neither be turned on and off rapidly, nor synchronized with the stimulus on the screen. Therefore, in the psychophysical experiments of this dissertation (see Chapter 3), stabilization had to be enabled for the whole duration of a 25-trial block. A second limitation of this method is that it does not allow the objective assessment of the quality of stabilization. The experimenter has to rely on the observer to subjectively judge whether retinal image motion has been eliminated.

To overcome these limitations, a different stabilization system needs to be designed,

which would include real-time processing of eye movement data and subject response. While the present doctoral project was being pursued, several members of the laboratory have been developing a new, versatile system for Eye-Movement Contingent Display (EMCD). This integrated hardware and software system, called EyeRIS, is based on a digital signal processor and enables accurate control of the position and motion of the stimulus displayed on a CRT monitor (Santini et al., 2006). In particular, the stimulus can be modified in real time according to the gaze-contingent procedure specified by the experimenter. EyeRIS is designed to update the stimulus within a delay of 10 ms at a monitor refresh rate of 200 Hz. When coupled with the DPI eyetracker, the spatial resolution of the system is $1'$. EyeRIS outperforms other EMCD systems, which to our knowledge use eyetrackers with lower resolutions than the DPI eyetracker (e.g., Geisler et al., 2003, Nikolov et al., 2004, and others reviewed in Loschky et al., 2003).

EyeRIS allows the study of a new experimental condition called “stabilization-after-saccade”, in which each trial starts in the unstabilized condition, and stabilization is only turned on at the end of the initial guided saccade. We could compare subject performances during stabilized and unstabilized conditions after the subject performed an initial saccade, because this is the condition closer to natural viewing circumstances. Stabilizing the image after a saccade would allow a fairer comparison with the unstabilized condition (called normal-fixation-after-saccade). The stabilization-after-saccade condition was not available to us in the psychophysical experiments reported in Chapter 3. Instead, we could only compare the two conditions of normal-fixation-after-saccade and stabilization-without-saccade (Experiments 1 and 2), or normal-fixation-without-saccade and stabilization-without-saccade (Experiment 3). With EyeRIS, stabilization-after-saccade can be compared to normal-fixation-after-saccade for the first time. In particular, new psychophysical experiments can be designed based on our neural modeling result to differentiate the effect of fixational eye movements on low vs. high spatial frequencies. The current goal in our lab is to analyze the influence of fixational eye movements on the discrimination of gratings masked by noise with a power spectrum decreasing as $1/f^2$ with spatial

frequency, like the average power spectrum of natural images. Using EyeRIS, we can selectively eliminate the retinal image motion that normally occurs during the intersaccadic intervals of visual fixation, and only during these intervals, while allowing saccades to occur normally. Our lab has conducted these experiments, and results show that fixational eye movements improve discrimination of high-spatial frequency, but not low-spatial frequency, stimuli (Rucci et al., submitted manuscript). Contrast sensitivity is correspondingly impaired at high spatial frequencies in the absence of the retinal image motion produced by fixational eye movements. These results show that fixational eye movements create a dynamic visual input to the eye that enhances the high-frequency harmonics of the stimulus, supporting our hypothesis that, in a natural visual world dominated by low spatial frequencies, fixational eye movements constitute an effective sampling strategy by which the visual system enhances the processing of spatial detail.

A second possible extension of our work would be to investigate the influence of fixational eye movements on peripheral vision. Fading of low-contrast objects, called the Troxler effect, works especially well in the periphery (see section 2.1.5). Martinez-Conde et al. (2004) suggested that fixational eye movements might have different effects on foveal vs. peripheral vision. They proposed that microsaccades may be more important for peripheral vision, whereas drifts and tremor would maintain foveal vision. However, conducting experiments in the periphery presents a number of challenges. It is difficult for the subjects to attend a location in the visual field that, by design, they cannot foveate. Besides, the size of current displays (whether CRT monitors or others) usually limits the accessible visual field to a fraction of the whole visual field. Monocular experiments also restrict stimulus presentations to the corresponding hemifield. Future experiments will have to address these challenges in order to study peripheral vision in the presence (or absence) of fixational eye movements.

Third, an oft-asked question regards the perceived difference between a subject's own eye movements and external object motion. Is it equivalent for the visual system that the eye moves by a certain amount, and that an object (or the full field) moves by the same

amount? A priori, both are distinct, since people are not aware of the constant motion of the world on the retina due to fixational eye movements. Besides, a quick and easy experiment proves that proprioceptive information is not enough for the brain to compensate for eye motion: Wiggling one's eyeball through the eyelid leads to perceived motion of the world, unlike the apparent stability of the world in the presence of incessant eye movements of all sizes. The comparative study of retinal image motion due to eye movements vs. external object motion could be addressed by experiments with "reconstructed eye movements", in which the visual field is stabilized and, at the same time, moved along with previously recorded patterns of fixational eye movements. It would be very interesting to investigate whether "reconstructed eye movements" can restore the quality of vision experienced in normal vision, in comparison with the stabilized condition. Experiments could also be designed to exchange patterns of eye movements between subjects, such that a given subject is presented with eye movements performed by another subject, to test if each individual visual system is tuned to its own eye movement characteristics.

Beyond human psychophysics, studying the physiological responses of neurons in the presence of fixational eye movements offers promising perspectives. The results from our neural modeling study need to be confirmed by neurophysiological experiments. Do cells in the early visual system actually discard the broad spatial correlations present in natural scenes, when viewing them in the presence of fixational eye movements? Moreover, in Chapter 4 we proposed the existence of a multiplexing scheme that would allow each M cell to encode different spatial frequencies at different times during visual fixation, from low frequencies at the onset of fixation to higher frequencies towards the end of a normal fixation period. As discussed in section 4.4, this coarse-to-fine integration of visual information was found in at least some conditions in psychophysical experiments (Parker et al., 1992; Schyns and Oliva, 1994; Parker and Costen, 1999). Since a multiplexing code also requires the existence of a reference time, it would be interesting to verify experimentally whether a "reset" signal exists that indicates the occurrence of a saccade or the beginning of a new fixation. This signal could be provided either by an efference copy of the saccade motor

command (Gaarder, 1968; Usrey and Reid, 1999), or by a sudden change in the structure of correlated activity in retinal ganglion cells.

According to Gibson (1979), visual perception is an active process which should not be studied in isolation from behavior, but instead in “ecological” conditions. Investigating vision in the presence of fixational eye movements is only one step towards understanding visual processes as they occur in natural behavior, but it is an important step that has too often been neglected, particularly in neurophysiological experiments in which the animals are either anesthetized and paralyzed, or awake but required to perform steady fixation. The results of this dissertation indicate that fixational eye movements play an important role in the neural representation of visual information. A number of recent neurophysiological studies of fixational eye movements in awake macaques (Gur et al., 1997; Martinez-Conde et al., 2000; Ramcharan et al., 2001; Snodderly et al., 2001; Reppas et al., 2002) and in isolated retinas (Ölveczky et al., 2003; Pitkow, 2006) demonstrate renewed interest in this field. We hope that this trend reflects a turning point in vision research that will lead to considering eye movements as an integral part of natural vision.

References

- Abeles, M. (1991). *Corticonics: Neural Circuits of the Cerebral Cortex*. Cambridge University Press.
- Ahissar, E. and Arieli, A. (2001). Figuring space by time. *Neuron*, 32(2):185–201.
- Albus, K. and Wolf, K. (1984). Early postnatal development of neuronal function in the kitten's visual cortex: a laminar analysis. *Journal of Physiology (London)*, 348:153–185.
- Alitto, H. J. and Usrey, W. M. (2005). Dynamic properties of thalamic neurons for vision. *Progress in Brain Research*, 149:83–90.
- Alonso, J. M., Usrey, W. M., and Reid, R. C. (1996). Precisely correlated firing in cells of the lateral geniculate nucleus. *Nature*, 383(6603):815–819.
- Andrews, T. J. and Coppola, D. M. (1999). Idiosyncratic characteristics of saccadic eye movements when viewing different visual environments. *Vision Research*, 39:2947–2953.
- Applegate, R. A., Bradley, A., and van W. A. Heuven (1990). Entoptic visualization of the retinal vasculature near fixation. *Investigative Ophthalmology and Visual Science*, 31(10):2088–98.
- Arend, L. E. (1973). Spatial differential and integral operations in human vision: Implications of stabilized retinal image fading. *Psychological Review*, 80(5):374–395.
- Arend, L. E. and Timberlake, G. T. (1986a). What is psychophysically perfect image stabilization? Do perfectly stabilized images always disappear? *Journal of the Optical Society of America. A, Optics and Image Science*, 3(2):235–241.
- Arend, L. E. and Timberlake, G. T. (1986b). What is psychophysically perfect image stabilization? Do perfectly stabilized images always disappear? *Journal of the Optical Society of America*, 3(2):235–241.
- Arend, L. E. and Timberlake, G. T. (1987). What is psychophysically perfect image stabilization? do perfectly stabilized images always disappear?: Reply to comment. *Journal of the Optical Society of America. A, Optics and Image Science*, 4(2):407–408.
- Arieli, A., Shoham, D., Hildesheim, R., and Grinvald, A. (1995). Coherent spatiotemporal patterns of ongoing activity revealed by real-time optical imaging coupled with single-unit recording in the cat visual cortex. *Journal of Neurophysiology*, 73(5):2072–93.
- Arnett, D. and Spraker, T. E. (1981). Cross-correlation analysis of the maintained discharge of rabbit retinal ganglion cells. *Journal of Physiology*, 317:29–47.

- Atick, J. J. (1992). Could information theory provide an ecological theory of sensory processing? *Network: Computation in Neural Systems*, 3(2):213–251.
- Atick, J. J. and Redlich, A. (1990). Towards a theory of early visual processing. *Neural Computation*, 2:308–320.
- Atick, J. J. and Redlich, A. (1992). What does the retina know about natural scenes? *Neural Computation*, 4:196–210.
- Attneave, F. (1954). Some informational aspects of visual perception. *Psychological Review*, 61(3):183–93.
- Avant, L. L. (1965). Vision in the Ganzfeld. *Psychological Bulletin*, 64(4):246–58.
- Averbeck, B. B., Latham, P. E., and Pouget, A. (2006). Neural correlations, population coding and computation. *Nature Reviews Neuroscience*, 7:358–366. 10.1038/nrn1888.
- Averill, H. I. and Weymouth, F. W. (1925). Visual perception and the retinal mosaic, II. The influence of eye movements on the displacement threshold. *Journal of Comparative Psychology*, 5:147–176.
- Backus, B. T. and Oruç, I. (2005). Illusory motion from change over time in the response to contrast and luminance. *Journal of Vision*, 5(11):1055–1069.
- Baddeley, R., Abbott, L. F., Booth, M. C., Sengpiel, F., Freeman, T., Wakeman, E. A., and Rolls, E. T. (1997). Responses of neurons in primary and inferior temporal visual cortices to natural scenes. *Proceedings of the Royal Society, Series B: Biological Sciences*, 264(1389):1775–83.
- Bair, W. and O’Keefe, L. P. (1998). The influence of fixational eye movements on the response of neurons in area mt of the macaque. *Visual Neuroscience*, 15(4):779–786.
- Barlow, H. (2001). Redundancy reduction revisited. *Network: Computation in Neural Systems*, 12(3):241–53.
- Barlow, H. B. (1961). Possible principles underlying the transformations of sensory messages. In Rosenblith, W. A., editor, *Sensory Communication*, pages 217–234. MIT Press, Cambridge MA.
- Barlow, H. B. (1963). Slippage of contact lenses and other artefacts in relation to fading and regeneration of supposedly stable retinal images. *The Quarterly Journal of Experimental Psychology*, 15:36–51.
- Barlow, H. B. and Levick, W. R. (1969). Changes in the maintained discharge with adaptation level in the cat retina. *Journal of Physiology (London)*, 202(3):699–718.
- Bartfeld, E. and Grinvald, A. (1992). Relationships between orientation-preference pinwheels, cytochrome oxidase blobs, and ocular-dominance columns in primate striate cortex. *Proceedings of the National Academy of Sciences of the United States of America*, 89(24):11905–9.

- Benardete, E. A. and Kaplan, E. (1997a). The receptive field of the primate P retinal ganglion cell, I: Linear dynamics. *Visual Neuroscience*, 14(1):169–185.
- Benardete, E. A. and Kaplan, E. (1997b). The receptive field of the primate P retinal ganglion cell, II: Nonlinear dynamics. *Visual Neuroscience*, 14(1):187–205.
- Benardete, E. A. and Kaplan, E. (1999a). The dynamics of primate M retinal ganglion cells. *Visual Neuroscience*, 16(2):355–368.
- Benardete, E. A. and Kaplan, E. (1999b). Dynamics of primate P retinal ganglion cells: responses to chromatic and achromatic stimuli. *Journal of Physiology (London)*, 519 Pt 3:775–790.
- Benardete, E. A., Kaplan, E., and Knight, B. W. (1992). Contrast gain control in the primate retina: P cells are not X-like, some M cells are. *Visual Neuroscience*, 8(5):483–486.
- Bolger, C., Bojanic, S., Sheahan, N. F., Coakley, D., and Malone, J. F. (1999). Dominant frequency content of ocular microtremor from normal subjects. *Vision Research*, 39(11):1911–5.
- Born, R. T. and Bradley, D. C. (2005). Structure and function of visual area MT. *Annual Review of Neuroscience*, 28:157–89.
- Born, R. T., Groh, J. M., Zhao, R., and Lukasewycz, S. J. (2000). Segregation of object and background motion in visual area MT: effects of microstimulation on eye movements. *Neuron*, 26(3):725–34.
- Brady, N. and Field, D. J. (2000). Local contrast in natural images: normalisation and coding efficiency. *Perception*, 29(9):1041–55.
- Breitmeyer, B. and Julesz, B. (1975). The role of on and off transients in determining the psychophysical spatial frequency response. *Vision Research*, 15:411–415.
- Britten, K. H. (2004). The middle temporal area: Motion processing and the link to perception. In Chalupa, L. M. and Werner, J. S., editors, *The Visual Neurosciences*, chapter 81, pages 1203–1216. Cambridge: MIT Press.
- Brivanlou, I. H., Warland, D. K., and Meister, M. (1998). Mechanisms of concerted firing among retinal ganglion cells. *Neuron*, 20(3):527–39.
- Buisseret, P. and Imbert, M. (1976). Visual cortical cells: their developmental properties in normal and dark-reared kittens. *Journal of Physiology (London)*, 255:511–525.
- Bullier, J. and Nowak, L. G. (1995). Parallel versus serial processing: new vistas on the distributed organization of the visual system. *Current Opinion in Neurobiology*, 5(4):497–503.
- Burbeck, C. A. and Kelly, D. H. (1982). Eliminating transient artifacts in stabilized-image contrast thresholds. *Journal of the Optical Society of America*, 72(9):1238–1243.

- Burbeck, C. A. and Kelly, D. H. (1984). Role of local adaptation in the fading of stabilized images. *Journal of the Optical Society of America. A, Optics and Image Science*, 1:216–220.
- Burr, D. C. and Morrone, M. C. (1996). Temporal impulse response functions for luminance and colour during saccades. *Vision Research*, 36(14):2069–78.
- Burr, D. C. and Morrone, M. C. (2004). Visual perception during saccades. In Chalupa, L. M. and Werner, J. S., editors, *The Visual Neurosciences*, chapter 93, pages 1391–1401. Cambridge: MIT Press.
- Burr, D. C., Morrone, M. C., and Ross, J. (1994). Selective suppression of the magnocellular visual pathway during saccadic eye movements. *Nature*, 371(6497):511–3.
- Cai, D., DeAngelis, G. C., and Freeman, R. D. (1997). Spatiotemporal receptive field organization in the lateral geniculate nucleus of cats and kitten. *Journal of Neurophysiology*, 78(2):1045–1061.
- Campbell, F. W. and Robson, J. G. (1961). A fresh approach to stabilized retinal images. *Journal of Physiology (London)*, 158:11P–12P.
- Campbell, F. W. and Wurtz, R. H. (1978). Saccadic omission: why we do not see a grey-out during a saccadic eye movement. *Vision Research*, 18(10):1297–303.
- Carpenter, R. H. S. (1988). *Movements of the Eyes*. Pion, London.
- Casagrande, V. A. and Norton, T. T. (1991). Lateral geniculate nucleus: A review of its physiology and function. In Leventhal, A. G., editor, *The Neural Basis of Visual Function, vol. 4: Vision and Visual Dysfunction*. London: MacMillan Press.
- Casile, A. and Rucci, M. (2006). A theoretical analysis of the influence of fixational instability on the development of thalamo-cortical connectivity. *Neural Computation*, 18(3):569–590.
- Chander, D. and Chichilnisky, E. J. (2001). Adaptation to temporal contrast in primate and salamander retina. *Journal of Neuroscience*, 21(24):9904–16.
- Changeux, J. P. and Danchin, A. (1976). Selective stabilization of developing synapses as a mechanism for the specification of neuronal networks. *Nature*, 264:705–712.
- Chapman, B. and Stryker, M. P. (1993). Development of orientation selectivity in ferret visual cortex and effects of deprivation. *Journal of Neuroscience*, 13(12):5251–5262.
- Chechik, G., Globerson, A., Anderson, M., Young, E., Nelken, I., and Tishby, N. (2002). Group redundancy measures reveal redundancy reduction in the auditory pathway. In Dietterich, T. G., Becker, S., and Ghahramani, Z., editors, *Advances in Neural Information Processing Systems (NIPS 2001)*, volume 14, pages 173–180, Cambridge, MA. MIT Press.

- Cheng, H., Chino, Y. M., 3rd, E. L. S., Hamamoto, J., and Yoshida, K. (1995). Transfer characteristics of lateral geniculate nucleus X neurons in the cat: effects of spatial frequency and contrast. *Journal of Neurophysiology*, 74(6):2548–57.
- Chklovskii, D. B., Schikorski, T., and Stevens, C. F. (2002). Wiring optimization in cortical circuits. *Neuron*, 34(3):341–7.
- Clarke, F. J. J. (1957). Rapid light adaptation of localised areas of the extra-foveal retina. *Optica Acta (London)*, 4:69–77.
- Clarke, F. J. J. (1960). A study of troxler’s effect. *Optica Acta (London)*, 7:219–236.
- Clarke, F. J. J. (1961). Visual recovery following local adaptation of the peripheral retina (troxler’s effect). *Optica Acta (London)*, 8:121–135.
- Clarke, F. J. J. (1962). On the localization of troxler’s effect in the visual pathway. *Vision Research*, 2:53–68.
- Clowes, M. B. and Ditchburn, R. W. (1959). An improved apparatus for producing a stabilized retinal image. *Optica Acta*, 6(3):252–265.
- Collewijn, H. and van der Mark, F. (1972). Ocular stability in variable feedback conditions in the rabbit. *Brain Research*, 36(1):47–57.
- Conway, B. R., Kitaoka, A., Yazdanbakhsh, A., Pack, C. C., and Livingstone, M. S. (2005). Neural basis for a powerful static motion illusion. *Journal of Neuroscience*, 25(23):5651–6.
- Conway, J. L., Timberlake, G. T., and Skavenski, A. A. (1981a). Oculomotor changes in cats reared without experiencing continuous retinal image motion. *Experimental Brain Research*, 43(2):229–232.
- Conway, J. L., Timberlake, G. T., and Skavenski, A. A. (1981b). Oculomotor changes in cats reared without experiencing continuous retinal image motion. *Experimental Brain Research*, 43:229–232.
- Coppola, D. and Purves, D. (1996). The extraordinary rapid disappearance of entopic images. *Proceedings of the National Academy of Sciences of the United States of America*, 23(93):8001–8004.
- Corfield, R., Frosdick, J. P., and Campbell, F. W. (1978). Grey-out elimination: the roles of spatial waveform, frequency and phase. *Vision Research*, 18(10):1305–11.
- Cornsweet, T. N. (1958). New technique for the measurement of small eye movements. *Journal of the Optical Society of America*, 48:808–811.
- Cornsweet, T. N. and Crane, H. D. (1973). Accurate two-dimensional eyetracker using first and fourth purkinje images. *Journal of the Optical Society of America*, 63(8):921–928.

- Crair, M. C., Gillespie, D. C., and Stryker, M. P. (1998). The role of visual experience in the development of columns in cat visual cortex. *Science*, 279(5350):566–570.
- Crane, H. D. (1994). The Purkinje Image Eyetracker, Image Stabilization, and Related Forms of Stimulus Manipulation. In Kelly, D. H., editor, *Visual Science and Engineering: Models and Applications*, chapter 2, pages 15–89. New York: Marcel Dekker Inc.
- Crane, H. D. and Clarke, M. (1978). Three-dimensional visual stimulus deflector. *Applied Optics*, 17(5):706–714.
- Crane, H. D. and Steele, C. M. (1978). Accurate three-dimensional eyetracker. *Applied Optics*, 17(5):691–705.
- Crane, H. D. and Steele, C. M. (1985). Generation V dual Purkinje-image eyetracker. *Applied Optics*, 24(4):527–537.
- Croner, L. J. and Kaplan, E. (1995). Receptive fields of P and M ganglion cells across the primate retina. *Vision Research*, 35(1):7–24.
- Dacey, D. M. (2000). Parallel pathways for spectral coding in primate retina. *Annual Review of Neuroscience*, 23:743–75.
- Dan, Y., Alonso, J. M., Usrey, W. M., and Reid, R. C. (1998). Coding of visual information by precisely correlated spikes in the lateral geniculate nucleus. *Nature Neuroscience*, 1(6):501–507.
- Dan, Y., Atick, J. J., and Reid, R. C. (1996). Efficient coding of natural scenes in the lateral geniculate nucleus: Experimental test of a computational theory. *Journal of Neuroscience*, 16(10):3351–3362.
- David, S. V., Vinje, W. E., and Gallant, J. L. (2004). Natural stimulus statistics alter the receptive field structure of V1 neurons. *Journal of Neuroscience*, 24(31):6991–7006.
- Dawis, S., Shapley, R., Kaplan, E., and Tranchina, D. (1984). The receptive field organization of X-cells in the cat: spatiotemporal coupling and asymmetry. *Vision Research*, 24(6):549–564.
- de Bie, J. (1985). An afterimage vernier method for assessing the precision of eye movement monitors: results for the scleral coil technique. *Vision Research*, 25(9):1341–3.
- de Boer, E. and Kuyper, P. (1968). Triggered correlation. *IEEE Transactions on Biomedical Engineering*, 15:169–179.
- de Ruyter Van Steveninck, R. R., Bialek, W., Potters, M., and Carlson, R. H. (1994). Statistical adaptation and optimal estimation in movement computation by the blowfly visual system. In *IEEE International Conference on Systems, Man, and Cybernetics. 'Humans, Information and Technology'*, volume 1, pages 302–307.

- De Valois, R. L. (2004). Neural coding of color. In Chalupa, L. M. and Werner, J. S., editors, *The Visual Neurosciences*, chapter 65, pages 1003–1016. Cambridge: MIT Press.
- Derrington, A. M. and Lennie, P. (1984). Spatial and temporal contrast sensitivities of neurones in lateral geniculate nucleus of macaque. *Journal of Physiology (London)*, 357:219–240.
- Deubel, H. and Bridgeman, B. (1995). Fourth Purkinje image signals reveal eye-lens deviations and retinal image distortions during saccades. *Vision Research*, 35(4):529–538.
- Diesmann, M., Gewaltig, M. O., and Aertsen, A. (1999). Stable propagation of synchronous spiking in cortical neural networks. *Nature*, 402(6761):529–33.
- Ditchburn, R. W. (1955). Eye movements in relation to retinal action. *Optica Acta (London)*, 1:171–176.
- Ditchburn, R. W. (1973). *Eye-movements and visual perception*. Oxford: Clarendon Press.
- Ditchburn, R. W. (1980). The function of small saccades. *Vision Research*, 20:271–272.
- Ditchburn, R. W. (1987). What is psychophysically perfect image stabilization? Do perfectly stabilized images always disappear?: Comment. *Journal of the Optical Society of America. A, Optics and Image Science*, 4(2):405–406.
- Ditchburn, R. W. and Foley-Fisher, J. A. (1986). Retinal image stabilizing systems for experiments in colour. *Optica Acta*, 33:91–96.
- Ditchburn, R. W. and Ginsborg, B. L. (1952). Vision with a stabilized retinal image. *Nature*, 170(4314):36–37.
- Ditchburn, R. W. and Ginsborg, B. L. (1953). Involuntary eye movements during fixation. *Journal of Physiology (London)*, 119:1–17.
- Dobkins, K. R. and Albright, T. D. (2004). Merging processing streams: Color cues for motion detection and interpretation. In Chalupa, L. M. and Werner, J. S., editors, *The Visual Neurosciences*, chapter 82, pages 1217–1228. Cambridge: MIT Press.
- Dong, D. W. and Atick, J. J. (1995a). Statistics of natural time-varying images. *Network: Computation in Neural Systems*, 6:345–358.
- Dong, D. W. and Atick, J. J. (1995b). Temporal decorrelation: a theory of lagged and nonlagged responses in the lateral geniculate nucleus. *Network: Computation in Neural Systems*, 6(2):159–178.
- Drysdale, A. E. (1975). The visibility of retinal blood vessels. *Vision Research*, 15(7):813–8.

- Eizenman, M., Hallett, P., and Frecker, R. C. (1985). Power spectra for ocular drift and tremor. *Vision Research*, 25(11):1635–1640.
- Ejima, Y., Takahashi, S., Yamamoto, H., Fukunaga, M., Tanaka, C., Ebisu, T., and Umeda, M. (2003). Interindividual and interspecies variations of the extrastriate visual cortex. *Neuroreport*, 14(12):1579–1583.
- Enroth-Cugell, C., Robson, J. G., Schweitzer-Tong, D. E., and Watson, A. B. (1983). Spatio-temporal interactions in cat retinal ganglion cells showing linear spatial summation. *Journal of Physiology (London)*, 341:279–307.
- Erdmann, B. and Dodge, R. (1898). *Psychologische Untersuchungen über das Lesen*. Halle, Germany:Niemeyer.
- Evans, C. R. (1965). Some studies of pattern perception using a stabilized retinal image. *The British Journal of Psychology*, 56(2,3):121–133.
- Ferman, L., Collewijn, H., and den A. V. Berg, V. (1987a). A direct test of Listing's law—II. Human ocular torsion measured under dynamic conditions. *Vision Research*, 27(6):939–51.
- Ferman, L., Collewijn, H., Jansen, T. C., and den A. V. Berg, V. (1987b). Human gaze stability in the horizontal, vertical and torsional direction during voluntary head movements, evaluated with a three-dimensional scleral induction coil technique. *Vision Research*, 27(5):811–28.
- Field, D. J. (1987). Relations between the statistics of natural images and the response properties of cortical cells. *Journal of the Optical Society of America. A, Optics and Image Science*, 4(12):2379–94.
- Field, D. J. (1994). What is the goal of sensory coding? *Neural Computation*, 6:559–601.
- Franz, M. O. and Scholkopf, B. (2005). Implicit wiener series for higher-order image analysis. In Saul, L. K., Weiss, Y., and Bottou, L., editors, *Advances in Neural Information Processing Systems (NIPS 2004)*, volume 17, pages 465–472, Cambridge, MA. MIT Press.
- Frazor, R. A., Albrecht, D. G., Geisler, W. S., and Crane, A. M. (2004). Visual cortex neurons of monkeys and cats: temporal dynamics of the spatial frequency response function. *Journal of Neurophysiology*, 91(6):2607–27.
- Fregnac, Y. and Imbert, M. (1978). Early development of visual cortical cells in normal and dark-reared kittens: relationship between orientation selectivity and ocular dominance. *Journal of Physiology (London)*, 278:27–44.
- Gaarder, K. (1968). Interpretive study of evoked responses elicited by gross saccadic eye movements. *Perceptual and Motor Skills*, 27(3):683–703.

- Gallant, J. L., Connor, C. E., and Essen, V. D. C. (1998). Neural activity in areas V1, V2 and V4 during free viewing of natural scenes compared to controlled viewing. *Neuroreport*, 9(9):2153–2158.
- Garcia-Perez, M. A. and Peli, E. (2001). Intrасaccadic perception. *Journal of Neuroscience*, 21(18):7313–22.
- Gawne, T. J., Kjaer, T. W., Hertz, J. A., and Richmond, B. J. (1996). Adjacent visual cortical complex cells share about 20% of their stimulus-related information. *Cerebral Cortex*, 6(3):482–9.
- Gawne, T. J. and Richmond, B. J. (1993). How independent are the messages carried by adjacent inferior temporal cortical neurons? *Journal of Neuroscience*, 13(7):2758–71.
- Geisler, W. S., Perry, J. S., and Najemnik, J. (2003). Visual search: Gaze contingent displays and optimal search strategies [abstract]. *Journal of Vision*, 3(9):68a.
- Gerrits, H. J. M., de Haan, B., and Vندrick, A. J. H. (1966). Experiments with retinal stabilized images. Relations between the observations and neural data. *Vision Research*, 6:427–440.
- Gerrits, H. J. M. and Vندrick, A. J. H. (1970). Artificial movements of a stabilized image. *Vision Research*, 10:1443–1456.
- Gerrits, H. J. M. and Vندrick, A. J. H. (1972). Eye movements necessary for continuous perception during stabilization of retinal images. *Bibliotheca Ophthalmologica: Supplementa ad Ophthalmologica*, 82:339–347.
- Gerrits, H. J. M. and Vندrick, A. J. H. (1974). The influence of stimulus movements on perception in parafoveal stabilized vision. *Vision Research*, 14:175–180.
- Ghazanfar, A. A. and Nicolelis, M. A. (2001). The structure and function of dynamic cortical and thalamic receptive fields. *Cerebral Cortex*, 11(3):183–193.
- Gibson, J. J. (1979). *The Ecological Approach to Visual Perception*. Boston: Houghton-Mifflin.
- Greschner, M., Bongard, M., Rujan, P., and Ammermüller, J. (2002). Retinal ganglion cell synchronization by fixational eye movements improves feature estimation. *Nature Neuroscience*, 5(4):341–7.
- Guido, W., Lu, S. M., Vaughan, J. W., Godwin, D. W., and Sherman, S. M. (1995). Receiver operating characteristic (ROC) analysis of neurons in the cat’s lateral geniculate nucleus during tonic and burst response mode. *Visual Neuroscience*, 12(4):723–41.
- Guido, W. and Weyand, T. (1995). Burst responses in thalamic relay cells of the awake behaving cat. *Journal of Neurophysiology*, 74(4):1782–6.
- Gur, M. (1989). Color and brightness fade-out in the ganzfeld is wavelength dependent. *Vision Research*, 29(10):1335–1341.

- Gur, M. (1991). Perceptual fade-out occurs in the binocularly viewed ganzfeld. *Perception*, 20:645–654.
- Gur, M., Beylin, A., and Snodderly, D. M. (1997). Response variability of neurons in primary visual cortex (V1) of alert monkeys. *Journal of Neuroscience*, 17(8):2914–20.
- Gur, M., Kagan, I., and Snodderly, D. M. (2005). Orientation and direction selectivity of neurons in V1 of alert monkeys: functional relationships and laminar distributions. *Cerebral Cortex*, 15(8):1207–21.
- Gur, M. and Snodderly, D. M. (1987). Studying striate cortex neurons in behaving monkeys: Benefits of image stabilization. *Vision Research*, 27(12):2081–2087.
- Gur, M. and Snodderly, D. M. (1997). Visual receptive fields of neurons in primary visual cortex (V1) move in space with the eye movements of fixation. *Vision Research*, 37(3):257–65.
- Harris, C. M., Hainline, L., Abramov, I., Lemerise, E., and Camenzuli, C. (1988). The distribution of fixation durations in infants and naive adults. *Vision Research*, 28(3):419–432.
- Harrison, C. W. (1952). Experiments with linear prediction in television. *Bell System Technical Journal*, 31:764–783.
- Hebbard, F. W. and Marg, E. (1960). Physiological nystagmus in the cat. *Journal of the Optical Society of America*, 50:151–155.
- Heidenreich, S. M. and Turano, K. A. (1996). Speed discrimination under stabilized and normal viewing conditions. *Vision Research*, 36(12):1819–1825.
- Helmholtz, H. (1866). *Treatise on Physiological Optics*. New York: Dover Publications. This 1962 edition by James P. C. Southall was translated from the third German edition from 1909.
- Hendry, S. H. and Reid, R. C. (2000). The koniocellular pathway in primate vision. *Annual Review of Neuroscience*, 23:127–53.
- Hinds, O. P., Polimeni, J. R., Blackwell, M. L., Wiggins, C. J., Wiggins, G. C., van der Kouwe, A., Wald, L. L., Schwartz, E. L., and Fischl, B. (2005). Reconstruction and analysis of human V1 by imaging the stria of Gennari using MRI at 7T [Abstract]. In *Society for Neuroscience Abstracts*.
- Hirsch, H. V. B. (1985). The role of visual experience in the development of cat striate cortex. *Cellular and Molecular Neurobiology*, 5:103–121.
- Hirsch, J. A. and Martinez, L. M. (2006). Circuits that build visual cortical receptive fields. *Trends in Neurosciences*, 29(1):30–39.

- Horton, J. C. and Hedley-Whyte, E. T. (1984). Mapping of cytochrome oxidase patches and ocular dominance columns in human visual cortex. *Philosophical Transactions of the Royal Society of London. Series B, Biological Sciences*, 304(1119):255–72.
- Horton, J. C. and Hubel, D. H. (1981). Regular patchy distribution of cytochrome oxidase staining in primary visual cortex of macaque monkey. *Nature*, 292(5825):762–4.
- Hubel, D. H. and Wiesel, T. N. (1962). Receptive fields, binocular interaction and functional architecture in the cat's visual cortex. *Journal of Physiology (London)*, 160:106–54.
- Ikeda, M. (1986). Temporal impulse response. *Vision Research*, 26(9):1431–40.
- Ikegaya, Y., Aaron, G., Cossart, R., Aronov, D., Lampl, I., Ferster, D., and Yuste, R. (2004). Synfire chains and cortical songs: temporal modules of cortical activity. *Science*, 304(5670):559–64.
- Irving, E. L., Zacher, J. E., Allison, R. S., and Callender, M. G. (2003). Effects of scleral search coil wear on visual function. *Investigative Ophthalmology and Visual Science*, 44(5):1933–8.
- Jones, R. M. and Tuluay-Keesey, Ü. (1975). Accuracy of image stabilization by an optical-electronic feedback system. *Vision Research*, 15:57–61.
- Jones, R. M., Webster, J. G., and Tuluay-Keesey, Ü. (1972). An active feedback system for stabilizing visual images. *IEEE Transactions on Biomedical Engineering*, 19(1):29–33.
- Kagan, I., Gur, M., and Snodderly, D. M. (2002). Spatial organization of receptive fields of V1 neurons of alert monkeys: comparison with responses to gratings. *Journal of Neurophysiology*, 88(5):2557–74.
- Kandel, E. R., Schwartz, J. H., and Jessell, T. M., editors (2000). *Principles of Neural Science*. McGraw-Hill, fourth edition.
- Kaplan, E. and Shapley, R. M. (1986). The primate retina contains two types of ganglion cells, with high and low contrast sensitivity. *Proceedings of the National Academy of Sciences of the United States of America*, 83(8):2755–7.
- Kapoula, Z. A., Robinson, D. A., and Hain, T. C. (1986a). Motion of the eye immediately after a saccade. *Experimental Brain Research*, 61(2):386–394.
- Kapoula, Z. A., Robinson, D. A., and Hain, T. C. (1986b). Motion of the eye immediately after a saccade. *Experimental Brain Research*, 61(2):386–394.
- Keesey, Ü. T. (1960). Effects of involuntary eye movements on visual acuity. *Journal of the Optical Society of America*, 50:769–774.

- Keesey, Ü. T. (1969). Visibility of a stabilized target as a function of frequency and amplitude of luminance variation. *Journal of the Optical Society of America*, 59:604–610.
- Kelly, D. H. (1979a). Motion and vision. I. Stabilized images of stationary gratings. *Journal of the Optical Society of America*, 69(9):1266–1274.
- Kelly, D. H. (1979b). Motion and vision. II. Stabilized spatio-temporal threshold surface. *Journal of the Optical Society of America*, 69(10):1340–1349.
- Kelly, D. H. (1981). Disappearance of stabilized chromatic gratings. *Science*, 214(11):1257–1258.
- Kerr, J. N., Greenberg, D., and Helmchen, F. (2005). Imaging input and output of neocortical networks in vivo. *Proceedings of the National Academy of Sciences of the United States of America*, 102(39):14063–8.
- Koenderink, J. J. (1972). Contrast enhancement and the negative afterimage. *Journal of the Optical Society of America*, 62(5):685–689.
- Kowler, E. and Steinman, R. M. (1980). Small saccades serve no useful purpose. *Vision Research*, 20(3):273–276.
- Krahe, R. and Gabbiani, F. (2004). Burst firing in sensory systems. *Nature Reviews Neuroscience*, 5(1):13–23.
- Krauskopf, J., Cornsweet, T. N., and Riggs, L. A. (1960). Analysis of eye movements during monocular and binocular fixation. *Journal of the Optical Society of America*, 50:572–8.
- Kremers, J., Lee, B. B., Pokorny, J., and Smith, V. C. (1993). Responses of macaque ganglion cells and human observers to compound periodic waveforms. *Vision Research*, 33(14):1997–2011.
- Kretzmer, E. R. (1952). Statistics of television signals. *Bell System Technical Journal*, 31:751–763.
- Lakshminarayanan, V., Knowles, R. A., Enoch, J. M., and Vasuvedan, R. (1992). Measurement of fixational stability while performing a hyperacuity task using the scanning laser ophthalmoscope: Preliminary studies. *Clinical Vision Science*, 7:557–563.
- Lee, B. B. (1996). Receptive field structure in the primate retina. *Vision Research*, 36(5):631–44.
- Lee, B. B., Pokorny, J., Smith, V. C., and Kremers, J. (1994). Responses to pulses and sinusoids in macaque ganglion cells. *Vision Research*, 34(23):3081–96.
- Lee, B. B., Pokorny, J., Smith, V. C., Martin, P. R., and Valberg, A. (1990). Luminance and chromatic modulation sensitivity of macaque ganglion cells and human observers. *Journal of the Optical Society of America. A, Optics and Image Science*, 7(12):2223–36.

- Lee, D. and Malpeli, J. G. (1998). Effects of saccades on the activity of neurons in the cat lateral geniculate nucleus. *Journal of Neurophysiology*, 79(2):922–936.
- Lennie, P. (2003). The cost of cortical computation. *Current Biology*, 13(6):493–7.
- Leopold, D. A. and Logothetis, N. K. (1998). Microsaccades differentially modulate neural activity in the striate and extrastriate visual cortex. *Experimental Brain Research*, 123:341–345.
- Li, Y., Fitzpatrick, D., and White, L. E. (2006). The development of direction selectivity in ferret visual cortex requires early visual experience. *Nature Neuroscience*, 9(5):676–681.
- Linsenmeier, R. A., Frishman, L. J., Jakiela, H. G., and Enroth-Cugell, C. (1982). Receptive field properties of X and Y cells in the cat retina derived from contrast sensitivity measurements. *Vision Research*, 22:1173–1183.
- Lisberger, S. G., Morris, E. J., and Tychsen, L. (1987). Visual motion processing and sensory-motor integration for smooth pursuit eye movements. *Annual Review of Neuroscience*, 10:97–129.
- Lisman, J. E. (1997). Bursts as a unit of neural information: making unreliable synapses reliable. *Trends in Neurosciences*, 20(1):38–43.
- Liu, J. and Newsome, W. T. (2005). Correlation between speed perception and neural activity in the middle temporal visual area. *The Journal of Neuroscience*, 25(3):711–22.
- Livingstone, M. S., Freeman, D. C., and Hubel, D. H. (1996). Visual responses in V1 of freely viewing monkeys. *Cold Spring Harbor Symposia on Quantitative Biology*, 61:27–37.
- Livingstone, M. S. and Hubel, D. H. (1984). Anatomy and physiology of a color system in the primate visual cortex. *Journal of Neuroscience*, 4(1):309–56.
- Loschky, L. C., Mcconkie, G. W., Reingold, E. M., and Stampe, D. M. (2003). Gaze-contingent multiresolutional displays: An integrative review. *Human Factors*, 45.
- Maldonado, P. E., Godecke, I., Gray, C. M., and Bonhoeffer, T. (1997). Orientation selectivity in pinwheel centers in cat striate cortex. *Science*, 276(5318):1551–5.
- Manteuffel, G., Plasa, L., Sommer, T. J., and Wess, O. (1977). Involuntary eye movements in salamanders. *Naturwissenschaften*, 64(10):533–4.
- Marmarelis, P. Z. and Marmarelis, V. Z. (1978). *Analysis of Physiological Systems*. New York: Plenum Press.
- Marshall, W. H. and Talbot, S. A. (1942). Recent evidence for neural mechanisms in vision leading to a general theory of sensory acuity. In Kluver, H., editor, *Biological Symposia—Visual Mechanisms*, volume 7, pages 117–164, Lancaster, PA. Cattell.

- Martinez, L. M., Wang, Q., Reid, R. C., Pillai, C., Alonso, J. M., Sommer, F. T., and Hirsch, J. A. (2005). Receptive field structure varies with layer in the primary visual cortex. *Nature Neuroscience*, 8(3):372–379.
- Martinez-Conde, S., Macknik, S. L., and Hubel, D. H. (2000). Microsaccadic eye movements and firing of single cells in the striate cortex of macaque monkeys. *Nature Neuroscience*, 3(3):251–258.
- Martinez-Conde, S., Macknik, S. L., and Hubel, D. H. (2002). The function of bursts of spikes during visual fixation in the awake primate lateral geniculate nucleus and primary visual cortex. *Proceedings of the National Academy of Sciences of the United States of America*, 99(21):13920–13925.
- Martinez-Conde, S., Macknik, S. L., and Hubel, D. H. (2004). The role of fixational eye movements in visual perception. *Nature Reviews Neuroscience*, 5:229–240.
- Martinez-Conde, S., Macknik, S. L., Troncoso, X. G., and Dyar, T. A. (2006). Microsaccades counteract fading during fixation. *Neuron*, 49(2):297–305.
- Mastrorarde, D. N. (1983a). Correlated firing of cat retinal ganglion cells. I. Spontaneously active inputs to X- and Y-cells. *Journal of Neurophysiology*, 49(2):303–24.
- Mastrorarde, D. N. (1983b). Interactions between ganglion cells in cat retina. *Journal of Neurophysiology*, 49(2):350–65.
- Mastrorarde, D. N. (1989). Correlated firing of retinal ganglion cells. *Trends in Neurosciences*, 12(2):75–80.
- Matin, L., Picoult, E., Stevens, J. K., Jr, M. W. E., Young, D., and MacArthur, R. (1982). Oculoparalytic illusion: visual-field dependent spatial mislocalizations by humans partially paralyzed with curare. *Science*, 216(4542):198–201.
- Mazer, J. A., Vinje, W. E., McDermott, J., Schiller, P. H., and Gallant, J. L. (2002). Spatial frequency and orientation tuning dynamics in area V1. *Proceedings of the National Academy of Sciences of the United States of America*, 99(3):1645–50.
- Mechler, F. and Ringach, D. L. (2002). On the classification of simple and complex cells. *Vision Research*, 42(8):1017–33.
- Meister, M. (1996). Multineuronal codes in retinal signaling. *Proceedings of the National Academy of Sciences of the United States of America*, 93(2):609–14.
- Meister, M., Lagnado, L., and Baylor, D. A. (1995). Concerted signaling by retinal ganglion cells. *Science*, 270(5239):1207–10.
- Merigan, W. H. and Maunsell, J. H. (1993). How parallel are the primate visual pathways? *Annual Review of Neuroscience*, 16:369–402.
- Miller, K. D., Erwin, E., and Kayser, A. (1999). Is the development of orientation selectivity instructed by activity? *Journal of Neurobiology*, 41(1):44–57.

- Møller, F., Laursen, M. L., Tygesen, J., and Sjølie, A. K. (2002). Binocular quantification and characterization of microsaccades. *Graefe's Archive for Clinical and Experimental Ophthalmology*, 240(9):765–770.
- Morrison, D. J. and Schyns, P. G. (2001). Usage of spatial scales for the categorization of faces, objects, and scenes. *Psychonomic Bulletin and Review*, 8(3):454–69.
- Motter, B. C. and Poggio, G. F. (1984). Binocular fixation in the rhesus monkey: spatial and temporal characteristics. *Experimental Brain Research*, 54:304–314.
- Movshon, J. A., Adelson, E. H., Gizzi, M. S., and Newsome, W. T. (1985). The analysis of moving visual patterns. In Chagas, C., Gattass, R., and Gross, C., editors, *Study Week on Pattern Recognition Mechanisms (April 25–29, 1983)*, volume 54, pages 117–151. Vatican City: Pontifica Academia Scientiarum.
- Movshon, J. A., Albright, T. D., Stoner, G. R., Majaj, N. J., and Smith, M. A. (2003). Cortical responses to visual motion in alert and anesthetized monkeys. *Nature Neuroscience*, 6(1):3; author reply 3–4.
- Movshon, J. A., Thompson, I. D., and Tolhurst, D. J. (1978a). Receptive field organization of complex cells in the cat's striate cortex. *Journal of Physiology (London)*, 283:79–99.
- Movshon, J. A., Thompson, I. D., and Tolhurst, D. J. (1978b). Spatial summation in the receptive fields of simple cells in the cat's striate cortex. *Journal of Physiology (London)*, 283:53–77.
- Murakami, I. and Cavanagh, P. (1998). A jitter after-effect reveals motion-based stabilization of vision. *Nature*, 395(6704):798–801.
- Murakami, I., Kitaoka, A., and Ashida, H. (2006). A positive correlation between fixation instability and the strength of illusory motion in a static display. *Vision Research*, 46(15):2421–2431.
- Nachmias (1959). Two-dimensional motion of the retinal image during monocular fixation. *Journal of the Optical Society of America*, 49:901–907.
- Navon, D. (1977). Forest before trees: The precedence of global features in visual perception. *Cognitive Psychology*, 9(3):353–383.
- Newsome, W. T., Wurtz, R. H., and Komatsu, H. (1988). Relation of cortical areas MT and MST to pursuit eye movements. II. Differentiation of retinal from extraretinal inputs. *Journal of Neurophysiology*, 60(2):604–20.
- Nikolov, S. G., Newman, T. D., Jones, M. G., Gilchrist, I. D., Bull, D. R., and Canagarajah, N. C. (2004). Gaze-contingent display using texture mapping and OpenGL: System and applications. In *Eye Tracking Research and Applications Symposium 2004*, San Antonio, TX.
- Oliver, B. M. (1952). Efficient coding. *Bell System Technical Journal*, 31:724–750.

- Olson, J. D., Tulunay-Keesey, Ü., and Saleh, B. E. A. (1993). Fading time of retinally-stabilized images as a function of background luminance and target width. *Vision Research*, 33(15):2127–2138.
- Olson, J. D., Tulunay-Keesey, Ü., and Saleh, B. E. A. (1994). Adaptation with a stabilized retinal image: effect of luminance and contrast. *Vision Research*, 34(21):2907–2915.
- Ölveczky, B. P., Baccus, S. A., and Meister, M. (2003). Segregation of object and background motion in the retina. *Nature*, 423(6938):401–8.
- Orban, G. A., Van Essen, D., and Vanduffel, W. (2004). Comparative mapping of higher visual areas in monkeys and humans. *Trends in Cognitive Sciences*, 8(7):315–324.
- Ott, D. and Daunicht, W. (1992). Eye movement measurement with the scanning laser ophthalmoscope. *Clinical Vision Science*, 7:551–556.
- Ott, D. and Eckmiller, R. (1989). Ocular torsion measured by TV- and scanning laser ophthalmoscopy during horizontal pursuit in humans and monkeys. *Investigative Ophthalmology and Visual Science*, 30(12):2512–20.
- Ott, D., Lades, M., Holthoff, K., and Eckmiller, R. (1990). A general numerical method evaluating three-dimensional eye rotations by scanning laser ophthalmoscopy. *Ophthalmic and Physiological Optics: the Journal of the British College of Ophthalmic Opticians (Optometrists)*, 10(3):286–90.
- Ouchi, H. (1977). *Japanese Optical and Geometrical Art*. New York: Dover.
- Oyster, C. W. (1999). *The Human Eye: Structure and Function*. Sinauer Associates.
- Pack, C. C., Berezovskii, V. K., and Born, R. T. (2001). Dynamic properties of neurons in cortical area MT in alert and anaesthetized macaque monkeys. *Nature*, 414(6866):905–8.
- Pack, C. C. and Born, R. T. (2001). Temporal dynamics of a neural solution to the aperture problem in visual area MT of macaque brain. *Nature*, 409(6823):1040–2.
- Pack, C. C., Conway, B. R., Born, R. T., and Livingstone, M. S. (2006). Spatiotemporal structure of nonlinear subunits in macaque visual cortex. *The Journal of Neuroscience*, 26(3):893–907.
- Pack, C. C., Hunter, J. N., and Born, R. T. (2005). Contrast dependence of suppressive influences in cortical area MT of alert macaque. *Journal of Neurophysiology*, 93(3):1809–1815.
- Panzeri, S., Schultz, S. R., Treves, A., and Rolls, E. T. (1999). Correlations and the encoding of information in the nervous system. *Proceedings of the Royal Society London. B, Biological Sciences*, 266(1423):1001–12.
- Parker, D. M. and Costen, N. P. (1999). One extreme or the other or perhaps the golden mean? Issues of spatial resolution in face processing. *Current Psychology*, 18:118–127.

- Parker, D. M., Lishman, J. R., and Hughes, J. (1992). Temporal integration of spatially filtered visual images. *Perception*, 21(2):147–60.
- Perez-Reyes, E. (2003). Molecular physiology of low-voltage-activated t-type calcium channels. *Physiological Reviews*, 83(1):117–61.
- Pettigrew, J. D. (1974). The effect of visual experience on the development of stimulus specificity by kitten cortical neurons. *Journal of Physiology (London)*, 237:49–74.
- Piotrowski, L. N. and Campbell, F. W. (1982). A demonstration of the visual importance and flexibility of spatial-frequency amplitude and phase. *Perception*, 11(3):337–46.
- Pirenne, M. H. (1962). *Light adaptation. I. The Troxler phenomenon.*, volume 2, pages 197–199. Academic, New York.
- Pitkow, X. (2006). *Optimality principles for the visual code.* PhD thesis, Biophysics, Harvard University, Cambridge, MA.
- Polimeni, J. R., Granquist-Fraser, D., Wood, R. J., and Schwartz, E. L. (2005a). Physical limits to spatial resolution of optical recording: clarifying the spatial structure of cortical hypercolumns. *Proceedings of the National Academy of Sciences of the United States of America*, 102(11):4158–63.
- Polimeni, J. R., Hinds, O. P., Balasubramanian, M., van der Kouwe, A. J. W., Wald, L. L., Dale, A. M., Fischl, B., and Schwartz, E. L. (2005b). The human V1–V2–V3 visuotopic map complex measured via fMRI at 3 and 7 Tesla [Abstract]. In *Society for Neuroscience Abstracts*.
- Priebe, N. J., Mechler, F., Carandini, M., and Ferster, D. (2004). The contribution of spike threshold to the dichotomy of cortical simple and complex cells. *Nature Neuroscience*, 7(10):1113–22.
- Pritchard, R. M. and Heron, W. (1960). Small eye movements of the cat. *Canadian Journal of Psychology*, 14:131–137.
- Puchalla, J. L., Schneidman, E., Harris, R. A., and Berry, M. J. (2005). Redundancy in the population code of the retina. *Neuron*, 46(3):493–504.
- Purkinje, J. (1825). *Beobachtungen und Versuche zur Physiologie der Sinne. II. Neue Beiträge zur Kenntniss des Sehens in subjectiver Hinsicht.* Berlin: Reiner.
- Putnam, N., Hofer, H. J., Doble, N., Chen, L., Carroll, J., and Williams, D. R. (2005). The locus of fixation and the foveal cone mosaic. *Journal of Vision*, 5(7).
- Ramcharan, E. J., Gnadt, J. W., and Sherman, S. M. (2001). The effects of saccadic eye movements on the activity of geniculate relay neurons in the monkey. *Visual Neuroscience*, 18(2):253–258.
- Ratliff, F. and Riggs, L. A. (1950). Involuntary motions of the eye during monocular fixation. *Journal of Experimental Psychology*, 40:687–701.

- Reid, R. C. and Shapley, R. M. (2002). Space and time maps of cone photoreceptor signals in macaque lateral geniculate nucleus. *Journal of Neuroscience*, 22(14):6158–6175.
- Reppas, J. B., Usrey, W. M., and Reid, R. C. (2002). Saccadic eye movements modulate visual responses in the lateral geniculate nucleus. *Neuron*, 35(5):961–974.
- Rieke, F., Bodnar, D. A., and Bialek, W. (1995). Naturalistic stimuli increase the rate and efficiency of information transmission by primary auditory afferents. *Proceedings of the Royal Society of London. Series B, Biological sciences*, 262(1365):259–65.
- Riggs, L. A. and Niehl, E. W. (1960). Eye movements recorded during convergence and divergence. *Journal of the Optical Society of America*, 50:913–920.
- Riggs, L. A. and Ratliff, F. (1952). The effects of counteracting the normal movements of the eye. *Journal of the Optical Society of America*, 42:872–873.
- Riggs, L. A., Ratliff, F., Cornsweet, J. C., and Cornsweet, T. N. (1953). The disappearance of steadily fixated visual test objects. *Journal of the Optical Society of America*, 43(6):495–501.
- Riggs, L. A. and Schick, A. M. L. (1968). Accuracy of retinal image stabilization achieved with a plane mirror on a tightly fitting contact lens. *Vision Research*, 8:159–169.
- Riggs, L. A. and Tulunay, U. S. (1959). Visual effects of varying the extent of compensation for eye movements. *Journal of the Optical Society of America*, 49:741–745.
- Ringach, D. L., Hawken, M. J., and Shapley, R. (1997). Dynamics of orientation tuning in macaque primary visual cortex. *Nature*, 387(6630):281–284.
- Robinson, D. A. (1963). A method of measuring eye movement using a scleral search coil in a magnetic field. *IEEE Transactions in Biomedical Engineering*, 10:137–45.
- Rodieck, R. W. (1967). Maintained activity of cat retinal ganglion cells. *Journal of Neurophysiology*, 30(5):1043–71.
- Roorda, A. (2000). Adaptive optics ophthalmoscopy. *Journal of Refractive Surgery*, 16(5):S602–7.
- Ross, J., Morrone, M. C., Goldberg, M. E., and Burr, D. C. (2001). Changes in visual perception at the time of saccades. *Trends in Neurosciences*, 24(2):113–21.
- Royden, C. S., Banks, M. S., and Crowell, J. A. (1992). The perception of heading during eye movements. *Nature*, 360:583–585.
- Rozhkova, G. I., Nickolayev, P. P., and Shchadrin, V. E. (1982a). Perception of stabilized retinal stimuli in dichoptic viewing conditions. *Vision Research*, 22(2):293–302.
- Rozhkova, G. I., Nikolaev, P. P., and Dimentman, A. M. (1985). Binocular rivalry during monocular observation of a homogeneous field and of stabilized images. *Human Physiology*, 11(3):153–9.

- Rozhkova, G. I., Nikolaev, P. P., and Shchadrin, V. E. (1982b). Factors determining characteristics of perception of stabilized retinal images. *Human Physiology*, 8(4):247–53.
- Rucci, M. and Casile, A. (2004). Decorrelation of neural activity during fixational instability: Possible implications for the refinement of V1 receptive fields. *Visual Neuroscience*, 21(5):725–738.
- Rucci, M. and Casile, A. (2005). Fixational instability and natural image statistics: Implications for early visual representations. *Network: Computation in Neural Systems*, 16(2–3):121–138.
- Rucci, M. and Desbordes, G. (2003). Contributions of fixational eye movements to the discrimination of briefly presented stimuli. *Journal of Vision*, 3(11):852–64.
- Rucci, M., Desbordes, G., Iovin, R., and Santini, F. (2006). Miniature eye movements enhance fine spatial detail. (*submitted manuscript*).
- Rucci, M., Edelman, G. M., and Wray, J. (2000). Modeling LGN responses during free-viewing: A possible role of microscopic eye movements in the refinement of cortical orientation selectivity. *Journal of Neuroscience*, 20(12):4708–4720.
- Ruderman, D. L. (1994). Statistics of natural images. *Network: Computation in Neural Systems*, 5(4):517–548.
- Saleh, B. E. A. and Tulunay-Keese, Ü. (1986). A model for the fading of stabilized images in a visual system. *IEEE Transactions on Systems, Man and Cybernetics*, 16(1):84–92.
- Santini, F., Redner, G., Iovin, R., and Rucci, M. (2006). EyeRIS: A general-purpose system for eye movement contingent display control. *Behavior Research Methods (in press)*.
- Schneidman, E., Bialek, W., and 2nd, M. J. B. (2003). Synergy, redundancy, and independence in population codes. *Journal of Neuroscience*, 23(37):11539–53.
- Schuchard, R. A. and Raasch, T. W. (1992). Retinal locus for fixation: Pericentral fixation targets. *Clinical Vision Science*, 7:511–520.
- Schulz, E. (1984). Binocular micromovements in normal persons. *Graefe's Archive for Clinical and Experimental Ophthalmology*, 222(2):95–100.
- Schyns, P. G. and Oliva, A. (1994). From blobs to boundary edges: Evidence for time- and spatial-scale-dependent scene recognition. *Psychological Science*, 5:195–200.
- Shannon, C. E. and Weaver, W. (1949). *The Mathematical Theory of Communication*. Univ. Illinois Press, Urbana Champagne, IL.
- Shapley, R. (1990). Visual sensitivity and parallel retinocortical channels. *Annual Review of Psychology*, 41:635–58.

- Shapley, R. M. and Victor, J. D. (1978). The effect of contrast on the transfer properties of cat retinal ganglion cells. *Journal of Physiology (London)*, 285:275–98.
- Shapley, R. M. and Victor, J. D. (1979). Nonlinear spatial summation and the contrast gain control of cat retinal ganglion cells. *Journal of Physiology (London)*, 290(2):141–61.
- Sharpe, C. R. (1972). The visibility and fading of thin lines visualized by their controlled movement across the retina. *Journal of Physiology (London)*, 222(1).
- Sherk, H. and Stryker, M. (1976). Quantitative study of cortical orientation selectivity in visually inexperienced kitten. *Journal of Neurophysiology*, 39(1):63–70.
- Sherman, S. M. (1996). Dual response modes in lateral geniculate neurons: mechanisms and functions. *Visual Neuroscience*, 13(2):205–213.
- Sherman, S. M. and Guillery, R. W. (1996). Functional organization of thalamocortical relays. *Journal of Neurophysiology*, 76(3):1367–1395.
- Sherman, S. M. and Guillery, R. W. (2004). The visual relays in the thalamus. In Chalupa, L. M. and Werner, J. S., editors, *The Visual Neurosciences*, chapter 35, pages 565–591. Cambridge: MIT Press.
- Sherrington, C. (1906). *The Integrative Action of the Nervous System*. Yale University Press, New Haven.
- Sillito, A. M. and Jones, H. E. (2002). Corticothalamic interactions in the transfer of visual information. *Philosophical transactions of the Royal Society of London. Series B, Biological sciences*, 357(1428):1739–52.
- Sincich, L. C., Park, K. F., Wohlgenuth, M. J., and Horton, J. C. (2004). Bypassing V1: a direct geniculate input to area MT. *Nature Neuroscience*, 7(10):1123–8.
- Singer, W. (1999). Time as coding space? *Current Opinion in Neurobiology*, 9:189–194.
- Singer, W. and Gray, C. M. (1995). Visual feature integration and the temporal correlation hypothesis. *Annual Review of Neuroscience*, 18:555–586.
- Skavenski, A. A., Robinson, D. A., Steinman, R. M., and Timberlake, G. T. (1975a). Miniature eye movements of fixation in rhesus monkey. *Vision Research*, 15(11):1269–1273.
- Skavenski, A. A., Robinson, D. A., Steinman, R. M., and Timberlake, G. T. (1975b). Miniature eye movements of fixation in rhesus monkey. *Vision Research*, 15(11):1269–1273.
- Skottun, B. C., Valois, D. R. L., Grosf, D. H., Movshon, J. A., Albrecht, D. G., and Bonds, A. B. (1991). Classifying simple and complex cells on the basis of response modulation. *Vision Research*, 31(7-8):1079–86.
- Smirnakis, S. M., Berry, M. J., Warland, D. K., Bialek, W., and Meister, M. (1997). Adaptation of retinal processing to image contrast and spatial scale. *Nature*, 386(6620):69–73.

- Smith, M. A., Majaj, N. J., and Movshon, J. A. (2005). Dynamics of motion signaling by neurons in macaque area MT. *Nature Neuroscience*, 8(2):220–8.
- Smith, V. C., Lee, B. B., Pokorny, J., Martin, P. R., and Valberg, A. (1992). Responses of macaque ganglion cells to the relative phase of heterochromatically modulated lights. *Journal of Physiology (London)*, 458:191–221.
- Snodderly, D. M. (1987). Effect of light and dark environments on macaque and human fixational eye movements. *Vision Research*, 27:401–415.
- Snodderly, D. M., Kagan, I., and Gur, M. (2001). Selective activation of visual cortex neurons by fixational eye movements: implications for neural coding. *Visual Neuroscience*, 18(2):259–77.
- Snodderly, D. M. and Kurtz, D. (1985). Eye position during fixation tasks: Comparison of macaque and human. *Vision Research*, 25:83–98.
- So, Y. T. and Shapley, R. (1981). Spatial tuning of cells in and around lateral geniculate nucleus of the cat: X and Y relay cells and perigeniculate interneurons. *Journal of Neurophysiology*, 45(1):107–20.
- Spauschus, A., Marsden, J., Halliday, D. M., Rosenberg, J. R., and Brown, P. (1999). The origin of ocular microtremor in man. *Experimental Brain Research*, 126(4):556–62.
- Spillmann, L., Tulunay-Keesey, U., and Olson, J. (1993). Apparent floating motion in normal and stabilized vision. *Investigative Ophthalmology and Visual Science*, Supplement 34:1031p.
- Srinivasan, M. V., Laughlin, S. B., and Dubs, A. (1982). Predictive coding: a fresh view of inhibition in the retina. *Proceedings of the Royal Society, Series B: Biological Sciences*, 216(1205):427–59.
- St Cyr, G. J. and Fender, D. H. (1969). The interplay of drifts and flicks in binocular fixation. *Vision Research*, 9(2):245–65.
- Steinbach, M. J. and Money, K. E. (1973). Eye movements of the owl. *Vision Research*, 13(4):889–891.
- Steinman, R. M. (2004). Gaze control under natural conditions. In Chalupa, L. M. and Werner, J. S., editors, *The Visual Neurosciences*, chapter 90. Cambridge: MIT Press.
- Steinman, R. M., Cunitz, R. J., Timberlake, G. T., and Herman, M. (1967). Voluntary control of microsaccades during maintained monocular fixation. *Science*, 155:1577–1579.
- Steinman, R. M., Haddad, G. M., Skavenski, A. A., and Wyman, D. (1973). Miniature eye movement. *Science*, 181(102):810–819.
- Steinman, R. M. and Levinson, J. Z. (1990). The role of eye movements in the detection of contrast and spatial detail. In Kowler, E., editor, *Eye movements and their role in visual and cognitive processes*, chapter 3, pages 115–212. Elsevier Science Publishers BV.

- Steinman, R. M., Levinson, J. Z., Collewijn, H., and J. van der Steen (1985). Vision in the presence of known natural retinal image motion. *Journal of the Optical Society of America. A, Optics and Image Science*, 2(2):226–233.
- Stent, G. S. (1973). A physiological mechanism for Hebb's postulate of learning. *Proceedings of the National Academy of Sciences of the United States of America*, 70:997–1001.
- Stetter, M., Sendtner, R. A., and Timberlake, G. T. (1996). A novel method for measuring saccade profiles using the scanning laser ophthalmoscope. *Vision Research*, 36(13):1987–94.
- Stevens, J. K., Emerson, R. C., Gerstein, G. L., Kallos, T., Neufeld, G., Nichols, C. W., and Rosenquist, A. C. (1976). Paralysis of the awake human: visual perceptions. *Vision Research*, 16:93–98.
- Stevenson, S. B. and Roorda, A. (2005). Correcting for miniature eye movements in high resolution scanning laser ophthalmoscopy. In Manns, F., Soderberg, P. G., Ho, A., Stuck, B. E., and Belkin, M., editors, *Ophthalmic Technologies XV*, volume 5688 of *Proceedings of SPIE*, pages 145–151. SPIE—The International Society for Optical Engineering, Bellingham, WA.
- Sylvester, R., Haynes, J. D., and Rees, G. (2005). Saccades differentially modulate human LGN and V1 responses in the presence and absence of visual stimulation. *Current Biology*, 15(1):37–41.
- Tolhurst, D. J., Tadmor, Y., and Chao, T. (1992). Amplitude spectra of natural images. *Ophthalmic and Physiological Optics*, 12(2):229–32.
- Troxler, I. P. V. (1804). *Über das Verschwinden gegebener Gegenstände innerhalb unseres Gesichtskreises*, volume II, pages 1–53. F. Fromann, Jena, Germany.
- Tulunay, Ü. S. (1959). *Effects of retinal image motions on acuity*. PhD thesis, Brown University Psychology Department.
- Tulunay-Keeseey, Ü. (1982). Fading of stabilized retinal images. *Journal of the Optical Society of America*, 72(4):440–447.
- Tulunay-Keeseey, Ü. and Bennis, B. J. (1979). Effects of stimulus onset and image motion on contrast sensitivity. *Vision Research*, 19:767–774.
- Tulunay-Keeseey, Ü. and Jones, R. M. (1976). The effect of micromovements of the eye and exposure duration on contrast sensitivity. *Vision Research*, 16:481–488.
- Tulunay-Keeseey, Ü. and Jones, R. M. (1980). Contrast sensitivity measures and accuracy of image stabilization systems. *Journal of the Optical Society of America*, 70(11):1306–1310.
- Tulunay-Keeseey, Ü. and Olson, J. D. (1996). Brightness of uniform stabilized fields. *Vision Research*, 36(3):351–359.

- Tulunay-Keeseey, Ü., Saleh, B. E. A., VerHoeve, J. N., and Hom, M. (1987). Apparent phase reversal during stabilized image fading. *Journal of the Optical Society of America. A, Optics and Image Science*, 4(11):2166–2175.
- Tulunay-Keeseey, Ü. and VerHoeve, J. N. (1987). The role of eye movements in motion detection. *Vision Research*, 27(5):747–754.
- Usrey, W. M. and Reid, R. C. (1999). Synchronous activity in the visual system. *Annual Review of Physiology*, 61:435–456.
- Van Essen, D. C. (2004). Organization of visual areas in macaque and human cerebral cortex. In Chalupa, L. M. and Werner, J. S., editors, *The Visual Neurosciences*, chapter 32, pages 507–521. Cambridge: MIT Press.
- Van Essen, D. C., Lewis, J. W., Drury, H. A., Hadjikhani, N., Tootell, R. B., Bakircioglu, M., and Miller, M. I. (2001). Mapping visual cortex in monkeys and humans using surface-based atlases. *Vision Research*, 41(10–11):1359–1378.
- van Hateren, J. H. (1992). A theory of maximizing sensory information. *Biological Cybernetics*, 68(1):23–9.
- van Hateren, J. H. and Ruderman, D. L. (1998). Independent component analysis of natural image sequences yields spatio-temporal filters similar to simple cells in primary visual cortex. *Proceedings of the Royal Society, Series B: Biological Sciences*, 265:2315–2320.
- van Hateren, J. H., Ruttiger, L., Sun, H., and Lee, B. B. (2002). Processing of natural temporal stimuli by macaque retinal ganglion cells. *Journal of Neuroscience*, 22(22):9945–60.
- van Hateren, J. H. and van der Schaaf, A. (1998). Independent component filters of natural images compared with simple cells in primary visual cortex. *Proceedings of the Royal Society, Series B: Biological Sciences*, 265:359–366.
- Verheijen, F. J. (1961). A simple after image method demonstrating the involuntary multidirectional eye movements during fixation. *Optica Acta (London)*, 8:309–11.
- Victor, J. D. (1987). The dynamics of the cat retinal X cell centre. *Journal of Physiology (London)*, 386:219–246.
- Vinje, W. E. and Gallant, J. L. (2000). Sparse coding and decorrelation in primary visual cortex during natural vision. *Science*, 287(5456):1273–6.
- Vinje, W. E. and Gallant, J. L. (2002). Natural stimulation of the nonclassical receptive field increases information transmission efficiency in V1. *Journal of Neuroscience*, 22(7):2904–15.
- von Holst, E. and Mittelstaedt, H. (1950). Das Reafferenzprinzip Wechselwirkungen zwischen Zentralnervensystem und Peripherie. *Naturwissenschaften*, 37(20):464–476.

- Westheimer, G. (1990). The grain of visual space. *Cold Spring Harbor Symposia on Quantitative Biology*, 55:759–63.
- Winterson, B. J. and Robinson, D. A. (1975). Fixation by the alert but solitary cat. *Vision Research*, 15:1349–1352.
- Yarbus, A. L. (1956). Perception of a stabilized retinal image. *Biofizika*, 1:435–437. In Russian.
- Yarbus, A. L. (1967). *Eye Movements and Vision*. New York: Plenum Press. Translated from Russian by Basil Haigh. Original Russian edition published in Moscow in 1965.
- Zanker, J. M. (2004). Looking at Op Art from a computational viewpoint. *Spatial Vision*, 17(1-2):75–94.
- Zanker, J. M., Doyle, M., and Robin, W. (2003). Gaze stability of observers watching Op Art pictures. *Perception*, 32(9):1037–49.
- Zohary, E., Shadlen, M. N., and Newsome, W. T. (1994). Correlated neuronal discharge rate and its implications for psychophysical performance. *Nature*, 370(6485):140–3.
- Zuber, B. L. and Stark, L. (1965). Microsaccades and the velocity-amplitude relationship for saccadic eye movements. *Science*, 150:1459–1460.

Gaëlle Desbordes

born January 15, 1977 in Paris, France

Current contact information:

Harvard Biocontrols Laboratory
Harvard University
60 Oxford St
Cambridge, MA 02138 USA
tel: (+1) 617 495 3206
desbordes@gmail.com

EDUCATION **Boston University, Boston, MA USA:**

Ph.D. candidate in Cognitive and Neural Systems, 2006.
Graduate courses in computational neuroscience and neural models of: vision, audition, sensory-motor control & adaptive movement planning, speech production, memory & attention, conditioning & reinforcement.

Laval University, Quebec City, QC Canada:

M.Sc., Computer Science, August 2001.
Graduate courses in artificial intelligence, software agents, neural networks, natural language processing, knowledge representation, machine learning, advanced object-oriented projects.

Ecole Nationale Supérieure des Mines, Saint-Etienne, France:

Ingénieur des Mines, March 2001.

Corresponding to BA/MA in Multidisciplinary Engineering and Management. This college is one of the engineering *Grandes Ecoles*: “Prestige university-level colleges with competitive entrance examinations”, which require 2 to 3 years of *Math Sup–Math Spé*, i.e., intensive courses and weekly exams in undergraduate mathematics, physics, chemistry, computer science, French, and foreign languages.

French *baccalauréat* (high school graduation), Rouen, France:

Mathematics & Physics major, June 1994, with *Mention Très Bien* (Very High Honors).

- HONORS AND AWARDS**
- November 2004: Fellowship to Okinawa Computational Neuroscience Course (Japan)
 - 2001–2004: Boston University, Arts and Sciences Dean’s Fellowship (USA)
 - 2000–2001: Laval University Scholarship (Canada)
 - 1999–2000: *Région Rhône-Alpes* Scholarship (France)
- MEMBERSHIPS**
- Society for Neuroscience
 - Visual Sciences Society
 - Association of Women in Science
- RESEARCH EXPERIENCE**
- | | |
|--|---|
| <i>Research Assistant (Ph.D. Student)</i> | Boston University,
Department of Cognitive and
Neural Systems
Boston, MA USA |
| May 2002–present | |
| Active Perception Lab. Advisor: Prof. Michele Rucci. | |
| Project funded by the National Science Foundation (grants number EIA-0130851 and EMT-0432104) and the National Institute of Health (grant number EY015732-01). | |
| Investigating the role of fixational eye movements in perception, by conducting psychophysical experiments on human subjects and modeling and simulating biological neural networks in the early visual pathway. | |
| <i>Research Assistant (M.Sc. Student)</i> | Laval University, Department
of Computer Science
Québec, QC Canada |
| May 2000–June 2001 | |
| Advisor: Prof. Bernard Moulin. | |
| Project funded by the Defence Research Establishment Valcartier, Val-Bélair, Québec. | |
| M.Sc. thesis: “An Argumentation-Based Framework For Software Agents”. | |
| Wrote a review of explanation and argumentation in knowledge-based systems (see Publications). Designed an argumentation-based and agent-based system using logic programming and conceptual graphs. | |

- TEACHING EXPERIENCE *Teaching Fellow* **Boston University,
Department of Cognitive and
Neural Systems**
Boston, MA USA
- Spring 2003
with Prof. Dan Bullock.
Course CN540: Neural and Computational Models of Adaptive Move-
ment Planning and Control.
- Teaching Assistant* **Laval University, Department
of Computer Science**
Québec, QC Canada
- Fall 2000
with Prof. Karim Khelifi.
Course IFT-21027: Introduction to Scientific Programming.
- OTHER PROFESSIONAL EXPERIENCE *Visual C++ Programmer
(Internship)* **Fujisoft ABC Inc.**
Summer 1999 Kamakura, JAPAN
- Windsurfing Teacher and Teacher
Assistant* **French Sailing Federation**
Summers of 1993, 1994, 1995, 1998 Boat Clubs and Summer Camps,
France
- VOLUNTARY ACTIVITIES *Co-organizer of Journal Club*
2004-present
Organizing weekly meetings for faculty and graduate students inter-
ested in discussing research articles about visual neuroscience.
- Webmaster*
2002-2004
Active Perception Lab's webpage: <http://cns.bu.edu/aplab/>
- JOURNAL PUBLICATIONS G. Desbordes and M. Rucci. Fast decorrelation across primate retinal
ganglion cells due to fixational eye movements. (*in preparation*)
- M. Rucci, G. Desbordes, R. Iovin, F. Santini. Miniature eye move-
ments enhance fine spatial detail. (*submitted*)
- M. Rucci and G. Desbordes (2003). Contributions of fixational eye
movements to the discrimination of briefly presented stimuli. *Journal
of Vision*, 3 (11): 852-864.
<http://journalofvision.org/3/11/18/>

B. Moulin, H. Irandoust, M. Bélanger, G. Desbordes (2002). Explanation and argumentation capabilities: Towards the creation of more persuasive agents. *Artificial Intelligence Review*, 17 (3): 169-222, May 2002.

CONFERENCES M. Rucci, G. Desbordes, R. Iovin, F. Santini (2006). Fixational eye movements and the perception of spatial detail. Society for Neuroscience 36th Annual Meeting, Atlanta, GA, Oct 2006 (*accepted abstract*).

G. Desbordes and M. Rucci (2006). Modeling the dynamics of retinal ganglion cells during natural viewing. 10th International Conference on Cognitive and Neural Systems, Boston, MA, May 2006.

M. Rucci, G. Desbordes, R. Iovin, F. Santini (2006). Contributions of fixational eye movements to visual discrimination. Vision Sciences Society 2006 meeting, Sarasota, FL, May 2006.

M. Rucci, R. Iovin, and G. Desbordes (2006). Fixational eye movements and the representation of natural scenes. CoSyNe conference, Salt Lake City, UT, March 2006.

G. Desbordes and M. Rucci (2005). A model of visual discrimination in the presence of fixational instability. Society for Neuroscience 35th Annual Meeting, Washington D.C., Nov 2005.

M. Rucci and G. Desbordes (2005). Influences of fixational eye movements on the statistics of visual input: Implications for early visual representations. Society for Neuroscience 35th Annual Meeting, Washington D.C., Nov 2005.

M. Rucci, G. Desbordes, and A. Casile (2005). Fixational eye movements and the neural encoding of natural visual stimuli: A theoretical perspective. Gordon Research Conference on Oculomotor System Biology, Lewiston, ME, June 2005.

G. Desbordes and M. Rucci (2004). Modeling the responses of LGN neurons during fixational eye movements. Society for Neuroscience 34th Annual Meeting, San Diego, CA, Oct 2004.

G. Desbordes and M. Rucci (2004). Discrimination of briefly presented stimuli in the presence and absence of fixational eye movements. Vision Sciences Society 2004 meeting, Sarasota, FL, May 2004.

F. Santini, J.D. Watts, G. Desbordes and M. Rucci (2004). A system for experiments of eye movements contingent display. Vision Sciences Society 2004 meeting, Sarasota, FL, May 2004.

G. Desbordes and M. Rucci (2004). Modeling the response of geniculate neurons during fixational instability. 8th International Conference on Cognitive and Neural Systems, Boston, MA, May 2004.

G. Desbordes and M. Rucci (2003). Stimulus identification in the presence and absence of eye movements. 7th International Conference on Cognitive and Neural Systems, Boston, MA, May 2003.

COMPUTER SKILLS Languages: C/C++, Matlab, L^AT_EX, HTML, Java, Perl, Lisp, Prolog.
Operating Systems: Unix/Linux, Microsoft Windows.

LANGUAGE SKILLS French (mother tongue)
English (fluent)
German (ZDFB: German Language for Business diploma)
Japanese and Italian (basic conversation).

OTHER PAST AND PRESENT INTERESTS Kung-fu, tai-chi, yoga
Music: singing, guitar, saxophone, recorder (baroque flute); multiple live performances in rock, jazz, and classical music
Windsurfing: official Sailing Teacher of the French Sailing Federation
Reading (neuroscience, vision, evolution; French, American, and English literature)
Improvisational theatre, including several on-stage performances
Travel.